

**The role of thylakoid ATP synthase subunit gamma
and attempts to transform the organelles of
*A. thaliana***

**Dissertation der Fakultät für Biologie
der Ludwig-Maximilians-Universität München**

**vorgelegt von
Cristina Dal Bosco
aus Italien**

2006

1. Gutachter: Prof. Dr. Reinhold G. Herrmann

2. Gutachter: Prof. Dr. Hugo Scheer

Tag der mündlichen Prüfung: März, den 31, 2006

CONTENT

ABBREVIATIONS.....	6
1 INTRODUCTION.....	8
1.1 THYLAKOID MEMBRANE PHOTOSYNTHETIC COMPLEXES IN HIGHER PLANTS.....	8
1.2 ATP SYNTHASE: STRUCTURE, FUNCTION AND REGULATION.....	9
1.3 ATP SYNTHASE γ SUBUNIT.....	11
1.3.1 REDOX REGULATION.....	11
1.3.2 ATPC1 VERSUS ATPC2.....	12
1.4 PHOTOCHEMISTRY.....	13
1.4.1 NON-PHOTOCHEMICAL QUENCHING - NPQ.....	13
1.4.2 THE CENTRAL ROLE OF PSBS FOR qE.....	14
1.5 TOWARDS ORGANELLE TRANSFORMATION IN ARABIDOPSIS THALIANA.....	14
1.5.1 ARABIDOPSIS THALIANA: A MODEL FOR HIGHER PLANTS.....	15
1.5.2 PLASTID TRANSFORMATION.....	16
1.6 GOALS OF THE PROJECT.....	19
2 MATERIALS.....	20
2.1 CHEMICALS, RADIOACTIVE SUBSTANCES, WORKING MATERIAL.....	20
2.2 PLANT MATERIAL.....	20
2.3 BACTERIAL STRAINS.....	21
2.4 PLASMIDS.....	21
2.4.1 CLONING VECTORS.....	21
2.4.2 EXPRESSION VECTORS.....	21
2.4.3 BINARY VECTORS.....	21
2.5 OLIGONUCLEOTIDES.....	22
2.6 MEDIA.....	24
2.6.1 MEDIA FOR BACTERIA.....	24
2.6.2 SOLUTIONS AND MEDIA FOR PROTOPLAST AND TISSUE CULTURE.....	24
2.7 ENZYMES.....	26
2.8 ANTIBODIES.....	27
3 METHODS.....	28
3.1 BACTERIA GROWTH AND MANIPULATION.....	28
3.1.1 CULTIVATION OF BACTERIA.....	28
3.1.2 PREPARATION OF COMPETENT CELLS.....	28
3.1.3 TRANSFORMATION OF BACTERIA (HEAT SHOCK).....	29
3.2 PLANT GROWTH AND MANIPULATION.....	29
3.2.1 SEED STERILIZATION, PLANT GROWTH AND MUTANT SELECTION.....	29
3.2.2 PROTOPLAST ISOLATION.....	30
3.2.3 PEG TREATMENT OF PROTOPLAST.....	30
3.2.4 DNA TRANSFER BY THE BIOLISTIC METHOD.....	31

3.2.5	<i>AGROBACTERIA</i> MEDIATED NUCLEAR TRANSFORMATION OF <i>ARABIDOPSIS</i>	31
3.2.6	GUS ASSAY	32
3.3	<i>NUCLEIC ACID MANIPULATION</i>	32
3.3.1	RAPID ISOLATION OF GENOMIC DNA FOR PCR USE	32
3.3.2	ISOLATION OF TOTAL RNA	33
3.3.3	ISOLATION OF DNA FOR PCR USE FROM YEAST	33
3.3.4	PLASMID ISOLATION FROM <i>E. COLI</i>	33
3.3.5	ENZYMATIC ASSAYS	34
3.3.6	NORTHERN ANALYSIS	35
3.3.7	HYBRIDIZATION OF NUCLEIC ACIDS	35
3.3.8	REVERSE TRANSCRIPTION (RT)-PCR	36
3.3.9	QUANTITATIVE REAL-TIME RT-PCR	36
3.4	<i>PROTEIN AND PIGMENT ANALYSES</i>	37
3.4.1	EXTRACTION OF THYLAKOID MEMBRANE PROTEINS	37
3.4.2	EXTRACTION OF TOTAL PROTEINS	38
3.4.3	ISOLATION OF MAJOR THYLAKOID MEMBRANE COMPLEXES OF <i>ARABIDOPSIS</i>	39
3.4.4	ISOELECTRO FOCUSING OF THYLAKOID MEMBRANE PROTEINS	40
3.4.5	<i>IN VIVO</i> LABELLING OF LEAF PROTEINS	40
3.4.6	MEASUREMENT OF PROTEIN AND CHLOROPHYLL CONCENTRATION	41
3.4.7	SODIUM DODECYL SULFATE POLYACRYLAMIDE GEL ELECTROPHORESIS (SDS-PAGE)	41
3.4.8	PROTEIN DETECTION	41
3.5	<i>CHLOROPHYLL A FLUORESCENCE ANALYSIS</i>	43
3.6	<i>GENETIC METHODS</i>	44
3.6.1	MAPPING OF THE <i>DPA1</i> MUTATION	44
3.6.2	GENERATION OF THE <i>PSBSxDPAI</i> DOUBLE MUTANT	44
3.7	<i>ELECTRON MICROSCOPY</i>	45
3.8	<i>PHOTOPHOSPHORYLATION</i>	45
4	RESULTS	46
4.1	<i>KNOCK-OUT MUTANT OF THE ATP SYNTHASE γ SUBUNIT, DPA1 (DEFICIENCY OF PLASTID ATP SYNTHASE 1)</i>	46
4.1.1	ISOLATION AND PHENOTYPE OF THE <i>DPA1</i> MUTANT	46
4.1.2	INACTIVATION OF THE <i>ATPC1</i> GENE	47
4.1.3	ACCUMULATION OF THE MAJOR PHOTOSYNTHETIC COMPLEXES IN <i>DPA1</i>	49
4.1.4	PLASTID ATP SYNTHASE ACTIVITY IN <i>DPA1</i> MUTANT	50
4.1.5	PHOTOSYNTHETIC ACTIVITY IN <i>DPA1</i>	51
4.1.6	LIGHT INDUCED THYLAKOID SWELLING IN <i>DPA1</i>	55
4.1.7	<i>PSBSxDPA1</i> DOUBLE MUTANT	55
4.1.8	EXPRESSION OF NUCLEAR-ENCODED GENES IN <i>DPA1</i>	58
4.2	<i>DPA1 COMPLEMENTED WITH A MUTATED FORM OF ATPC1</i>	60
4.2.1	ATP SYNTHASE ACCUMULATION IN ATPC-MOD TRANSFORMED LINES	61
4.2.2	CHLOROPHYLL A FLUORESCENCE TRANSIENT AND THYLAKOID Δ pH IN ATPCMOD-C	62
4.3	<i>THE ATPC2 GENE</i>	64
4.3.1	ATPC2 IS LOCALIZED IN THE PLASTID	64
4.3.2	ATPC2 IS EXPRESSED AT A VERY LOW LEVEL IN GREEN TISSUES	65
4.3.3	OVEREXPRESSION OF <i>ATPC2</i> IN THE <i>DPA1</i> MUTANT	66
4.3.4	ATPC2 KNOCK-OUT LINES	70
4.3.5	EXPRESSION ANALYSIS OF THE <i>ATPC2</i> PROMOTER	71

4.4	<i>TOWARDS ORGANELLE TRANSFORMATION IN ARABIDOPSIS</i>	73
4.4.1	EFFICIENT REGENERATION FROM COTYLEDON PROTOPLASTS	73
4.4.2	DEVELOPMENT OF A SELECTABLE MARKER FOR <i>ARABIDOPSIS</i> PLASTID TRANSFORMATION.....	76
4.4.3	DHPS AND FOLATE BIOSYNTHESIS IN <i>ARABIDOPSIS</i>	80
4.4.4	SULFONAMIDE RESISTANCE BY MITOCHONDRIAL TRANSLOCATION OF DHPS.	82
4.4.5	BACTERIAL DHPS SPECIFIC ANTIBODY	83
5	DISCUSSION	85
5.1	<i>THE γ SUBUNIT IS ESSENTIAL FOR ASSEMBLY OF THE PLASTID ATP SYNTHASE</i>	85
5.2	<i>LOSS OF THE CHLOROPLAST ATP SYNTHASE CAUSES HIGH NON-PHOTOCHEMICAL QUENCHING</i>	86
5.3	<i>POST-ILLUMINATION FLUORESCENCE INCREASE IS DUE TO RELAXATION OF THE THYLAKOID PROTON GRADIENT</i>	87
5.4	<i>PHOTOPROTECTIVE ROLE OF qE</i>	88
5.5	<i>UP-REGULATION OF NUCLEAR PHOTOSYNTHETIC GENE EXPRESSION IN <i>DPA1</i></i>	89
5.6	<i>ATPC2 IN ARABIDOPSIS AND HIGHER PLANTS</i>	90
5.7	<i>IS ATPC2 A FUNCTIONAL γ SUBUNIT?</i>	90
5.8	<i>REGULATION OF ATPC1 AND ATPC2 EXPRESSION</i>	92
5.9	<i>IN VIVO ANALYSIS OF ATP SYNTHASE THIOL MODULATION</i>	95
5.10	<i>EFFICIENT IN VITRO REGENERATION FROM COTYLEDON PROTOPLASTS OF <i>ARABIDOPSIS THALIANA</i></i>	96
5.11	<i>DEVELOPMENT OF <i>SUL</i> AS A SELECTABLE MARKER</i>	97
6	SUMMARY	101
	LITERATURE	103
	ACKNOWLEDGEMENTS	114
	CURRICULUM VITAE	116

ABBREVIATIONS

μE	microeinstein (1 E = 1 mol of photons)
Å	Ångstrom
ATP	adenosine 5'-triphosphate
bp	base pairs
BAP	6-benzylaminopurine
BSA	bovine serum albumin
cDNA	complementary DNA
Ci	Curie
cpm	counts per minute
Cyt _{b₆f}	cytochrome <i>b₆f</i> complex
DNA	deoxyribonucleic acid
DTT	1,4-dithiothreitol
dNTPs	deoxynucleoside triphosphates
EDTA	ethylenediaminetetraacetic acid
EGTA	ethylene glycol-bis(2-aminoethylether)- <i>N,N,N',N'</i> -tetraacetic acid
EMS	ethyl methanesulfonate
ESTs	expressed sequence tags
FTR	ferredoxin-thioredoxin reductase
g	gravity force, gramme
GFP	green fluorescent protein
GTP	guanosine 5'-triphosphate
hcf	high chlorophyll fluorescence
IAA	indole-3-acetic acid
HEPES	N-[2-Hydroxyethyl]piperazine-N'-[2-ethanesulfonic acid]
kb	kilobases
kDa	kilodalton
LHCI	chlorophyll-binding PSI light-harvesting complex
Mb	megabases
MES	2-Morpholinoethanesulfonic acid
MOPS	3-[N-Morpholino]propanesulfonic acid
mRNA	messenger RNA

NADP ⁺	nicotinic adenine dinucleotide phosphate
NPQ	non-photochemical chlorophyll <i>a</i> fluorescence quenching
P700	PSI primary electron donor chlorophyll <i>a</i>
PAM	pulse amplitude–modulated fluorometer
PCR	polymerase chain reaction
PEG	polyethylene glycol
PSI	photosystem I
PSII	photosystem II
PVDF	polyvinylidene difluoride
qE	energy-dependent chlorophyll <i>a</i> fluorescence quenching
qP	photochemical chlorophyll <i>a</i> fluorescence quenching
rbcS	Rubisco small subunit
RNA	ribonucleic acid
rpm	revolutions per minute
rRNA	ribosomal RNA
RT-PCR	reverse transcription PCR
SD	standard deviation
SDS	sodium dodecyl sulfate
SDS-PAGE	SDS-polyacrylamide gel electrophoresis
SSLP	simple sequence length polymorphism
Suc	sucrose
TAL	thin alginate layer
T-DNA	transferred DNA
TP	transit peptide
Tricine	N-Tris-(hydroxymethyl)-methylglycine
Tris	Tris-(hydroxymethyl)-aminomethane
tRNA	transfer RNA
Tween	polyoxyethylenesorbitan monolaurate
U	unit, enzyme activity
UTR	untranslated region
v/v	volume per volume
w/v	weight per volume
X-Gluc	5-bromo-4-chloro-3-indolyl-beta-D-glucuronic acid

1 INTRODUCTION

1.1 THYLAKOID MEMBRANE PHOTOSYNTHETIC COMPLEXES IN HIGHER PLANTS

Photosynthesis is a physicochemical process by which photosynthetic organisms use sunlight energy to drive the synthesis of organic compounds. Photosynthesis is carried out by various organisms ranging from prokaryotes to higher plants. In higher plants the entire enzymatic machinery required for photosynthesis is located in highly organized, chlorophyll-containing organelles, the chloroplasts. The principal structural units of the chloroplast are thylakoid membranes, flattened vesicles consisting of approximately 50% of each lipid and protein. The major photosynthetic proteins are organized in multi-subunit protein complexes which span the lipid bilayer and are associated with both peripheral and soluble polypeptides in stroma and lumen, respectively. The protein complexes are designated photosystem II (PSII) with the water oxidation system, photosystem I (PSI), antenna light harvesting complexes (LHCI and LHCII) associated with both photosystems, cytochrome *b₆f* complex, ATP synthase and NAD(P)H dehydrogenase (reviewed in Wollman *et al.*, 1999; Herrmann and Westhoff, 2001), (Fig. 1.1).

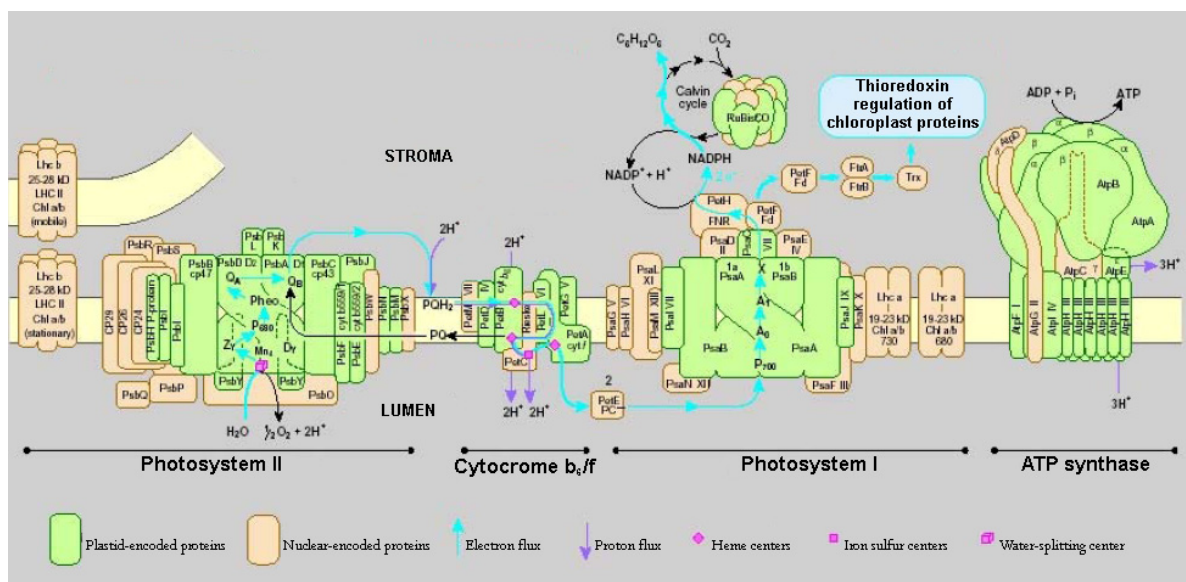


Figure 1.1. Scheme of the thylakoid membrane system. The four major complexes are shown, while a fifth minor abundant complex, the NADH-dehydrogenase complex, is not shown (Race *et al.*, 1999).

These assemblies catalyze the photosynthetic light reaction, i.e. they utilize light energy to drive an electron transport from water to NADP^+ in concert with coupled proton translocation across the thylakoid membrane that generates a proton motive force for the synthesis of ATP.

1.2 ATP SYNTHASE: STRUCTURE, FUNCTION AND REGULATION

The chloroplast ATP synthase belongs to the family of F-type ATPases that are also present in bacteria and mitochondria (Nelson, 1992). It generates ATP from ADP and inorganic phosphate (photophosphorylation) using energy derived from a *trans*-thylakoid electrochemical proton gradient.

The basic organization, structure, and composition of this protein complex have been extensively investigated at the eubacterial level as well as in mitochondria and plastids, and it was found to be highly conserved (Strotmann *et al.*, 1998, Groth and Pohl, 2001). The plastid ATP synthase complex consists of nine different subunits. Four of them are localized in the membrane integral CF_o subcomplex (subunits I, II, III, and IV₁₄ encoded by the genes *atpF*, *atpG*, *AtpH* and *atpI*, respectively) which is responsible for proton translocation. The other five subunits constitute the extrinsic CF₁ subcomplex (α_3 , β_3 , γ , δ , and ϵ , encoded by the genes *atpA*, *atpB*, *atpC*, *atpD* and *atpE*) in which ATP is synthesized or hydrolyzed (Groth and Strotmann, 1999). In purple bacteria the genes of both subcomplexes are organized in two separate operons, thus suggesting that the enzyme evolutionary derived from a proton channel (Fo) and an ATPase with ATP hydrolysis activity (F₁) (Falk and Walker, 1988). The $\alpha_3\beta_3\gamma$ subcomplex from F₁ is the minimum core complex that maintains the feature as an ATPase. In *Chlamydomonas* the ATP synthase genes are spread over the entire chloroplast genome. In higher plants *atpC*, *atpD* and *atpG* reside in the nucleus and regulatory mechanisms co-ordinate the expression of the CF_oCF₁ genes. These nuclear genes are expressed synchronously in response to light, to organ specific factors and plastid derived signals (Bolle *et al.*, 1996).

The organization of the genes also reflects a possible mechanism of assembly. The bacterial Fo and F₁ are accumulated independently and then associate to the membrane to assemble a

functional complex (Klionsky and Simoni, 1985). However, only little is known about the assembly of the chloroplast enzyme. In *Chlamydomonas* neither CF_o nor CF₁ is assembled, although the unimpaired polypeptides are synthesized, if one of the nine subunits is missing (Strotmann *et al.*, 1998). The supramolecular organization of the ATP synthase has been resolved by x-ray crystallography (Abrahams *et al.*, 1994, Stock *et al.*, 1999, Menz *et al.*, 2001). From a mechanical point of view the enzyme is represented as an assembly of a stator and a rotor portion (Fig. 1.2). The stator is composed of the F_o subunits a, b, b', and the F₁ subunits α , β and δ . The rotor comprises F₁ subunits γ and ϵ and the 10 - 12 subunits of F_o subunits c (reviewed in Junge, 2004).

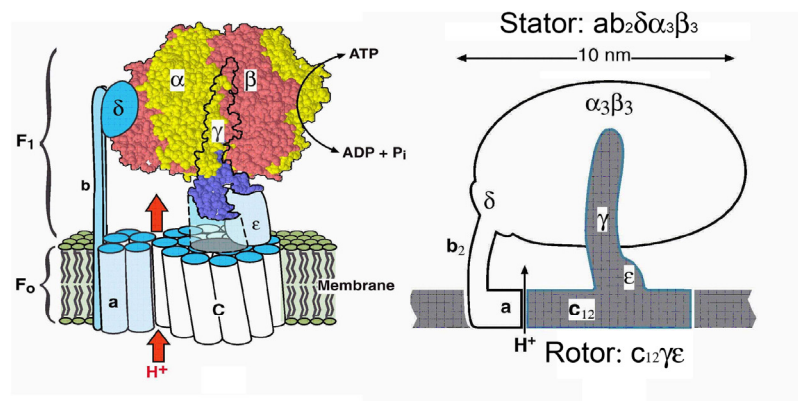


Figure 1.2. *E. coli* ATP synthase composition. The F₁ domain is made up of five subunits with the stoichiometry $\alpha_3\beta_3\gamma\delta\epsilon$. The F_o comprises a, b, b' and the ring of 10 - 12 c subunits (14 in chloroplast ATP synthase from spinach). From a functional point of view the subunits are organized in a stator: $abb'\delta\alpha_3\beta_3$ and a rotor $c_{10-12}\gamma\epsilon$ (Oster and Wang, 1999)

The catalytic sites reside in the β subunits at the α/β subunit interface which can adopt three distinct nucleotide binding conformations, empty site, ADP/Pi binding site and ATP binding site. The central γ subunit rotates within the $\alpha\beta$ hexamer, and drives the enzyme through three successive configurations that are required for ATP synthesis. The membrane-embedded ring, comprised of 10 - 14 identical subunits c (Seelert *et al.*, 2000), works as a turbine powered by protons, converting electrochemical energy into chemical energy stored in ATP (Arechaga and Jones, 2001).

The proton gradient in addition of being the driving force for ATP synthesis is also a kinetic factor. Membrane energization causes a hidden disulfide bridge of the γ subunit to become accessible and reduced. Upon reduction of two Cys residues, the activation profile of ATP synthase is shifted towards lower proton gradients (Ketcham *et al.*, 1984, Junesch and Gräber, 1987). This is why only chloroplast CF₀CF₁ is able of ATP hydrolysis after transition from light to dark, until a critical ADP/ATP ratio is reached and ADP, tightly bound, deactivates the enzyme. An additional regulation is due to the ϵ subunit which acts as an intrinsic inhibitor of CF₁. It was shown that the affinity of ϵ to the γ subunit depends on the redox state of the γ subunit (Hisabori *et al.*, 1998). The ϵ subunit did not inhibit the ATPase activity of the complex which contained oxidized γ subunit. It was suggested that the region adjacent to the Cys bridge is responsible for the interaction with the ϵ subunit and that the conformational change caused by the Cys bridge formation directly affects the affinity between the two subunits.

1.3 ATP SYNTHASE γ SUBUNIT

1.3.1 REDOX REGULATION

The γ subunit is responsible for the so-called thiol- or redox-modulation which is only observed in chloroplast CF₁ (Nalin and Mc Carty, 1984). The structural basis of the regulation is assigned to a sequence of nine amino acid residues containing two Cys residues able to form an intra-peptide disulfide bond upon reduction. *In vivo* the natural reductant is thioredoxin-*f* which is itself reduced by electrons supplied by the photosystems (Schwarz *et al.*, 1997). The 35 amino acid residues including the two cysteins (Cys199 - Cys205, numbering in *Arabidopsis*) are present only in higher plants and green algae such as *Chlamydomonas reinhardtii* (Ross *et al.*, 1995). In cyanobacteria 9 amino acids including the two critical cysteins are missing (Fig. 1.3). The thiol modulation could be induced upon introduction of the 2 cysteins in the cyanobacterial γ subunit (Werner-Grune *et al.*, 1994).

Although many enzyme activities are regulated by thioredoxins in the chloroplast, the molecular mechanism of such regulation remains unclear. In order to understand the redox regulation of CF₁ γ subunit, lacking three dimensional structure information of the regulatory region, the entire or part of the CF₁ γ subunit were combined with the rest of the

enzyme complex from prokaryotic species. More often the redox modulation was tested on the ATP hydrolysis activity of purified chimeric $\alpha_3\beta_3\gamma$ complex, also by means of different mutations introduced into the γ regulatory region (Hisabori *et al.*, 1997, Hisabori *et al.*, 1998, Konno *et al.*, 2000, Bald *et al.*, 2001, Ueoka-Nakanishi *et al.*, 2004).



Figure 1.3. Sequence alignment of γ subunits from different organisms: higher plants *A. thaliana* (AtpC1 and AtpC2), *N. tabacum*, *O. sativa*, the unicellular algae *C. reinhardtii*, prokaryotic *E. coli* and photosynthetic bacteria *Nostoc*. Conserved residues are shadowed in grey, identical in black and similar ones in light grey. The dashes indicate the gap of 35 and 9 amino acids comprising the regulatory region or only the two Cys that are missing in *E. coli* and cyanobacteria, respectively.

1.3.2 *ATPC1 VERSUS ATPC2*

In *Arabidopsis* two genes, *atpC1* and *atpC2* (accession numbers M61741 and J05761), located on chromosomes 4 and 1, respectively, encode the plastid γ subunit (Inhoara *et al.*, 2001, Legen *et al.*, 2001). The similarity of the AtpC subunits from different plants species and AtpC1 in *Arabidopsis* is about 88 %, while it drops to 70 - 74% in AtpC2. The two AtpC proteins in *Arabidopsis* share 73% sequence similarity. Moreover, *atpC1* is expressed at much higher level than *atpC2* in plants grown under continuous illumination (Inhoara *et al.*, 2001). AtpC2, as all other known plant γ subunits, contains the domain responsible for the redox regulation of the enzyme (Fig. 1.3). This raises the intriguing question about the role(s) of the two *atpC* gene copies in *Arabidopsis* and whether the two genes possess distinct functions. The two *atpC* genes are not conserved in the amino-terminal part of the transit peptide and are not found in duplicated genomic blocks assuming two independent gene transfers to the nucleus (Vision *et al.*, 2002).

1.4 PHOTOCHEMISTRY

Plant photosynthesis is driven primarily by visible light (wavelengths from 400 to 700 nm) that is absorbed by pigment molecules, mainly chlorophyll *a*, *b* and carotenoids, associated to the two photosystems. Photochemistry in photosystem II is initiated by the charge separation between P680 and pheophytin, generating P680⁺/Pheo⁻. Subsequent to excitation by light electron transport is energetically downhill (from lower to higher redox potential) from the reduced pheophytin, through plastoquinone, the cytochrome *b_f* complex and plastocyanine to the photosystem I reaction centre P700. The oxidized reaction center P680⁺ can oxidize water, resulting in the release of O₂ into the atmosphere through the water splitting complex. From photosystem I electrons are transferred to NADP⁺ by intermediate ferredoxin, a small 2Fe2S protein, and ferredoxin-NADP oxidoreductase. The downhill flow of electrons provides free energy for the generation of a proton chemiosmotic gradient. The conversion of the proton electrochemical energy into chemical free energy is accomplished by the ATP synthase which catalyzes the formation of ATP by the addition of inorganic phosphate (P_i) to ADP, as outlined above.

1.4.1 NON-PHOTOCHEMICAL QUENCHING - NPQ

A singlet-state excitation of chlorophyll *a* molecule (¹Chl*) which drives photochemistry may show alternative fates. It can re-emit the energy as fluorescence, can be de-excited by a thermal dissipation process or can decay via the triplet state. While the fluorescence yield is generally low, under light excess conditions the triplet pathway can be as significant as well as harmful. The chlorophyll triplet can transfer energy to ground-state oxygen, thus generating singlet oxygen, an extremely damaging reactive oxygen species (Müller *et al.*, 2001).

Non-photochemical quenching (NPQ) designates protective mechanisms that quench singlet-excited chlorophylls and harmlessly dissipate excess excitation energy as heat. NPQ can be divided into at least three different components according to their relaxation kinetics in darkness:

- ✓ qE, energy dependent quenching, relaxes within seconds to minutes;

- ✓ qT, state transition quenching, relaxes within minutes and is more relevant for algae than for plants;
- ✓ qI, photoinhibitory quenching, shows the slowest relaxation and is related to photoinhibition of photosynthesis.

qE is considered the most important component of photoprotection in higher plants (review by Holt *et al.*, 2004).

1.4.2 THE CENTRAL ROLE OF PSBS FOR qE

qE, which results in the thermal dissipation of excess absorbed light energy in the light-harvesting antenna of PSII, is induced by a low thylakoid lumen pH that is generated by the photosynthetic electron transport. The low thylakoid lumen pH acts as a signal of excess light and plays a crucial role in activating the plant response. Under conditions of low lumen pH the violaxanthin de-epoxidase is activated, thus leading to the conversion of violaxanthin to antheraxanthin and zeaxanthin in a process known as xanthophyll cycle (Demming-Adams, 1990). Although xanthophylls are necessary for qE, they have an additional photoprotective role in longer-term high light protecting the thylakoid membrane against photooxidative damage.

The second role of low thylakoid lumen pH is to drive the protonation of several PSII proteins involved in qE. One of these proteins, PsbS, proved to be essential for plants to perform qE (Li *et al.*, 2000). PsbS was discovered over ten years ago as 22 kDa protein in PSII preparations (Wedel *et al.*, 1992), although its exact location is yet unknown. Also the biophysical mechanism of qE, whether zeaxanthin is directly de-exciting $^1\text{Chl}^*$ or acting indirectly as allosteric regulators of the LHCS, and how PsbS is participating remain enigmatic (Niyogi *et al.*, 2005).

1.5 TOWARDS ORGANELLE TRANSFORMATION IN *ARABIDOPSIS THALIANA*

The genetic information of plants is localized in three cellular compartments: the nucleus, the mitochondria and the plastids. Plastids are plant cellular organelles with their own genome and transcription-translation machinery. Most plastid proteins are encoded in the

nuclear genome, translated in the cytoplasm and imported into the plastids; however, many proteins comprising the photosynthetic complexes are encoded by plastid genes.

Chlamydomonas reinhardtii was the first species where plastid transformation was successfully achieved (Boynton *et al.*, 1988). In higher plants integration of foreign DNA into the plastome was performed first in tobacco (Svab *et al.*, 1990), which until now is the only species routinely transformed at high efficiency and three other *Solanaceae* species: *Nicotiana plumbaginifolia* (O'Neil *et al.*, 1993), potato (Sidorov *et al.*, 1999) and tomato (Ruf *et al.*, 2001). Plastid transformation in *Arabidopsis* (Sikdar *et al.*, 1998), the related *Brassica napus* (Hou *et al.*, 2003) and rice (Khan and Maliga, 1999) was reported but no fertile progeny or only low efficiency were obtained.

1.5.1 *ARABIDOPSIS THALIANA*: A MODEL FOR HIGHER PLANTS

In the last decade, a period of intense molecular and genetic research, *Arabidopsis thaliana* has become a very popular model plant for biological studies of flowering plants. Its small size, a short life cycle (6 - 8 weeks), the ability to self-fertilize and to produce a large number of seeds make possible easy cultivation relatively large progenies in restricted space and time.

Arabidopsis was the first plant species chosen for complete sequencing of its (relatively small) nuclear genome with five chromosomes comprising 125 Mb. The organelle genomes, plastome and chondriome, have also been completely sequenced (Arabidopsis Genome Initiative, 2000).

In an approach of reverse genetic studies, T-DNA insertional mutagenesis is the main technology for a high throughput analysis of the whole nuclear genome. A large number of knock out mutant collections has been generated (Feldmann, 1991; Martienssen, 1998; Krysan *et al.*, 1999; Szabados *et al.*, 2002; Alonso *et al.*, 2003; Kuromori *et al.*, 2004) and many sequenced T-DNA insertions are accessible (<http://www.Arabidopsis.org/links/insertion.html>). In addition, the TILLING (Targeting Induced Local Lesions in Genomes) strategy, based on production of allelic series of induced point mutations, provides a

complementary tool for the ultimate goal of determining the function of each gene in *Arabidopsis* (Till *et al.*, 2003). Improved techniques for *Agrobacterium*-mediated nuclear transformation (Bechtold and Pelletier, 1998; Clough and Bent, 1998) and selection of transformants (Hadi *et al.*, 2002) allow functional complementation of a mutation with a wild-type genomic DNA or cDNA.

1.5.2 PLASTID TRANSFORMATION

In basic science, the possibility to transform the chloroplast was of particular interest as a tool to study plastid encoded gene function, to disclose plastid molecular processes like RNA transcription or RNA editing and to address evolutionary questions on the nuclear gene transfer (reviewed by Maliga, 2003). *Nicotiana tabacum* is actually the higher plant species used for these purposes. *Arabidopsis thaliana*, in fact, even being established as the higher plant model for molecular biology studies, cannot compete with the well established *in vitro* culture and plastid transformation techniques developed for tobacco. The singular report on plastid transformation in *Arabidopsis* (Sikdar S.R. *et al.*, 1998) could only provide evidence for sterile transplastomic regenerates with relatively low transformation efficiency. Essential steps that need to be optimized for chloroplast transformation in a new plants species are efficient regeneration systems, and an appropriate selectable marker.

1.5.2.1 Sulfonamide resistance gene, a selectable marker for plant transformation

Sulfonamides are anti-microbial compounds which inhibit the folic acid biosynthesis pathway. Sulfonamides are *p*-aminobenzoic acid (*p*-ABA) analogues that are recognized by dihydropteroate synthase (DHPS) as alternate substrate (Fig. 1.4A). Plants as well as bacteria harbour the folic acid biosynthetic pathway and thus are sensitive to sulfonamides. Resistance to sulfonamides is conferred to bacteria by various R plasmids containing a sulfonamide resistance gene (*sul*) which encodes a mutated DHPS that is insensitive to inhibition by sulfonamides (Wise and Abou-Donia, 1975). The *sul* gene fused to the Rubisco transit peptide for chloroplast targeting could be used for efficient selection of transformed shoots on tobacco leaf explants after transfection with *Agrobacterium tumefaciens* (Guerineau *et al.*, 1990). The same chimeric gene has also been routinely used

as a selectable marker for *Arabidopsis* nuclear transformation (Amann *et al.*, 2004, Dal Bosco *et al.*, 2004, Lezhneva *et al.*, 2004).

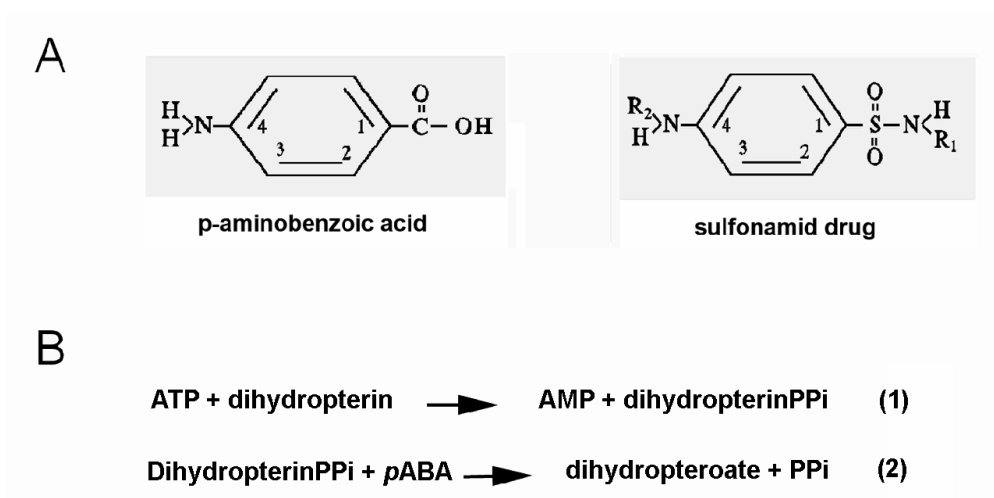


Figure 1.4. **A.** Chemical structure of DHPS substrates: *p*-aminobenzoic acid (*p*-ABA) and the inhibitor, *p*-ABA analogue, sulfonamide. **B.** First two reactions of the tetrahydrofolate biosynthetic pathway catalyzed by HPPK (1) and DHPS (2).

1.5.2.2 Folic acid biosynthesis in higher plants

A number of pathways such as those involved in the metabolisms of methionine, serine, glycine, purine or thymidylate in which one-carbon reactions occur, are dependent on endogenous supply of reduced folate cofactors. Plants, fungi and micro-organisms, in contrast to animals, are able to synthesize tetrahydrofolate (H₄F) *de novo* (Hanson and Roje, 2001).

Folates are tripartite molecules comprising a pterin moiety, a *p*-aminobenzoate (*p*-ABA) unit, and a glutamate chain with one to eight residues (Fig. 1.5A). Dihydropterin is synthesized from GTP in three steps. None of the enzymes required for this synthesis have predicted targeting peptides, suggesting that they are located in the cytosol. *p*-ABA is formed from chorismate in three steps. In higher plants, the two proteins catalyzing these reactions have been proved to be localized in the chloroplast (Basset *et al.*, 2004). Dihydropterin and *p*-ABA together with glutamate are combined in mitochondria in five

reactions. This requires the sequential operation of five enzymes: a dihydropterin pyrophosphokinase (HPPK), a dihydropteroate synthase (DHPS), a dihydrofolate synthetase (DHFS), a dihydrofolate reductase (DHFR), and a folylpolyglutamate synthetase (FPGS) (Fig. 1.5B).

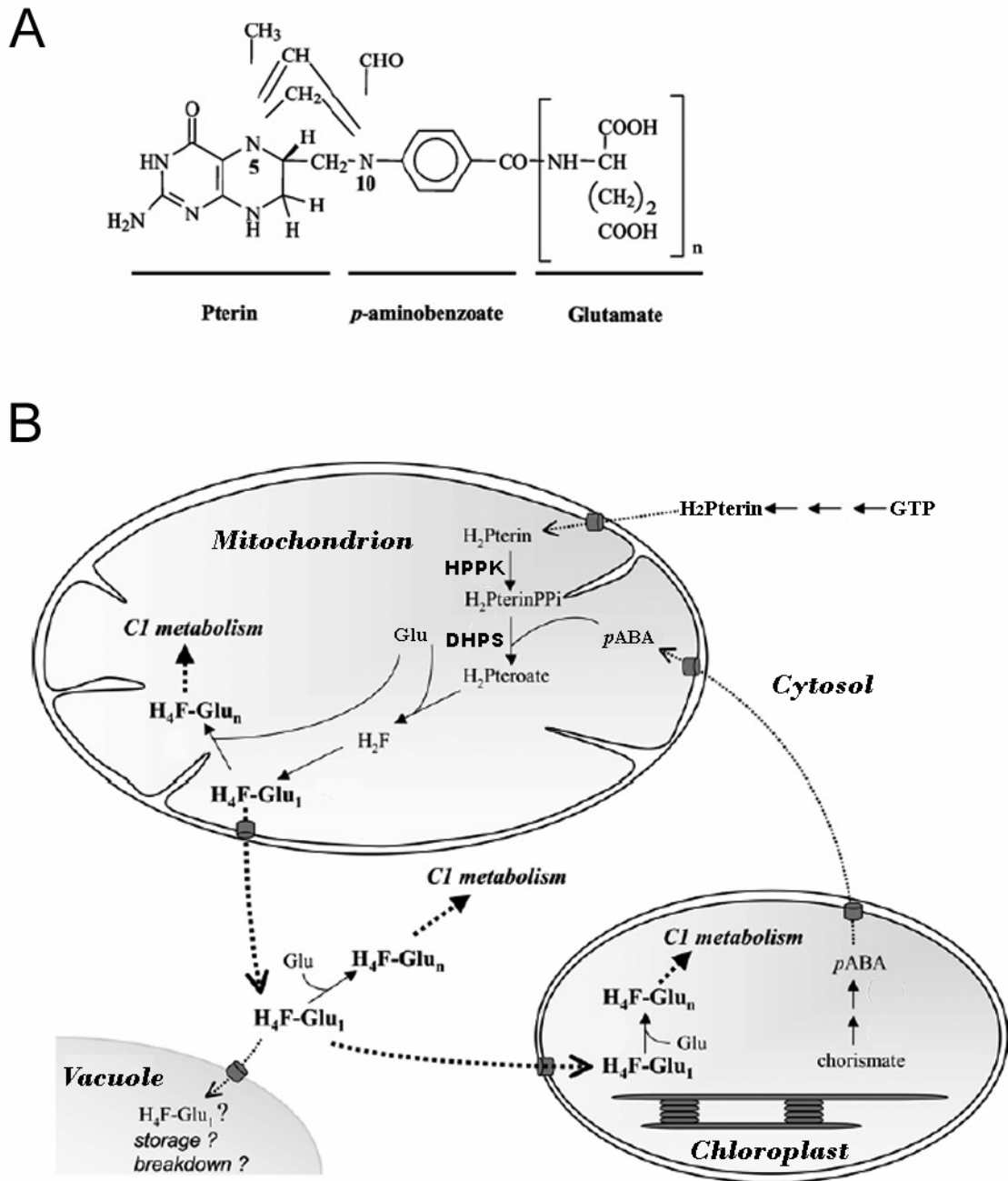


Figure 1.5. A. Structure of tetrahydrofolate underlying the tripartite structure composed of pterin, *p*-ABA and glutamate. B. Subcellular compartmentation of tetrahydrofolate synthesis in plant cells. Enzymes involved in tetrahydrofolate synthesis are indicated by plane arrows.

In higher plants, the first two steps (Fig 1.4B) are catalyzed by a single bifunctional enzyme, while in bacteria the two functions are spread in two separate proteins (Mouillon *et al.*, 2002). The DHPS, whether belonging to the mono- or to the bi-functional enzyme, is the target of antimicrobial sulfonamide drugs.

Plant food is a major source of folates for animals. Because folate deficiency is a worldwide health problem for humans there is much interest in engineering plants with enhanced folate content. In order to achieve this aim, at first the plant folate synthesis pathway has to be understood. In the last decade the knowledge of the structural organization, subcellular distribution and detailed kinetic properties of plant enzymes involved in tetrahydrofolate pathway increased greatly. A scheme of the current knowledge reviewed by Sahr *et al.* (2005) is shown in (Fig. 1.5B). The HPPK-DHPS enzyme, the target of sulfonamide drugs is located in the mitochondria. Surprisingly, its bacterial ortholog fused to the Rubisco small subunit transit peptide for targeting into chloroplasts could provide sulfonamide resistance in plants (Guerineau *et al.*, 1990).

1.6 GOALS OF THE PROJECT

The aim of this work was to extend knowledge about bioenergetic and physiological aspects of the thylakoid membrane complex ATP synthase in *A. thaliana*. The ATP synthase mutant *dpa1* was identified, which was shown to contain an insertion into the nuclear *atpC1* gene encoding the chloroplast γ subunit. This mutant was used (i) to characterise the assembly of the chloroplast ATP synthase complex, especially in functional correlation to photosynthetic processes; (ii) to study the function of a second gene, *atpC2*, encoding a putative γ subunit; (iii) to perform mutational studies on the γ subunit in order to investigate the regulation of the redox modulation *in vivo*.

Furthermore conditions for plastid transformation of *A. thaliana* were optimized. This included establishment of a protocol for efficient plant regeneration *in vitro* and identification of a suitable selection marker.

2 MATERIALS

2.1 CHEMICALS, RADIOACTIVE SUBSTANCES, WORKING MATERIAL

Chemicals used in this work were usually of p.a. quality and, if not mentioned, were purchased from the following companies: Applichem (Darmstadt, Germany), Biozym (Oldendorf, Germany), Fluka (Steinheim, Germany), ICN Biomedicals GmbH (Eschwege, Germany), Merck (Darmstadt, Germany), Pharmacia (Uppsala, Sweden), Roth (Karlsruhe, Germany), Serva (Heidelberg, Germany), Sigma-Aldrich Chemie GmbH (Taufkirchen, Germany), and USB (Cleveland, USA).

Radioactive nucleotides and [³⁵S]-methionine were purchased from Amersham Biosciences Europe GmbH (Freiburg, Germany).

Other materials were obtained from Biomol (Hamburg, Germany), Eppendorf (Hamburg, Germany), Greiner Bio-One GmbH (Frickenhausen, Germany), Millipore (Eschborn, Germany), Pall Bio Support Division (Dreieich, Germany), Qiagen (Hilden, Germany), and Schleicher and Schüll (Dassel, Germany). The manufacturers of commercial devices are mentioned in the text.

2.2 PLANT MATERIAL

The *dpa1* line, accession Wassilewskija, was originally identified in a T-DNA collection (Feldmann, 1991) obtained from the Arabidopsis Biological Resource Centre (Ohio State University, Columbus, USA). The mutation was propagated by heterozygous offspring. Homozygous *dpa1* plants were grown on sugar supplemented MS media at constant moderate light conditions ($10 \mu\text{E m}^{-2}\text{s}^{-1}$) and 21°C.

The *atpC2* knock-out mutant, accession Columbia, was obtained from the NASC T-DNA collection.

PsbS mutant plants were kindly provided by Dr. D. Leister, Max-Planck-Institute, Köln.

Protoplast regeneration from *Arabidopsis thaliana* cotyledons was performed on three wild type accessions: Columbia, Wassijleskja and C24. The seeds were placed on SCA medium and germinated at 25°C in continuous light. Prior to removing the cotyledons for protoplast isolation the seedling were subjected to cold treatment at +4°C for 24 h.

In vitro regeneration and plastid transformation experiments were performed with tobacco plants (*Nicotiana tabacum* L. cv. Petit Havana) grown aseptically under standard light conditions of 100 $\mu\text{E m}^{-2} \text{s}^{-1}$, 16/8 h light/dark cycles, and 25°C.

2.3 BACTERIAL STRAINS

<i>E. coli</i> DH5 α	(Bethesda Res. Lab., 1986)
<i>E. coli</i> XL10-Gold	Stratagene, Heidelberg
<i>Agrobacterium tumefaciens</i> GV3101 (pMP90RK)	(Koncz <i>et al.</i> , 1994)

2.4 PLASMIDS

2.4.1 CLONING VECTORS

pPCR-Script Amp SK(+) cloning vector	Stratagene, Heidelberg
pUC19	
pDONOR 207	Invitrogen, Karlsruhe, Germany
pBlueScript (SK- and SK+)	Stratagene, La Jolla, USA
puC19- <i>aadA</i>	(Regel <i>et al.</i> , 2001)
EcoRV- <i>aadA</i>	(Regel <i>et al.</i> , 2001)

2.4.2 EXPRESSION VECTORS

pOL-GFP	I. Small (INRA, Evry, France)
pGFP-2	

2.4.3 BINARY VECTORS

pSEX001-VS	(Reiss <i>et al.</i> , 1996)
------------	------------------------------

pPEX001
pKGWFS7,0

(Reiss *et al.*, 1996)
Invitrogen, Karlsruhe, Germany

2.5 OLIGONUCLEOTIDES

All oligonucleotides used for PCR, RT-PCR, cloning, or sequence analyses were obtained from MWG Biotech (Ebersberg, Germany), except the ones used for *atpC1* and *atpC2* promoter cloning which were provided by Invitrogen (Karlsruhe, Germany).

Table 2.1 Oligonucleotide primers used for amplification of genes and quantification of mRNAs

EXPERIMENT	TEMPLATE	PRIMER NAME	PRIMER SEQUENCE (5'→3')	FIG.
PCR analysis	<i>atpC1</i> , genomic DNA	AtpC1-prom	-CGAACCATCCACTAATACCCAGCC	4.2A, B
		AtpC1-5'-for	-CGTCTCTTCGTGAGCTCAGAGACCGTATCG	
		Atpc1-3'-rev	-GGTGATAAAGGCAGTAGCGTGTGGATCACG	
		35S-prom	-GCCATCGTTGAAGATGCCTCTGCCG	
		TDNA-LB	-CACATCATCTCATTGATGCTTGG	
		LBb1	-TAGCATCTGAATTCATAACCAATCTCGATACAC	
		AtpC2-rev-kpn	-CTAAGACTCGAAGAGCTTA	-
Promoter cloning	<i>atpC1</i> promoter	atpC1-prom-for	-GGGGACAAGTTTGTACAAAAAAGCAGGCTYY TTTCGTTCTAATTTCTAACCAAATATT	-
		atpC1-prom-rev	-GGGGACCACCTTTGTACAAGAAAGCTGGGTYT GTTGTTTGTTCAGACAGTGTTT	
	<i>atpC2</i> promoter	atpC2-prom -for	-GGGGACAAGTTTGTACAAAAAAGCAGGCTYYA AGACGGCGGCATTTTGAGAGC	4.20
		atpC2-prom-rev	-GGGGACCACCTTTGTACAAGAAAGCTGGGTYTTT GGGAAAGAAGACCCTGA	
<i>AtpC1/ AtpC1MOD</i> cloning	<i>atpC1</i>	atpC1-sma-for	-AACAAAAAATGGCTTGCTCTAATCTAACA	4.11A, B
AtpC1MOD cloning		atpC1-xba-rev	-AAGAGGGTTCTAGACAAATCAAACCTGTGC-	
		atpC1-mod-rev	-CCCTAGTTTTGTCGTTAACCTGAAAAACAGAA CTTCCGC	
		atpC1-mod-for	-GTTTTTCAGGTTAACGACAAAACCTAGGGAAATT	
Sequencing	pPCRScript Amp SK(+)	T7	-GTAATACGACTCACTATAC	-
		T3	-AATTAACCCTCACTAAAGGG	

	pKGWFS7,0	M13-for	-GTAAAACGACGGCCAGT	-	
		M13-rev	-CAGGAAACAGCTATGAC		
	<i>atpC1</i> promoter	atpC1prom-int-for	-TCCTTTGTCAGATATTTTCTCTCG	-	
	<i>atpC2</i> promoter	atpC2prom-int-for	-GTATTCATTTGTATTTAGTAACCCG		
N-term cloning	<i>atpC2</i>	atpC2-rev-kpn	-GGTTAATTGAGTAGAGAATCTCCACAAGAG	4.15	
<i>AtpC2</i> cloning		atpC2-sma-for	-AACAAAAAAATGACAGGTTTCGATCTCG		
		atpC2-xba-rev	-CACAGCTGTAGTTTCTACCTAAGACTCTCG		
Real time RT-PCR	<i>atpC1</i>	atpC1-18C-for	-CGTCTCTTCGTGAGCTCAGAGACCGTATCGA	4.16	
		atpC1-21H-rev	-GGTTAAGGGAACATCGACATCATCGG		
	<i>atpC2</i>	atpC2-69I-rev	-CCAGTAACAACAACCAAGCAACTCTC		
		atpC2-G16-for	-CGAATCGACAGTGTGAAGAATACCCAG		
	<i>Ycf-3</i>	ycf3-f	-GCTATGCGACTAGAAAATTGACCCC	-	
		ycf3-r	-CTCCTTGTTGAATGGCCTGTTCT		
<i>Dpa1</i> mapping	genomic DNA	Cer452226-marker	-CAGTCGAATCTTGATGACCGTCGATGATG -GTTTCGTCGAGAATCAGAGTGGCTC	-	
<i>Sul-gfp</i> fusion cloning	pSeX001	TPrbc-sma-for	-AGCTTTGCAATTCATACAGA	4.25	
		PhyBlink-rev	-GCTTATCGATACCTCCACCTCCGGCATGATCTA ACCTTCGGTCTC		
	pGFP2	PhyBlink-for	-AGGTGGAGGTATCGATAAGCTTGATCCCATGAG TAAAGGAGAAG		
		GFP-bam-xba-rev	-GGCATGGATGAACTATACAAA		
<i>Sul</i> cloning	pSeX001	5-sul-NcoI	-GCAATGGTGGAAAGAGTAAAGTCCATGGTG	4.27	
		3-sul-HindIII	-GAGAGAGAAAGCTTTGTAGAGAGAGACTGG		
coxIV-TP cloning	Yeast genomic DNA	coxIV-xho-for	-GGGACTCGAGATGTTGTCACCTACGTCAATC	4.29	
		coxIV-rev-xho	-ATACTCGAGGGGTTTTTGCTGAAGCAGATA		
Northern analysis	pZL1 (<i>petC</i> , <i>psbS</i> , <i>lhcB6</i> , <i>psaD1</i>)	pZL1-for	-TAATACGACTCACTATAGGG	-	
		pZL1-rev	-ATTTAGGTGACACTATAG		
	<i>atpC1</i>	atpC121H-rev	-GGTTAAGGGAACATCGACATCATCGG	4.2C	
		atpC158E-for	-ATGGCTTGCTCTAATCTAAC		

2.6 MEDIA

2.6.1 MEDIA FOR BACTERIA

LB medium

10 g/l Bactotryptone
5 g/l yeast extract
5 g/l NaCl
15 g/l agar for solid medium

YEB medium

5 g/l beef extract
5 g/l bacteriological peptone
1 g/l yeast extract
5 g/l sucrose
2 ml 1 M MgCl₂

SOC medium

10g/l bactotriptide
5g/l yeast extract
5g/l NaC
10 mM MgSO₄
10 mM MgCl₂
10mM glucose

pH 7.5 with NaOH

All media containing antibiotics were prepared by adding the antibiotic from stock solutions after sterilization and cooling down to approx. 50°C.

2.6.2 SOLUTIONS AND MEDIA FOR PROTOPLAST AND TISSUE CULTURE

MS-medium:

4.3 g/l MS salts (Murashige and Skoog, 1962)
15 g/l sucrose
2.5 mM MES
KOH, pH 5.7
7g/l agar or 3.5g/l gelrite

Table 2.2 Preplasmolysis and culture media

mg/l	F-PIN ^a	F-PCN ^b	PCA ^c	SCN ^d	SCA ^e	RMOP ^f	SRA ^g
KNO ₃	1012	1012	2527.5	2527.5	2527.5	1900	1900
CaCl ₂ ·2H ₂ O	640	640	450	150	150	440	440
MgSO ₄ ·7H ₂ O	370	370	746	246.5	1140	370	370
KH ₂ PO ₄	170	170				170	170
NaH ₂ PO ₄ ·H ₂ O			150	150	150		
NH ₄ NO ₃						1650	1650
(NH ₄) ₂ SO ₄			134	134	134		
NH ₄ -succinate (mM) ^h	20	20					
EDTA Fe(III) Na Salt	40	40	40	40	40	40	40
KI	0.83	0.83	0.75	0.75	0.75	0.83	0.83
H ₃ BO ₃	6.2	6.2	3	3	3	6.2	6.2
MnSO ₄ ·H ₂ O	22.3	22.3	10	10	10	22.3	22.3
ZnSO ₄ ·7H ₂ O	8.6	8.6	2	2	2	8.6	8.6
Na ₂ MoO ₄ ·2H ₂ O	0.25	0.25	0.25	0.25	0.25	0.25	0.25
CuSO ₄ ·5H ₂ O	0.025	0.025	0.025	0.025	0.025	0.025	0.025
CoCl ₂ ·6H ₂ O	0.025	0.025	0.025	0.025	0.025	0.025	0.025
inositol	200	200	200	100	100	100	50
pyridoxine-HCl	2	2	2	1	1		0.25
thiamin-HCl	1	1	1	10	10	1	0.05
Ca-panthotenate	2	2	2				
Biotin	0.02	0.02	0.02				
nicotinic acid	2	2	2	1	1		0.25
L-glutamine			50				
glycine							1
MES	976	976	976				
sucrose (g)	130	20		20	15	30	15
glucose (g)		65	80				
Agar (g)				8		8	8
Gelrite (g)					2		
casein hydrolysate			100				
coconut water (ml)			20				
BAP	1	1				1	
Kinetin							2
NAA	0.1	0.1	0.5			0.1	0.05
Dicamba			3				

All media were autoclaved, except of media F-PIN, F-PCN and PCA which had to be filter sterilized.

- ^a – Fast Protoplast Incubation Nicotiana (according to Dovzhenko *et al.* 1998)
^b – Fast Protoplast Culture Nicotiana
^c – Protoplast Culture Arabidopsis (according to Dovzhenko *et al.*, 2003)
^d – Shoot Culture Nicotiana
^e – Shoot Culture Arabidopsis
^f – RMOP (according to Svab and Maliga, 1993)
^g – Shoot Regeneration Arabidopsis (Luo and Koop, 1997)
^h – prepared as 2 M stock solution (NH₄Cl 106 g/l, KOH 224 g/l, succinic acid 236 g/l)

Table 2.3 Contents of media for protoplast isolation, transformation, and embedding

	Alg-A ^a	Ca2+-A ^b	MMM ^c	MMC ^d	MSC ^e	PEG ^f	TrafoM ^g
MES	7 mM	10 mM	10	10	10		5
CaCl ₂ ·2H ₂ O		20 mM		20			
Ca(NO ₃) ₂ ·4H ₂ O						67	
MgCl ₂ ·6H ₂ O	20 mM		10		20		15
MgSO ₄ ·7H ₂ O			10				
mannitol	550 mOsm	550 mOsm	550 mOsm	550 mOsm		270	550 mOsm
sucrose					550 mOsm		
PEG 1500 (g/l)						38.461	
alginic acid (g/l)	28						
Agar (g/l)		10					

All media were autoclaved except of PEG solution which had to be filter sterilised.

- ^a – Alginic Acid solution (according to Dovzhenko *et al.* 2003);
^b – Calcium²⁺ Agar medium (according to Dovzhenko *et al.* 1998);
^c – MES Mannitol Magnesium
^d – MES Mannitol Calcium
^e – MES Sucrose Calcium
^f – PEG solution (according to Koop *et al.* 1996);
^g – Transformation medium

2.7 ENZYMES

Restriction enzymes	MBI Fermentas (St. Leon-Rot, Germany)
T4 DNA ligase	GIBCO Life technologies
Alkaline Phosphatase CIP	New England BioLabs
Alkaline Phosphatase SHRIMP	Roche Molecular Biochemicals
Taq polymerase	Quiagen (Hilden; Germany)
<i>Pfu</i> Turbo polymerase	Stratagene (Heidelberg, Germany)
Klenow fragment (exo-)	MBI Fermentas (St. Leon-Rot, Germany)
Reverse transcriptase Super Script II	Invitrogen (Karlsruhe, Germany)

DNase I (RNase-free)

Roche Molecular Biochemicals

Macerozyme R-10

Yakult Pharmaceutical Industry, Japan

Cellulase, Onozuka R-10

Yakult Pharmaceutical Industry, Japan

2.8 ANTIBODIES

Table 2.4 Antisera used for protein identification in Western analysis.

PROTEIN OR PROTEIN COMPLEX	SUBUNIT	SOURCE OF ANTIBODY
Photosystem I	PsaC	R. Herrmann
Photosystem II	LHCII PsbD (D2) PsbO (PSII-O)	R. Berzborn Barbato R. Berzborn
Cytochrome <i>b₆f</i> complex	Cytochrome <i>f</i> (PetA) Cytochrome <i>b₆</i> (PetB) Subunit IV (PetD)	G. Hauska G. Hauska G. Hauska
ATP synthase	CF ₁ α, (AtpA) CF ₁ β, (AtpB) CF ₁ γ1 CF ₁ γ2 CF ₁ δ CF ₁ ε CF _o c (AtpH) CF _o b Cfo b'	R. Berzborn R. Berzborn R. Berzborn Pineda Antibody service (Berlin) R. Berzborn R. Berzborn R. Berzborn R. Berzborn R. Berzborn
DHPS	SUL	Pineda Antibody service (Berlin)

3 METHODS

3.1 BACTERIA GROWTH AND MANIPULATION

3.1.1 CULTIVATION OF BACTERIA

E. coli strains were propagated in LB medium or on LB agar plates at 37°C as described in Sambrook *et al.* (1989). For transformation with plasmids carrying ampicillin resistance, 70 µg/ml ampicillin were added to the medium. For blue-white colour screening 70 µg/ml each of IPTG and X-Gal were added to the LB medium. The *Agrobacterium* GV3101 strain was propagated at 28°C in YEB medium supplemented with 100 µg/ml rifampicin and 25 µg/ml kanamycin. For transformation with binary vectors carrying ampicillin resistance, 100 µg/ml carbenicillin were used.

3.1.2 PREPARATION OF COMPETENT CELLS

E. coli DH5α cells were streaked on LB plates and incubated overnight at 37°C. Single colonies were picked and used for inoculation of 10 ml SOB medium of an overnight culture. 1.5 ml of the overnight culture were added to 30 ml of pre-warmed SOC broth and shaken at 37°C until an absorbance of 0.5 at 600 nm was reached (approximately 90 – 120 min). The culture was then chilled on ice for 10 - 15 min., transferred to sterile round-bottom tubes and centrifuged at low speed (4000 g, 2 min, 4°C). The supernatant was discarded and the cells resuspended in 10 ml ice-cold RF1 buffer (1/3 of starting culture volume). Then, the cells were collected by centrifugation (4000 g, 2 min, 4°C), the supernatant was discarded again and the cells resuspended in 2.5 ml ice-cold RF2 buffer (1/12 of starting culture volume). The suspension was kept on ice for an additional 15 min. Aliquots of 100 µl were prepared, frozen in liquid nitrogen, and stored at –80°C.

<u>RF1 –Medium *</u>		<u>RF2-Medium</u>	
100 mM	RbCl	10 mM	MOPS
50 mM	MnCl ₂ x 4 H ₂ O	10 mM	RbCl
10 mM	CaCl ₂ x 2 H ₂ O	75 mM	CaCl ₂ x 2H ₂ O
15 %(w/v)	glycerol	15 %(w/v)	glycerol
30 mM	potassium acetate	pH 6.8 with NaOH	

* First CaCl₂, glycerol and potassium acetate were mixed, adjust to pH 6,2 with acetic acid, and then the other components were added.

The solutions were sterilized by filtration through 0.22 µm filter.

3.1.3 TRANSFORMATION OF BACTERIA (HEAT SHOCK)

To 100 µl of competent DH5α cells, either 10 - 50 ng of plasmid DNA or 20 µl of ligation mixture were added and the suspension incubated for 30 min on ice. After a heat shock (2 min at 42°C, or 5 min at 37°C) and successive incubation on ice (2 min), 400 µl SOC-medium was added and the bacteria incubated at 37°C for 1 and 1/2 h. The cells were then centrifuged (10,000 g, 1 min, RT) and the supernatant was removed. The cells were resuspended in 100 µl of LB medium and plated onto LB plates containing the desired antibiotics. Plates were incubated overnight at 37°C.

3.2 PLANT GROWTH AND MANIPULATION

3.2.1 SEED STERILIZATION, PLANT GROWTH AND MUTANT SELECTION

Seed sterilization and growth conditions for wild-type and mutant plants were as described in Meurer *et al.* (1996b). For growth on MS-medium, seeds were sterilized with 70% ethanol for 1 min, 5% (w/v) Dimanin C for 10 min. and washed three times, 10 min. each, with sterile water. Seeds generated from plants transformed with *Agrobacteria* were resuspended, after standard sterilization, in 0.1% agar supplied with Claforan 40 mg/l. Seeds were plated on solid MS medium and placed for 2 days at 4°C to synchronize germination.

Seedlings were grown under continuous light (photon flux density of 10 - 50 $\mu\text{E m}^{-2} \text{sec}^{-1}$) and a constant temperature of 21°C. Selection of mutant plants was facilitated by a chlorophyll fluorescence video imaging system (FluorCam690M, Photon Systems Instruments, Brno, Czech Republic). The *dpa1* mutants were readily distinguishable from wild-type plants because of their high non-photochemical quenching of chlorophyll fluorescence.

Propagation of lethal mutants occurred via heterozygous offsprings grown on soil. In all experiments three-week-old plants were used if not differently indicated.

3.2.2 PROTOPLAST ISOLATION

1g each of the enzymes, Cellulase Onozuka R-10 and Macerozyme Onozuka R-10 (Yakult, Japan), were dissolved in 10 ml of MMM medium and filtrated through 0.2 μm sterilising filter. 0.5% or 0.25% of each enzyme were used for removal of cell walls in *Arabidopsis* and tobacco, respectively.

Protoplast isolation, embedding, culture and regeneration solutions and media are presented in Table 2.2 and 2.3.

Plant material for protoplast isolation was cut into small pieces and used for preplasmolysis either in F-PIN medium (leaves, tobacco) or in MMC solution (cotyledons, *Arabidopsis*). Then these media were replaced with fresh ones containing the enzymes in proper concentrations and incubation took place (overnight at 25°C). After filtration through metal sieves with a mesh diameter of 100 μm for tobacco or of 50 μm for *Arabidopsis*, protoplasts were purified and embedded using the TAL technique according to Dovzhenko *et al.* (1998) for tobacco and Dovzhenko *et al.* (2003) for *Arabidopsis*.

3.2.3 PEG TREATMENT OF PROTOPLAST

The PEG method of protoplast treatment for plastid transformation was performed as described by Koop *et al.* (1996).

3.2.4 DNA TRANSFER BY THE BIOLISTIC METHOD

The biolistic method was used for plastid transformation of tobacco leaves. The Biolistic[®] Particle Delivery System, Model PDS-1000/He (Bio-Rad Laboratories, California, USA) was utilized. Gold particles, 60 mg (0.6 μm in diameter, Bio-Rad Laboratories, California, USA), were suspended in 1 ml ethanol (100%), and 36 μl of the mixture were transferred into a new plastic tube. After pelleting by centrifugation for 10 sec at 15,000 g in an Eppendorf centrifuge, 25 μg of DNA dissolved in H_2O (this volume was adjusted with sterile water to 255 μl), 250 μl of 2.5 M CaCl_2 and 50 μl of spermidine (Sigma, St. Louis, USA) were added and mixed. The mixture was incubated on ice for 10 min and centrifuged for 1 min at 12,000 g. After complete removal of the supernatant, the gold colloid was suspended by pipetting and washed twice in 100% ethanol, each for 1 min at 12,000 g. Microprojectiles coated with DNA were resuspended in 72 μl of 100% ethanol and stored on ice prior to bombardment. 5.4 μl were used per bombardment. Petri dishes with the targeted material were placed on the middle shelf, stopping screens and macrocarriers containing microprojectiles coated with DNA were placed in the holder and rupture disks of 900 psi were used.

3.2.5 AGROBACTERIA MEDIATED NUCLEAR TRANSFORMATION OF *ARABIDOPSIS*

Plants of the appropriate genotype were grown in green house conditions. For each transformation 8 pots (diameter 3.5'') containing 15-20 plants were used. After four weeks the emerging bolts were cut off to encourage growth of multiple secondary bolts. Infiltration was performed 7-10 days after clipping. Two days ahead a colony of *Agrobacterium* carrying the appropriate construct was picked and grown in 25 ml (LB + antibiotics) for 24h. This culture was added to 400 ml (LB + antibiotics) the day before infiltration. When the bacterial culture reached the OD600 of 2.0 the cells were harvested by centrifugation (5000 g 10 min at room temperature) and resuspended in 2 volumes infiltration medium. The suspension was transferred in a beaker and the plants were inverted and completely submerged in the medium for few seconds. The pots were then laid on their side into a plastic container and covered. The next day the plants were uncovered and set upright. The plants were further grown until the siliques were very dry and the seeds could be harvested.

Infiltration medium

5% sucrose

0.05% Silvet L-77 (Clough and Bent, 1998)

3.2.6 GUS ASSAY

Seedlings were transferred in tubes and submerged in 3.7% formaldehyde for 10 min in a fixation step. The seedling were further washed twice for 20 min each time in water and incubated in X-Gluc solution over night at 37°C. For an optimal visualization of blue staining the chlorophyll was removed by incubation in 70% ethanol for a few hours.

XGluc Solution

phosphate buffer (Na ₂ HPO ₄ /NaH ₂ PO ₄ , pH 7.0)	100 mM
EDTA	1 mM
potassium hexacyanoferrate (II)	1 mM
potassium hexacyanoferrate (III)	1 mM
Triton X-100	0.3%
X-Gluc*	1 mM

*freshly add from a stock solution of X-Gluc dissolved in DMF and kept at -20°C.

3.3 NUCLEIC ACID MANIPULATION

3.3.1 RAPID ISOLATION OF GENOMIC DNA FOR PCR USE

DNA was isolated from *Arabidopsis* leaves (approx. 0.5 cm²). Plant material was homogenised in 1.5 ml Eppendorf tubes using a mechanical stirrer RW16 basic (Kika Labortechnik, Staufen, Germany) for approx. 5 sec, and immediately afterwards 400 µl extraction buffer was added. After a short vortexing step, the extract was centrifuged for 3 min at 16,000 g at room temperature. 300 µl supernatant were transferred to a new Eppendorf tube and 300 µl isopropanol was added. The mixture was vortexed, incubated at room temperature for 2 min and centrifuged for 5 min at 16,000 g at room temperature or at 4°C. The supernatant was discarded, and the pellet was air-dried then, 200 µl TE buffer

were added. DNA solubilization occurred at 4°C over night or at 37°C for 1 h, without mixing and disturbing the pellet. For PCR amplification 4 µl DNA were used.

Extraction buffer

0.2 M Tris/HCl, pH 7.5

0.25 M NaCl

0.025 M EDTA

0.5%(w/v) SDS

3.3.2 ISOLATION OF TOTAL RNA

Total cellular RNA was isolated from plant tissue using TRIZOL reagent (Invitrogen, Karlsruhe, Germany) following the supplier's protocol. The concentration of isolated RNA was estimated by spectroscopic measurement using a GENEQUANT spectrophotometer. As a quality control of isolated RNA, aliquots (2 µg) were fractionated on formaldehyde-containing denaturing gels with ethidium bromide in the RNA sample to visualize the ribosomal RNA (rRNAs).

3.3.3 ISOLATION OF DNA FOR PCR USE FROM YEAST

DNA was isolated from a fresh yeast plate. A medium size yeast colony was transferred to a 1.5 ml tube containing 30 µl 0.2% SDS. The sample was vortexed for 15 seconds, heated in a hot block at 90°C for 4 min and centrifuged in a microfuge for 1 min at 10,000g. The supernatant (crude DNA) was removed and stored at -20°C or used for PCR amplification.

3.3.4 PLASMID ISOLATION FROM *E. COLI*

Plasmid DNA for cloning or sequencing was isolated using QIAprep Spin Mini or QIAfilter Maxi prep Kit (Qiagen, Hilden, Germany).

3.3.5 ENZYMATIC ASSAYS

3.3.5.1 Restriction analysis of DNA

For restriction, the DNA was incubated for 2 h with an appropriate amount of enzyme in the recommended buffer. Restriction was terminated by incubation of the sample at 65°C for 15 min. For double digestion, if the conditions for the two chosen enzymes were incompatible with each other, the DNA was digested successively with the respective enzymes. The DNA was purified between the two digestion assays using the rapid purification kit (Life Technologies, Inc.).

3.3.5.2 Ligation of DNA fragments

Ligation of DNA fragments was performed with T4 DNA ligase following the recommendation of the supplied protocol.

3.3.5.3 Dephosphorylation of plasmid DNA

After restriction, plasmid DNA was purified by the gel purification method (described in Section 3.1.4.). Then, SAP buffer (Boehringer, Ingelheim) and 1 U SAP (shrimps alkaline phosphatase) per 100 ng plasmid DNA were added and the reaction was incubated at 37°C for 2 h and terminated by incubation at 70°C for 10 min. The plasmid DNA was used for ligation without further purification.

3.3.5.4 Polymerase chain reaction (PCR)

For PCR amplifications of DNA templates the following reaction was set up:

0.5 mM	oligonucleotide primers
0.2 mM	dNTPs
1x PCR	buffer (Quiagen)
2.5 U	Taq polymerase
0.1 – 10 ng	DNA
30 µl final reaction volume.	

An initial denaturation step was performed at 95°C for 3 min, and afterwards 30 cycles of denaturation (95°C for 15 sec), annealing (58 - 62°C for 15 sec) and extension (72°C for 1 min per 1 kb DNA) were performed followed by a final extension step at 72°C for 5 min.

3.3.5.5 Sequence analyses

Nucleotide sequences were determined using the ABI377 system (Applied Biosystems, Foster City, CA). Sequences were evaluated using Sequencher 3.0 software (Gene Codes Corp., Ann Arbor, MI). Sequence alignments were performed using the BioEdit sequence alignment editor (North Carolina State University).

3.3.5.6 Radioactive labelling of DNA

DNA labelling was performed using the Random Primed DNA Labelling Kit (Roche Molecular Biochemicals, Mannheim, Germany) according to the supplied protocol.

3.3.6 NORTHERN ANALYSIS

For Northern analysis 10 µg of total cellular RNA was used. RNA was denatured through incubation with 30% glyoxal (McMaster and Carmichael, 1977), electrophoretically separated in 1.2% agarose gels in MOPS buffer and capillary transferred onto a Biotrans A nylon membrane (0.2 µm; Pall, Dreieich, Germany) in 20x SSC buffer (Grüne and Westhoff, 1988). RNA was fixed to the membrane by UV radiation.

3.3.7 HYBRIDIZATION OF NUCLEIC ACIDS

Hybridisations were performed in 5 ml ExpressHyb solution (Clontech Laboratories, Inc.) with continuous shaking at 68°C for 1 h. Prehybridisations were carried out in the same buffer for 30 min at 68°C. After hybridisation filters were washed several times at room temperature with Wash Solution 1 for 30 - 40 min followed by 40 min washing with Wash Solution 2 at 50°C. The filters were covered with plastic wrap, exposed to a phosphorimager screen and analysed by phosphorimaging (BASIII Fuji Bio Imaging plates and BAS2000

software package and the AIDA software package v3.25 beta; Raytest, Straubenhardt, Germany).

Wash Solution 1

SSC 2X

SDS 0.05%

Wash Solution 2

SSC 0.1X

SDS 0.1%

3.3.8 REVERSE TRANSCRIPTION (RT)-PCR

Reverse transcription was performed with 1 µg total RNA using SuperScript II RNase H⁻ Reverse Transcriptase and hexanucleotides (Roche Molecular Biochemicals, Mannheim, Germany) random primers according to the manufacturers instructions. DNase I (RNase-free) was used for removal of DNA from RNA preparations prior to RT-PCR reactions. For the case that some contaminating DNA remained in the RNA sample, primers were designed that anneal to sequences in exons at both sides of an intron to differentiate between amplification of cDNA and amplification of remaining, if any, DNA. With this approach PCR products derived from genomic DNA are longer compared to those derived from the intronless mRNA. If primers annealed to sequences in the same exon, the possibility of DNA contamination was controlled by using primer *ycf3-f* and *ycf3-r* (Table 2.1) annealing to the different exons of the *ycf3* gene and amplifying 202 and 990 bp fragments of cDNA and chloroplast DNA, respectively.

3.3.9 QUANTITATIVE REAL-TIME RT-PCR

Quantitative two-step RT-PCR was carried out using the LightCycler Thermal Cycler System (Roche Molecular Biochemicals, Mannheim, Germany) applying the SYBR Green protocol (Wittwer *et al.*, 1997a). Reverse transcription was performed as described in Chapter 3.3.8. Real-time PCR was performed using a commercially available master mix containing Taq DNA polymerase, SYBR-Green I dye and deoxyribonucleoside triphosphates (LightCycler - FastStart DNA master SYBR-Green I, Roche Molecular Biochemicals, Mannheim, Germany). Generation of PCR products was detected by measuring SYBR Green I fluorescence. SYBR Green I dye emits a fluorescence signal at

530 nm only when bound to double-stranded DNA. Therefore, during PCR the increase in SYBR Green I fluorescence is directly proportional to the amount of double-stranded DNA generated. After addition of primers (0.5 mM), MgCl₂ (4 mM) and template cDNA to the master mix, an initial denaturation step at 95°C for 10 min followed by 45 cycles of denaturation (95°C for 15 sec), annealing (58°C for 5 sec) and extension (72°C for 11 sec) were performed. All ramp rates were set to 20°C per sec. Detection of the fluorescent product was performed at the end of the extension period.

To verify that only the desired PCR product had been amplified, a melting curve analysis was performed after completion of PCR. For this, PCR products were denatured at 95°C, annealed at 55°C, and gradually heated to 95°C, whereas SYBR-Green I fluorescence was detected stepwise every 0.1°C. During such slow heating of the reaction mixture, melting of double-stranded DNA and a corresponding decrease of SYBR Green I fluorescence occurred. When the temperature of the reaction mixture reached the characteristic melting temperature of a particular DNA product (where the DNA is 50% double-stranded and 50% single-stranded), this was represented by a peak in a melting curve. If PCR generates only one amplicon, melting curve analysis shows only one melting peak. If primer-dimers or other non-specific products are present, they cause additional melting peaks. To estimate primer-dimer formation, a control without template DNA was included in each experiment.

The template quantification was determined by the crossing point using the LightCycler analysis software, as described in Wittwer *et al.* (1997b). Serially diluted samples of *Arabidopsis* total DNA, ranging from 15 ng to 1.5 µg of DNA were used for calibration.

3.4 PROTEIN AND PIGMENT ANALYSES

3.4.1 EXTRACTION OF THYLAKOID MEMBRANE PROTEINS

Plant tissue was ground in liquid nitrogen. The powder obtained was resuspended in extraction buffer and incubated on ice for 10 min. The homogenate was then filtered through two layers of Miracloth (100 µm, Calbiochem, La Jolla, USA) and centrifuged at 10,000 x g for 10 min at 4°C. The supernatant contained the soluble proteins. The membrane proteins,

present in the pellet, were washed once with the same buffer and resuspended in sample buffer. The resulting samples were frozen and stored at -20°C .

<u>Extraction buffer</u>		<u>Sample buffer</u>	
EDTA	10 mM	NaCO ₃	100 mM
EGTA	2 mM	sucrose	10% w/v
Tris-HCl, pH8.0	50 mM	DTT	50 mM
DTT	10 mM		

3.4.2 EXTRACTION OF TOTAL PROTEINS

Plant tissue was ground in liquid nitrogen. The powder obtained was transferred into a centrifuge tube and 5 ml/g of tissue buffer 1 were added. After mixing by vortexing the samples were frozen at -20°C for 45 min, followed by centrifugation at 10,000 g for 20 min at 4°C . The supernatant was removed and 9 ml of buffer 2 were added to the samples. After mixing and incubation at -20°C for 1 h a second centrifugation step was performed. The washing with buffer 2 was repeated and the pellet was successively dried in a desiccator. 5 mg of powder was taken and resuspended in 300 μl of sample buffer +10 μl Tris 1.5 M, pH 8.8.

Buffer 1

TCA	10 g/100 ml acetone
β -mercaptoethanol	70 μl

Buffer 2

β -mercaptoethanol	70 μl in 100 ml acetone
--------------------------	------------------------------------

3.4.3 ISOLATION OF MAJOR THYLAKOID MEMBRANE COMPLEXES OF *ARABIDOPSIS*

3 g of freshly harvested leaf material were homogenized in approximately 10 ml of Buffer A (5 sec. at maximal speed). The homogenate was filtrated through two layers of Miracloth (100 μ m, Calbiochem, La Jolla, USA), and centrifuged at 2000 g, for 2 min. The centrifugation was stopped without breaking power. The sediment was carefully suspended in 0.5 ml of Buffer B, centrifuged again at 2000 g for 4 min and suspended in TMK buffer in a ratio of 100 μ g chlorophyll to 0.5 ml buffer. The membranes were lysed for 10 min in darkness on ice and centrifuged for 3 - 5 min at 2000 g., the pellet was further washed twice by centrifugation in TMK buffer. The final pellet was resuspended in TMK buffer. Aliquots of the thylakoids were stored at -70°C or further treated for solubilization of membrane complexes. Membrane fractions equivalent to 100 μ g chlorophyll were resuspended in 100 μ l of 1% (w/v) β -dodecylmaltoside in TMK buffer. The suspension was incubated for 10 min on ice to solubilize the major thylakoid membrane proteins and centrifuged for 10 min, at 17,000 g in a microfuge. The supernatant containing the thylakoid lysate was loaded onto a linear 0.1 - 1.0 M sucrose gradient and centrifuged for 17 h at 125,000 g at 4°C in a SW60Ti rotor (Beckman, Munich, Germany). All preparation steps were performed at 4°C , and isolated membranes were stored in darkness on ice.

Buffer A

sorbitol	0.3 M
MgCl ₂	5 mM
Tricine/KOH	20 mM, pH8,4
EDTA	20 mM
BSA (w/v)	0.1%

Buffer B

0.3 M
5 mM
30 mM, pH7,6
2,5 mM
0.1%

TMK Buffer

Tris-HCl, pH6.8	10 mM
MgCl ₂	10 mM
KCl	20 mM

3.4.4 ISOELECTRO FOCUSING OF THYLAKOID MEMBRANE PROTEINS

Thylakoid membranes isolated according to chapter 3.4.3 corresponding to 200 µg of chlorophyll were collected by centrifugation at 700 g for 5 min, resuspended in 200 µl lyses buffer and osmotically treated for 30 min on ice. After centrifugation at 17,000 g for 10 min the sediment was washed once (17,000 g, 10 min) and then suspended with 200 µl lyses buffer. The proteins were precipitated with 4 volumes of 100% acetone at -20°C for 2 - 12 hours. The dried protein sediment was suspended in 350 µl solubilization buffer, incubated on ice for 30 min and centrifuged at 17,000 g for 10 min at 4°C. The supernatant was applied on to an IEF stripe 18 cm x 3 mm with a pH range between 4.0 – 9.0. The following program was used for focusing:

7 hours	30 V
13 hours	60 V
1 hour	200 V
1 hour	1,000 V
30 min	1,000 – 8,000 V
3 hours	8,000 V

Lyses Buffer

Tris-HCl, pH 8.0	10 mM
EDTA	5 mM
PMSF	5 mM
DFP	5 mM

Solubilisation Buffer

urea	7 M
thiourea	2 M
CHAPS	4%
DTT	1%
Pharmalyte 4 - 10	1%

3.4.5 *IN VIVO* LABELLING OF LEAF PROTEINS

In vivo labelling of leaf proteins was performed for 15 min as described in Meurer et al. (1998). Seedling were transferred in a Petri dish containing 1 mM KH₂PO₄ (pH 6.3), 0.1% (w/v) Tween 20 medium and, while keeping them in submersion to avoid embolism, the hypocotyls were cut. 20 µg/ml cycloheximide solution (to inhibit cytoplasmic translation) or chloramphenicol (to inhibit chloroplast translation) were added and after incubation for 5

min in the solution containing the antibiotic, the seedling were transferred to small vessels containing the same solution supplemented with 50 μCi [^{35}S]-methionine (>1000 Ci/mmol specific activity). Labelling was carried out at room temperature in a well illuminated place.

3.4.6 MEASUREMENT OF PROTEIN AND CHLOROPHYLL CONCENTRATION

Protein concentrations were measured according to Bradford (1976). Protein amounts of mutants were equalised to amounts in wild-type according to Coomassie-stained gels (Chapter 2.4.8.3). Chlorophyll concentrations were measured according to Arnon (1949).

3.4.7 SODIUM DODECYL SULFATE POLYACRILAMIDE GEL ELECTROPHORESIS (SDS-PAGE)

Soluble, membrane and total proteins were isolated and separated by SDS-PAGE as described in Meurer *et al.* (1996).

3.4.8 PROTEIN DETECTION

Protein gels were either subjected to Western blotting and further used for immunodecoration or exposed for radioactive detection in case of *in vivo* labelling, or were Coomassie Brilliant Blues/silver stained.

3.4.8.1 Western analysis

For immunodetection, proteins were transferred to polyvinylidene difluoride (PVDF) membranes (Amersham Buchler, Braunschweig, Germany) with a semi-dry blotting apparatus according to Khyse-Andersen (1984). The membrane was further blocked in 5% skimmed milk or BSA in TBS 1x solution for 1 h at RT or over night at 4°C.

3.4.8.2 Silver staining (Blum *et al.*, 1987)

After SDS-PAGE, gels were first incubated in fixation solution for 1h., then washed for three times 30 min each in ethanol (50%), incubated in Na₂SO₃ (0.02%) for 1.5 min and washed three times for 30 sec. with bi-distilled water. Subsequently the gels were incubated in staining solution for 30 min in darkness, washed once with water, and submerged in developing solution. The development reaction was relatively fast (few seconds to 1 min) and was stopped at the desired stage with the stop solution.

Fixation solution

ethanol	50%
acetic acid	12%
formaldehyde	0.05%

Staining solution

AgNO ₃	0.2%
formaldehyde	0.075%
(kept in darkness)	

Developing solution

NaCO ₃	6%
formaldehyde	0.05%
Na ₂ SO ₃	0.0004%

Stop solution

ethanol	50%
acetic acid	12%

3.4.8.3 Coomassie Brilliant Blue staining

The gels were stained by incubation in Coomassie Brilliant Blue staining solution for 1 h at 50°C or overnight at RT. Subsequently, the gels were destained in 12% (v/v) acetic acid with continuous agitation changing regularly the solution.

Coomassie Brilliant Blue staining solution

45% (v/v)	methanol
12% (v/v)	acetic acid
0.2% (w/v)	Coomassie Brilliant Blue R-250

3.5 CHLOROPHYLL *A* FLUORESCENCE ANALYSIS

Chlorophyll *a* fluorescence analyses were performed using plants of the same age grown under identical conditions. A pulse amplitude–modulated fluorometer (PAM101; Walz, Effeltrich, Germany) equipped with a data acquisition system (PDA-100; Walz, Effeltrich, Germany) and a personal computer using Wincontrol version 1.72 software (Walz, Effeltrich, Germany) for data collection were used to measure and analyze *in vivo* chlorophyll *a* fluorescence. The following settings were used for the PAM101 unit: light intensity, 4; gain, 6; damping, 9. After induction, saturating pulses of $4000 \mu\text{E m}^{-2} \text{sec}^{-1}$ light intensity and 1 sec duration were applied in 20 sec intervals to estimate quenching parameters. The actinic light intensity varied from 10 to $50 \mu\text{E m}^{-2} \text{sec}^{-1}$.

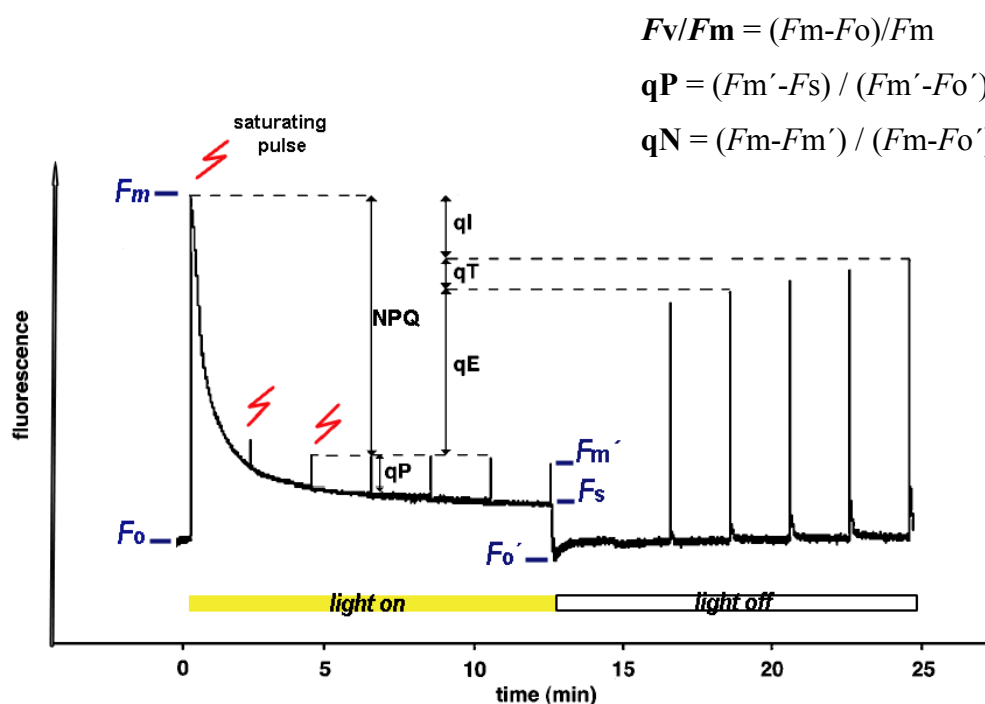


Figure 3.1 A typical chlorophyll fluorescence measurement. In the presence of only weak measuring light the minimal fluorescence (F_0) is seen. When a saturating light pulse is given, the photosynthetic light reactions are saturated and fluorescence reaches a maximal level (F_m). Upon continuous illumination with moderately excess light, a combination of qP and NPQ lowers the fluorescence yield. NPQ ($qE + qT + qI$) can be seen as the difference between F_m and the measured maximal fluorescence after a saturating light pulse during illumination (F_m'). (Graph adapted from Müller *et al.*, 2001)

The minimum fluorescence induced by weak measuring light in dark adapted leaves (F_0) was recorded. After a single saturation pulse that allowed to record the maximal fluorescence (F_m), the actinic light was switched on and fluorescence was recorded (F_s). During light induction fluorescence saturating pulses were applied to record the maximal fluorescence (F_m'). The minimum fluorescence after switching off the actinic light (F_0') was also estimated. These data were used to calculate the PSII efficiency (F_v/F_m), the photochemical quenching (qP) and the energetic component (qE) of non-photochemical quenching (NPQ) according to the formula shown in Fig 3.1.

3.6 GENETIC METHODS

3.6.1 MAPPING OF THE *DPAL* MUTATION

A mapping population was generated to identify the precise chromosomal location of the *dpa1* mutation. The F₁ populations were produced by pollinating emasculated flowers of the accession Landsberg *erecta* (*Ler*) with Wassilewskija plants heterozygous for the *dpa1* mutation. F₂ families selected for the mutant offsprings were grown on medium, and individual mutant plants were chosen for genetic mapping of the mutation with molecular markers with simple sequence length polymorphism marker Cer452226. The oligonucleotides used were located 850 kb upstream of the *atpC1* gene on the bacterial artificial chromosome F4C21. This marker is polymorphic between *Ler* and Wassilewskija producing 203 and 285 bp PCR products, respectively.

3.6.2 GENERATION OF THE *PSBSxDPAL* DOUBLE MUTANT

The F₁ generation was produced by pollinating emasculated *psbS* mutant with plants heterozygous for the *dpa1* mutation. Critical was the choice of the flowers development state. The emasculated flowers were at an early state of development with still short stamens not matured for pollen production while the pistils were rather elongated with a wet appearance at the top. The pollinating flowers contained elongated stamens with anthers covered by bright yellow pollen. The F₁ generation was heterozygous for the *psbS* mutation and heterozygous or wild type for the *dpa1* mutation. Only plants heterozygous for both

mutations were propagated and F₂ plants homozygous for *psbS* and segregating *dpa1* mutant offsprings were taken.

3.7 ELECTRON MICROSCOPY

Electron microscopy was performed by Prof. G. Wanner (LMU, München). Samples were prepared as described in Meurer *et al.* (1998).

3.8 PHOTOPHOSPHORYLATION

Chloroplast thylakoids from *Arabidopsis* leaves were prepared as described for spinach (Strotmann, H., and Bickel-Sandkötter, S., 1977). The reactions were conducted in a Δ pH clamp instrument as described (Strotmann, H. *et al.*, 1990). The reaction cell of 2.5 ml volume contained a medium consisting of 25 mM Tricine buffer, pH 8.0, 5 mM dithiothreitol, 5 mM MgCl₂, 5 mM ³²P-labeled Na₂HPO₄, 50 mM KCl, 50 μ M phenazine methosulfate, and thylakoids corresponding to a chlorophyll concentration of 25 μ g/ml. The experiments were conducted at pre-chosen Δ pH values which were kept constant throughout the experiment by the employed clamp device. Δ pH was continuously controlled by the fluorescence quenching of 9-aminoacridine. The thylakoids were pre-illuminated for 2 min to obtain the prechosen proton gradient. Then 0.5 mM ADP was added in the light. After 10, 20, and 30 sec, 0.2 ml samples were taken and deproteinized with HClO₄ (final concentration 0.6 M). The formed ³²P-labeled organic phosphate was then quantified.

4 RESULTS

4.1 KNOCK-OUT MUTANT OF THE ATP SYNTHASE γ SUBUNIT, *DPAL* (DEFICIENCY OF PLASTID ATP SYNTHASE 1)

4.1.1 ISOLATION AND PHENOTYPE OF THE *DPAL* MUTANT

The F2 progeny of 1100 EMS-treated seeds and 75 preselected pale mutants from T-DNA collections (Feldmann, 1991) obtained from the Arabidopsis Biological Resource Centre (Ohio State University, Columbus, OH) were used for screening 87 mutant plants. They developed pale green cotyledons but no primary leaves. Cultivation on sucrose-supplemented MS medium often rescued the mutant seedlings, leading to a nearly normal pigmentation and development. Under these conditions the mutants could often hardly be distinguished from wild type plants, although growth rates were slightly retarded. Seven plants showing a high dark level of fluorescence (F_0) but a lower level during light fluorescence induction were selected from the collection by imaging analysis (Fig. 4.1). In six plants, the lowest fluorescence level became apparent after about 1 - 2 min, and the fluorescence again slowly increased close to the F_0 level during light induction. This unusual fluorescence behaviour was already observed previously in several high chlorophyll fluorescence (*hcf*) mutant plants (Meurer *et al.*, 1996). In one of these mutants, *dpa1*, light-dependent quenching of F_0 was stable during induction. This increased non-photochemical quenching was indicative of photosynthetic electron transport activity in *dpa1* in contrast to a high chlorophyll fluorescence phenotype typical of photosystem I mutants such as *hcf101* (Fig. 4.1).

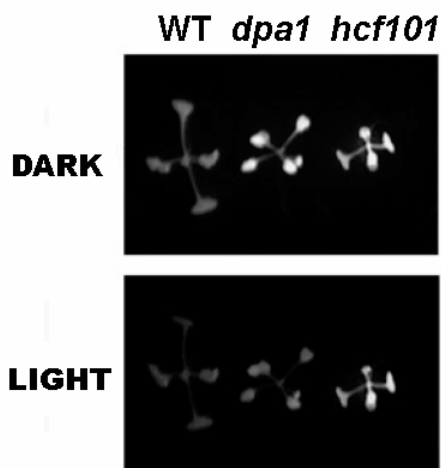


Figure 4.1. Chlorophyll fluorescence of seedling lethal mutants was initially recorded by fluorescence imaging. The *dpa1* mutant has been selected due to its high dark fluorescence level (F_0) and its normal steady state fluorescence level (F_s) during illumination. Photosynthetic electron transport mutants (*hcf101*) showed a high fluorescence level under both conditions,

4.1.2 INACTIVATION OF THE *ATPC1* GENE

In a first step the mutation was backcrossed in order to confirm a Mendelian segregation of *dpa1*, to remove possible background mutations and to generate a mapping population. The *dpa1* mutation was mapped to the upper part of chromosome 4 by the use of the molecular Cer452226 marker closely located to *atpC1* (see Methods). Forty-eight meiotic chromosome patterns of individual F2 mutant plants derived from backcrosses to the accession Landsberg *erecta* were used. No recombinations were identified, indicating that the *dpa1* mutation was closely linked to the *atpC1* gene. Southern blot analysis using probes of the T-DNA left border and the *atpC1* gene was performed on genomic DNA from *dpa1*, wild type, and heterozygous plants. Restriction fragment length polymorphisms demonstrated a T-DNA insertion in the region of *atpC1*. Due to the close location of the mutation to *atpC1* and the observed restriction fragment length polymorphism, primers of the *atpC1* gene and of the T-DNA borders were chosen in order to identify the site of the T-DNA insertion. Only the combination of the left border primer with the gene-specific primer (3 & 4, Fig. 4.2A) was able to amplify a product indicating that the right border was truncated (Fig. 4.2, A and B). After sequence analysis of the PCR products obtained the exact location of the T-DNA at position +603 bp relative to the start codon of the *atpC1* gene could be defined. The combination of primers before and after the T-DNA insertion in *atpC1* (2 & 4, Fig. 4.2A) generated no amplificate in the mutant, but the expected product of 578 bp in wild type and heterozygous plants (Fig. 4.2B). The PCRs also included the two primers of the actin3 gene as an internal control that amplified in both wild type and mutant plants.

The absence of expression of *atpC1* gene in the *dpa1* mutant was also demonstrated using Northern blot analysis. Transcript levels of plastid genes encoding other subunits of the chloroplast ATP synthase, i.e. *AtpA*, *AtpH/I*, and *AtpF*, were not altered in the mutant (Fig. 4.2C). The confirmation that the phenotype of the *dpa1* mutant was indeed caused solely by the insertional inactivation of the *atpC1* gene came from complementation studies. Mutant plants expressing the wild type *atpC1* gene under control sequences of the constitutive 35S RNA cauliflower mosaic virus (*dpa1-c*) were indeed able to rescue the wild type phenotype.

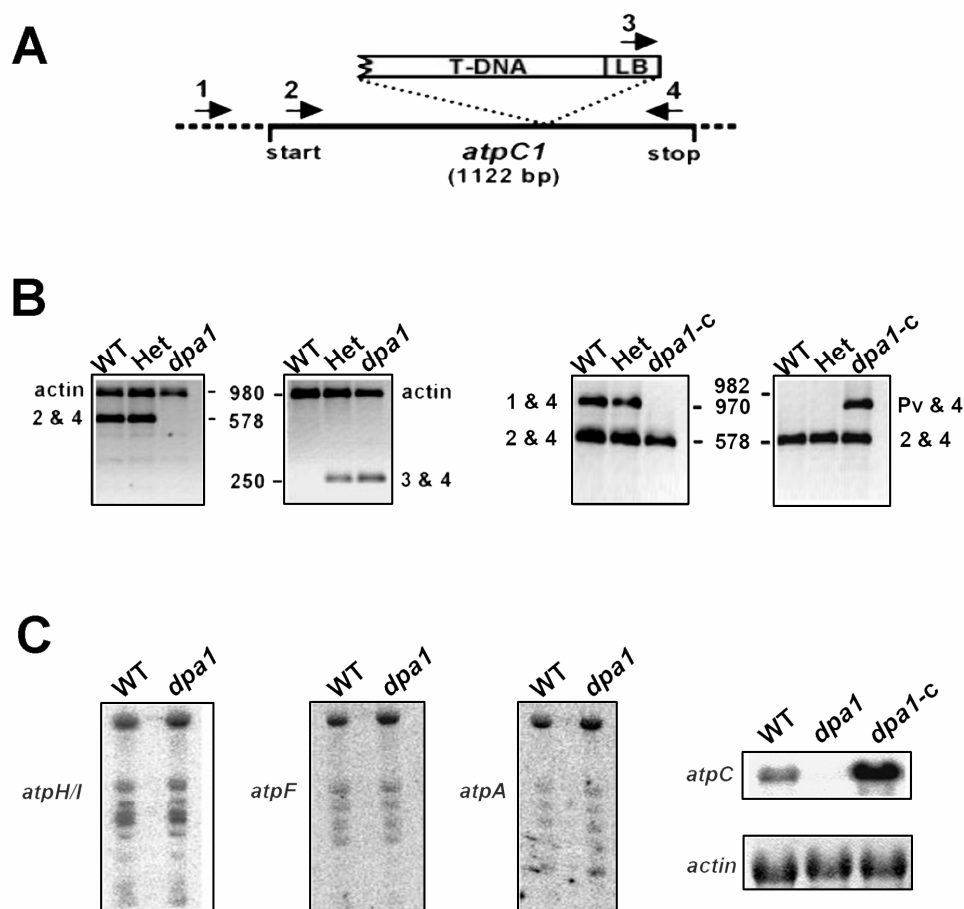


Figure 4.2. Analysis of the *dpa1* mutant. **A.** Schematic presentation of the insertion of the truncated T-DNA into the *atpC1* gene and of the primers used for the PCR analysis. Primer 1 (*atpC1*-prom) was chosen from the *atpC1* promoter, primers 2 (*atpC1*-5'-for) and 4 (*atpC1*-3'-rev) from the *atpC1* coding region, and primer 3 from the left border of the T-DNA (T-DNA-LB). **B.** PCR analysis of wild type (WT), heterozygous lines (Het), homozygous mutant (*dpa1*), and complemented mutant (*dpa1-c*). The data demonstrate homozygosis of *dpa1* because primers 2 and 4 did not amplify, whereas the internal control reaction using primers of the *actin3* gene was positive in *dpa1*. The PCR product using primers 3 and 4 demonstrates the insertion and the orientation of the T-DNA. In the complemented line primers 1 and 4 did not amplify due to the insertion of the T-DNA into the coding region of the endogenous gene while successful complementation was proven by amplification with primers 2 and 4 of *atpC1* as well as primers 4 and Pv, the primer designed from the 35S promoter of the binary vector used for complementation. **C.** Northern analysis to detect the expression of different ATP synthase genes. Only *atpC* expression is affected in *dpa1*.

4.1.3 ACCUMULATION OF THE MAJOR PHOTOSYNTHETIC COMPLEXES IN *DPA1*

In silver-stained gels it was already visible that the two large subunits α and β and the γ subunit of the ATP synthase were depleted in *dpa1* (Fig. 4.3C), although amounts and patterns of all the other thylakoid membrane proteins were comparable to those of the wild type. The accumulation of the ATP synthase and other thylakoid membrane complexes was further estimated in *dpa1* and wild type plants. A collection of antisera raised against eight individual ATP synthase polypeptides and representative polypeptides of PSI, PSII, and the cytochrome *b₆f* complex was used. All nuclear and plastid-encoded subunits of the ATP synthase analysed failed to accumulate in significant amounts in *dpa1* (Fig. 4.3A). The dilution series of wild type membranes demonstrated that the levels of ATP synthase subunits were reduced to less than 5%. Amounts of several subunits such as α , γ , c, δ , and b' were below the limit of detection. Only little differences in steady state levels were observed for other nuclear and plastome-encoded proteins of PSII, e.g. LHCII, PsbO, PsbD (D2), PSI, and PsaC, analyzed in *dpa1* (Fig. 4.3B).

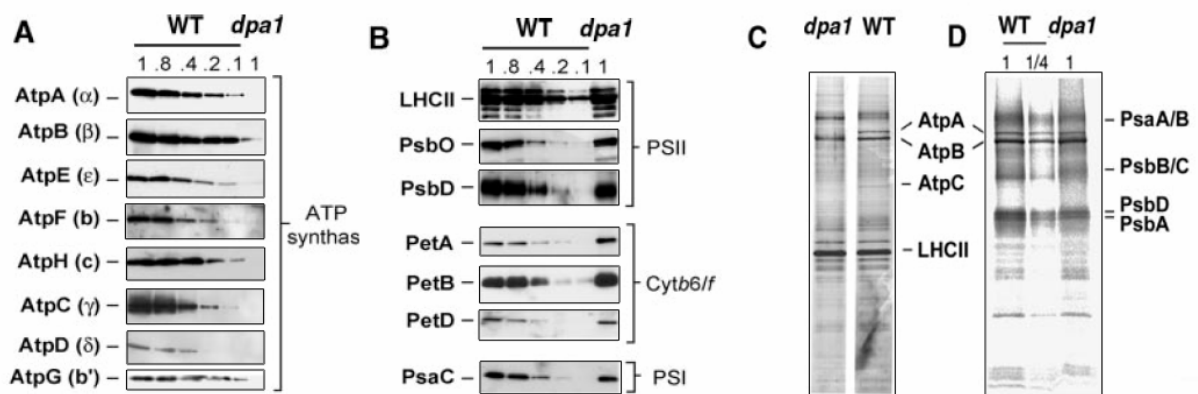


Figure 4.3. Accumulation and translation of thylakoid membrane proteins isolated from three-week-old *dpa1* and wild type (WT) plants. **A.** Immunodetection of ATP synthase subunits (α , β , γ , δ , ϵ , b, b', c), and **B.**, other photosynthetic membrane complexes: PSII (LHCII, PsbO, PsbD), *cytb₆f* (PetA, PetB, PetD) and PSI (PsaC). **C.** Silver staining and **D.**, *in vivo* labelling of thylakoid proteins. The *in vivo* labeling pattern is restricted to plastome encoded proteins as incorporation of ³⁵S-methionine occurred in the presence of the cytosolic translation inhibitor cycloheximide. 1 corresponds to 10 μ g of chlorophyll in the loaded sample.

In contrast, levels of proteins of the cytochrome *b₆f* complex, e.g. PetA and PetB, were increased in *dpal*. The rate of synthesis of plastid-encoded ATP synthase proteins was investigated by pulse labelling experiments with S³⁵-methionine (Fig. 4.3D). To reduce the complexity of labelling, synthesis of the nuclear encoded chloroplast proteins was inhibited with cycloheximide so that only plastome encoded proteins appeared. The appearing signals in the gels could be assigned to individual subunits of the thylakoid membrane, *i.e.* PsaA/B, AtpA/B, PsbB/C, and PsbA/D, due to their abundance and known electrophoretic mobilities and by mutant analysis (Meurer *et al.*, 2002). The protein labelling patterns in the mutant and wild type were identical with respect to the size and the numbers of all detectable polypeptides and their intensity of labelling. The PSII subunits PsbA, PsbB, PsbC, and PsbD, and the ATP synthase α (AtpA) and β (AtpB) subunits were synthesized at about normal rates in the mutant, whereas steady state levels of the α and β subunits were reduced by more than 95% as compared with the wild type (Fig. 4.3A).

Therefore, lack of the ATP synthase subunits in *dpal* is caused by a decreased stability of all subunits that constitute the complex in the mutant background. Some ATP synthase complexes might assemble in the mutant, which contains the *atpC2* gene product, and this could also explain the incorporation of the α and β subunits into the thylakoid membrane (Fig. 4.3D). However, expression of *atpC2* is not sufficient to allow photoautotrophic growth and significant accumulation of any subunit that belongs to the ATP synthase.

4.1.4 PLASTID ATP SYNTHASE ACTIVITY IN *DPAL* MUTANT

The immunological data were supported by analysis of ATP production with isolated thylakoids (Table 4.1). The rate of photophosphorylation depended on the magnitude of pH applied and attained 112.1 $\mu\text{mol of ATP chl}^{-1} \text{ h}^{-1}$ at $\Delta\text{pH } 3.0$ in wild type thylakoids. As reported for spinach chloroplasts, the ATP synthesis rate was increased in an intermediate ΔpH range from 2.5 to 3.0 under reducing conditions, indicating a lower ΔpH profile for the activation of the ATP synthase (Ross *et al.*, 1995). In mutant thylakoids, on the other hand, phosphorylation activity was low and ΔpH -independent both under oxidized and reduced conditions and probably unrelated to photophosphorylation.

Table 4.1. ATP production (photophosphorylation) in intact thylakoids from wild type (WT) and *dpa1*.

ΔpH	$\mu\text{molATP/mgChl}\cdot\text{h}$			
	WT		<i>dpa1</i>	
	Oxidized	Reduced	Oxidized	Reduced
2.4	15	15	2.7	6.6
2.5	31.7	64	1.9	6.2
2.8	73.1	116.5	1.9	5.4
2.9	89.3	140	2.6	6.8

Experiment performed in cooperation with Prof. H. Strotmann, Heinrich-Heine-Universität, Düsseldorf.

4.1.5 PHOTOSYNTHETIC ACTIVITY IN *DPA1*

Analysis of *dpa1* mutant seedlings revealed a decrease in F_v/F_m (0.60 +/- 0.05 versus 0.80 +/- 0.02 in the wild type) which is indicative of a partially impaired PSII photosynthetic activity.

4.1.5.1 High non-photochemical quenching is observed in the mutant

Light intensities of 2 $\mu\text{mol photons m}^{-2}\text{s}^{-1}$ for fluorescence induction did not significantly increase the F_s above the F_0 level in wild type plants, and saturating light pulses were able to completely induce the F_m level during induction (Fig. 4.4). In *dpa1* low light significantly increased the F_s to 20% of F_v indicating that electrons are not efficiently released from PSII. F_m could be reached during induction thus no significant proton accumulation or non-photochemical quenching (NPQ) takes place at this low intensity light in *dpa1*. Light-induced quenching of chlorophyll fluorescence severely depended on the chosen light intensity. Under low light of 2 $\mu\text{mol photons m}^{-2}\text{s}^{-1}$ NPQ was close to zero in both wild type and *dpa1*; under still moderate light intensities of 30 $\mu\text{mol photons m}^{-2}\text{s}^{-1}$ a strong NPQ was observed in *dpa1* reaching values of 1 after 2 min of induction, while in wild type NPQ was below 0.2 (Fig. 4.4). Depending on the light intensity the fluorescence

dropped far below the dark F_0 level which could be quenched up to 40% in the mutant. This high non-photochemical quenching mechanism did not allow light pulse-dependent increase of the fluorescence above the F_0 level after 2 min of dark adaptation.

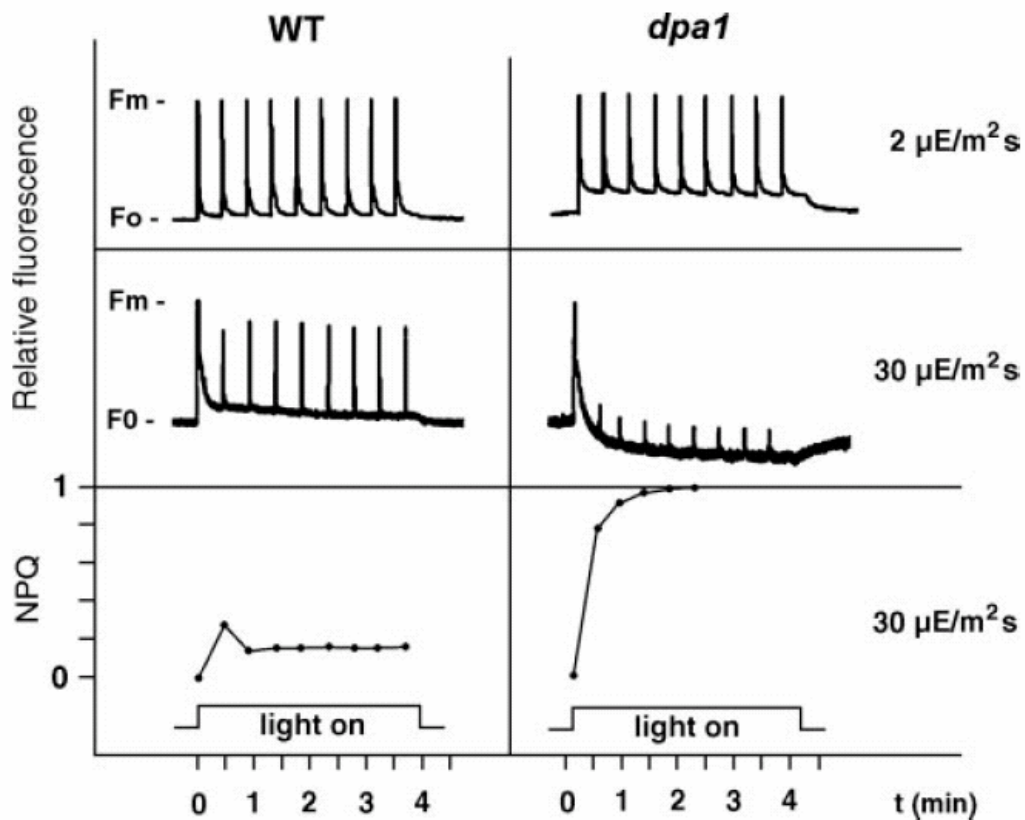


Figure 4.4. *In vivo* chlorophyll fluorescence induction and NPQ analysis in *dpa1* and wild type (WT). Actinic light was applied at time 0 to dark-adapted plants. The first saturating pulse allowed recording the maximal fluorescence; consecutive saturating pulses were applied at intervals of 30 sec. The actinic light intensity was 2 $\mu\text{mol of photons m}^{-2}\text{s}^{-1}$ and 30 $\mu\text{mol of photons m}^{-2}\text{s}^{-1}$.

4.1.5.2 The high NPQ can be totally ascribed to the trans-thylakoid electrochemical proton gradient in the mutant

The quenching below F_o was reversible and relaxed to about 90% within 5 min dark incubation; complete relaxation took about 10 min (Fig. 4.5A). Such post illumination increase of the fluorescence in *dpa1* could reflect the relaxation of the high energization of the thylakoid membrane. This assumption is consistent with the finding that the fluorescence increase was severely slowed down at a lower temperature when the thylakoid membrane is less leaky for protons (Fig. 4.5B). Lowering the temperature to 0°C decreased the relaxation rate considerably, and increasing the temperature to 35°C increased the relaxation rate. In addition, the kinetics of fluorescence quenching is also temperature-sensitive. Increasing the temperature to 35°C accelerated the quenching process, and decreasing the temperature to 0°C slowed down the kinetics. This might well be explained by the temperature dependence of the xanthophylls cycle, which plays a necessary role in NPQ.

Moreover, far-red light which selectively excites PSI was unable to change the relaxation rate, independently of which intensity has been used (Fig. 4.5A). Therefore, the fluorescence increase in the dark, after switching off actinic light, could not be caused by a reduction of quinones in *dpa1*.

To investigate further the quenching mechanism, fluorescence induction curves were analyzed in the presence of the ionophore nigericin (Fig. 4.5C). If quenching in *dpa1* was due to accumulation of protons in the lumen, the action of the uncoupler should prevent this tendency. Indeed, when nigericin was applied during induction, quenching of F_s started to relax in *dpa1* and fluorescence again reached levels above F_o (Fig. 4.5C). When nigericin was supplied 10 min before starting the fluorescence measurement, *dpa1* failed to perform strong NPQ, and the fluorescence traces were close to those found in wild type. Quenching of F_o in the darkness immediately after switching off actinic light was almost negligible (Fig. 4.5C).

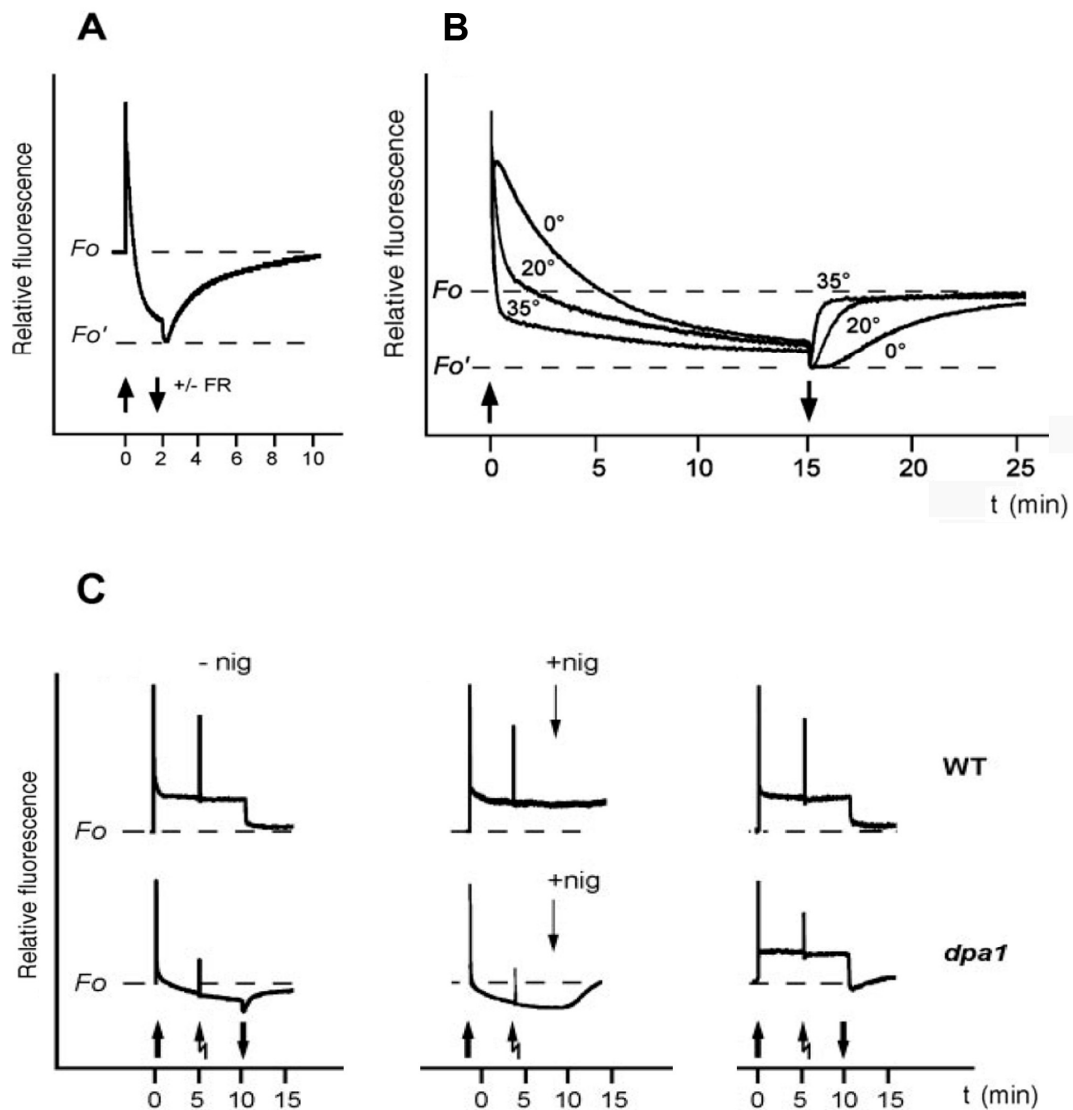


Figure 4.5. Analysis of the post-illumination fluorescence increase in *dpa1*. Induction and darkening are indicated by filled upward and downward arrows, respectively. **A.** The relaxation rate of fluorescence quenching was identical with or without far-red background light (intensity 8 of the PAM settings) after switching off actinic light, the actinic light intensity given for 2 min was $50 \mu\text{mol photons m}^{-2}\text{s}^{-1}$. **B.** Light-induced fluorescence quenching at $30 \mu\text{mol photons m}^{-2}\text{s}^{-1}$ and the dark relaxation after 15 min of induction was recorded at 0, 20, and 35°C . The curves were normalized to the F_o' level (lowest F_o value immediately after switching off the light). **C.** Effect of nigericin on fluorescence traces. The actinic light intensity was $30 \mu\text{mol photons m}^{-2}\text{s}^{-1}$. The continuous actinic light was switched on followed by a saturating pulse 5 min later (zigzag arrow). Ten minutes after, either the actinic light was switched off or $2 \mu\text{M}$ of the uncoupler nigericin was supplied (+nig). In the third panel nigericin was added 10 min. before fluorescence analysis. Chlorophyll fluorescence was recorded from leaves cut in small pieces to facilitate the entrance of the inhibitor.

4.1.6 LIGHT INDUCED THYLAKOID SWELLING IN *DPAI*

Ultra-thin sections of leaves from three-week-old plants grown under continuous light revealed an impaired structure of the chloroplast (Fig. 4.6). The mutant formed grana stacks which were disordered and not strictly oriented in parallel to each other probably because they were not always interconnected by stroma thylakoid membranes. The luminal space was swollen indicative of a light-dependent high proton gradient across the thylakoid membrane which leads to influx of osmotically active ions (Majeran *et al.*, 2001). The thylakoid membrane system was not reduced in *dpa1*, but mutant chloroplasts were deficient of any starch grains.

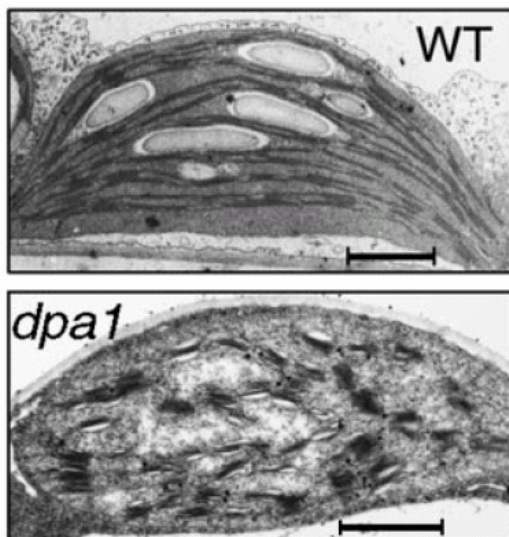


Figure 4.6. Ultrastructure of chloroplasts from three-week-old wild type (WT) and *dpa1* leaves. Both wild type and mutant plants were grown on sucrose-supplemented medium and illuminated prior to leaf fixation. Plants of the same age were selected for electron microscopic analyses. Bar, represents 1 μm (Experiment performed in cooperation with Prof. G. Wanner, Ludwig-Maximilians-Universität, München).

4.1.7 *PSBSXDPAI* DOUBLE MUTANT

Since a crucial role of PsbS protein in NPQ has been pointed out (Li *et al.*, 2000) and due to the abnormally high level of NPQ in *dpa1*, the involvement of PsbS in the mutant background was investigated. A classical genetic approach was chosen and a double mutation *psbSxdpa1* was generated by crossing *psbS* mutant plants with heterozygous *dpa1* mutant. The F1 generation, heterozygous for the *psbS* and *dpa1* mutations, were screened by PCR analysis. From these plants F2 progeny was obtained homozygous for *psbS* and heterozygous for *dpa1* allowing the segregation of *psbSxdpa1* double mutants.

4.1.7.1 Effect of the double mutation on NPQ

The absence of PsbS in *dpa1 Arabidopsis* mutant plants resulted in an incapability to perform NPQ (Li *et al.*, 2000). During fluorescence induction at high light F_m is not significantly quenched in *psbS* mutants while, at the same light condition, F_m could not be reached in the wild type, indicating that proton accumulation and NPQ take place (Fig. 4.7). As a consequence the F_s levels increased significantly in the mutant while in the wild type they remained almost unchanged compared to low light condition.

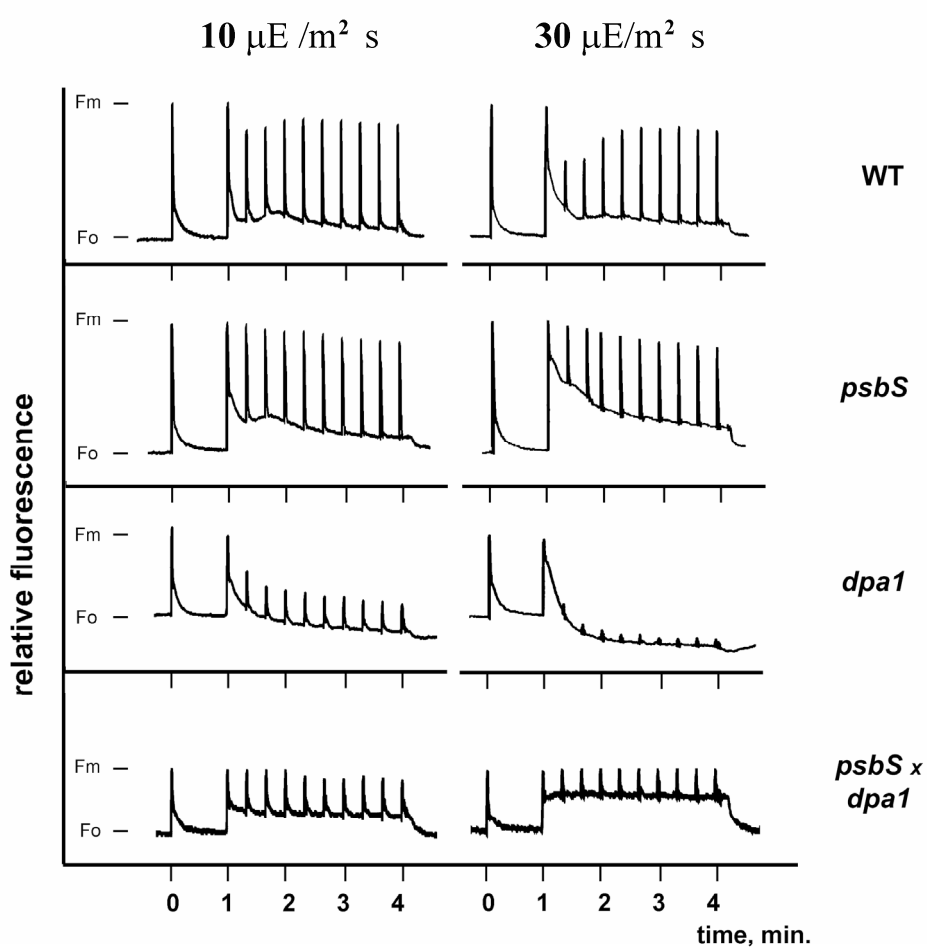


Figure 4.7. *In vivo* chlorophyll fluorescence induction and NPQ analysis in wild type (WT), *psbS* mutant, *dpa1* and *psbSxdpa1* double mutant. A first saturating pulse was applied at time 0 in order to record the maximal fluorescence (F_m). After 1 minute actinic light was switch on and consecutive saturating pulses were applied at intervals of 20 seconds. The actinic light intensity was $10 \mu\text{mol of photons m}^{-2}\text{s}^{-1}$ and $30 \mu\text{mol of photons m}^{-2}\text{s}^{-1}$.

The fluorescence analysis of the double mutant *psbSxdpa1* revealed that in the absence of PsbS no NPQ could develop in *dpa1*. The photosynthetic efficiency in the double mutant, recorded as F_v/F_m , was ~ 0.5 , comparable to *dpa1*. Nevertheless, at high light, when *dpa1* developed a high-non photochemical quenching that quenched F_o , the absence of PsbS resulted in an increase of F_s up to 70% of F_v (Fig. 4.7) and no induction of non-photochemical quenching.

4.1.7.2 Photoprotective role of qE

Single *dpa1* and double *psbSxdpa1* mutants grown at very low light were exposed to relatively high light ($100 \mu\text{mol}$ of photons $\text{m}^{-2}\text{s}^{-1}$) for increasing intervals of time. Photoinhibition during the high light (HL) treatment was measured by chlorophyll fluorescence. The maximal PSII photochemical efficiency, represented by the chlorophyll fluorescence parameter F_v/F_m , decreased gradually during exposure to HL (Fig. 4.8). The HL-induced decrease in F_v/F_m was significantly more pronounced in the double mutant than in *dpa1*. After four hours F_v/F_m of the double mutant was reduced to almost 50% of the initial value. The ability to perform non-photochemical quenching allowed *dpa1* to restrict the damage to 30 - 35%. The most significant difference was observed between 2 - 3 hours of high light treatment.

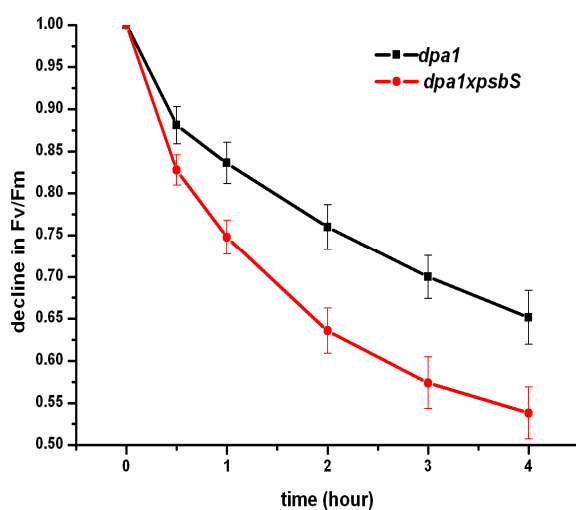


Figure 4.8. Three-week-old *dpa1* and *psbSxdpa1* mutants grown under dim light ($10 \mu\text{mol}$ of photons $\text{m}^{-2}\text{s}^{-1}$) were exposed at higher light intensity ($100 \mu\text{mol}$ of photons $\text{m}^{-2}\text{s}^{-1}$) and the values of F_v/F_m $[(F_m - F_o)/F_m]$ were recorded after 0.5, 1, 2, 3 and 4 hours. The data are shown as average of five measurements with standard deviation.

4.1.8 EXPRESSION OF NUCLEAR-ENCODED GENES IN *DPAI*

To investigate further effects of the *atpC1* mutation, the expression levels of nuclear genes that contribute to chloroplast functions were determined by DNA array analysis. This was carried out on a set of 3292 gene sequence tags, about 81% of which code for chloroplast-targeted proteins, and their expression patterns in *dpa1* mutants were compared with those in wild type (Kurth *et al.*, 2002; Richly *et al.*, 2003). Differential gene expression values (*dpa1* versus wild type) were determined by comparing hybridization signals. Statistical analysis of the expression data revealed that 1930 genes showed significant differential expression in *dpa1*. An unbalanced response of the nuclear chloroplast-related transcriptome was observed in the mutant, with the vast majority of differentially expressed genes being down-regulated (1765 genes down- and 165 genes up-regulated). The differentially expressed genes in *dpa1* were grouped into 13 major functional categories, including photosynthesis (dark or light reaction), primary and secondary metabolism, transcription, protein synthesis, transport, and others (Fig. 4.9). Most of the different functional gene classes followed the general trend of down-regulation. However, genes for the light and dark phase of photosynthesis were up-regulated more than others. Closer inspection of photosynthetic gene expression uncovered that in particular genes coding for proteins of the ATP synthase, the cytochrome *b6/f* complex, PSI, or the Calvin cycle were up-regulated in *dpa1* (Table 4.2), whereas differentially expressed genes coding for PSII tended to be up- or down-regulated. Because the analysis of the expression of photosynthetic proteins (Fig. 4.3B) and of chlorophyll fluorescence characteristics implied that photosynthetic electron flow still occurs in the *dpa1* mutant, the mRNA expression changes indicate that the plant is able to monitor the altered photosynthetic state of the chloroplast (*e.g.* the increased lumen acidification) and reacts by regulating appropriate photosynthetic genes. For example, from the analysis of steady state levels of photosynthetic proteins, it appears that the level of PSI-C is decreased in the mutant (Fig. 4.3B) and the up-regulation of other PSI genes could be a compensatory reaction of the plant to prevent an even higher reduction of this photosystem. In the same way expression of the two remaining nuclear genes of the ATP synthase, *atpD* and *atpG*, is increased in *dpa1* (Table 4.2).

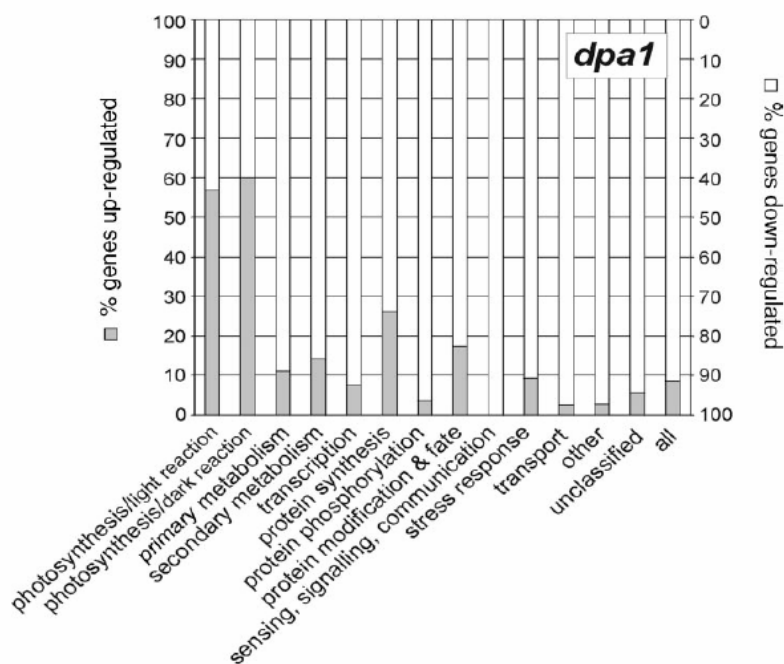


Figure 4.9. mRNA expression profiling of 3292 nuclear genes in *dpa1*. Total RNA isolated from 3-week-old plants grown under continuous light at a photon flux density of $20 \mu\text{mol photons m}^{-2} \text{s}^{-1}$ was used. Up- and down-regulated genes were classified in 13 major functional categories. Except for photosynthetic genes the expression of all other classes was strongly down-regulated. The array data were confirmed by Northern analysis with randomly chosen gene probes. Experiment performed in cooperation with Dr. D. Leister, Max Plank-Institute, Köln.

Table 4.2 Representative expression levels of up- and down-regulated nuclear photosynthetic genes in *dpa1*

	<i>Up-regulated</i>			<i>Down-regulated</i>		
	Accession no.	Annotation	Ratio <i>dpa1</i> /WT	Accession no.	Annotation	Ratio <i>dpa1</i> /WT
Electron carrier	At1g20340	PetE2	3.49	At4g14890	PetF5	0.40
				At5g10000	PetF4	0.13
PSI	<i>psaA</i>	PSI-A	3.69			
	At1g55670	PSI-G	2.63			
PSII	At1g79040	PSII-R	2.96	At1g03600	PSII protein family	0.36
	At1g4457	PsbS	2.41	At2g30790	PSII-P ₂	0.34
	At5g66570	PsbO1	2.17	At4g15510	PSII-P related protein	0.32
	At1g67740	psbY	1.73	At3g01440	PSII-Q related protein	0.19
	At2g06520	psbX	1.52			
Cytb6/f	At2g2650	PetM	1.91			
ATP synthase	At4g09650	AtpD	1.37			
	At4g32260	AtpG	1.37			
Dark reaction	At5g38420	Rubisco small subunit 2b	4.92	At1g73110	Putative rubisco activase	0.36
	<i>rbcl</i>	Rubisco large subunit	4.65	At3g55800	Sedoheptulose-bisphosphatase	0.34
	At5g38430	Rubisco small subunit 1b	4.43	At4g15530	Pyruvate, orthophosphate kinase	0.23
	At1g32060	Phosphoribulokinase	2.39			

4.2 *DPA1* COMPLEMENTED WITH A MUTATED FORM OF ATPC1

The γ subunit of higher plants and green algae is responsible for thiol modulation of the ATP synthase. The structural basis of this regulatory element resides in the reduction of two cysteins contained in a highly conserved segment of thirty amino acids in the γ subunit of CF₁ (Fig. 4.10). The substitution of three charged amino acids localized in the conserved region (E²¹⁰-E²¹² Fig. 4.10) with neutral ones made the γ subunit insensitive to thiol modulation (Konno *et al.*, 2000). The *dpa1* mutant was used to further characterize the thiol regulation and its physiological role *in vivo*.

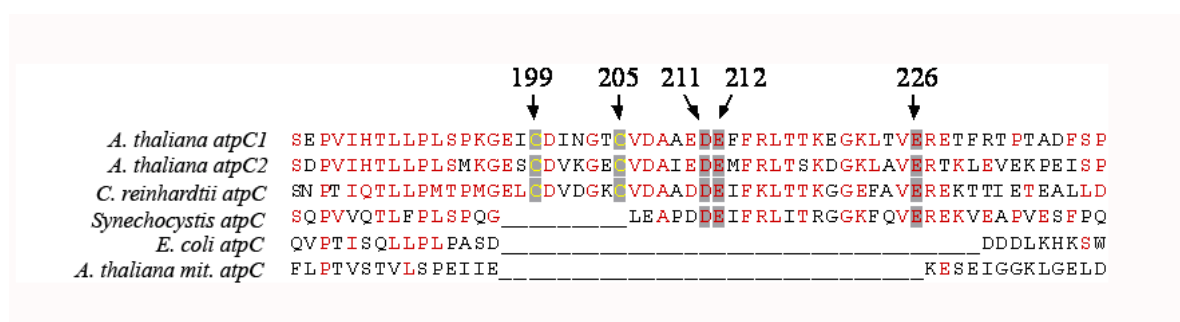


Figure 4.10. Alignment of partial protein sequences of γ subunits from different sources: chloroplast AtpC1 and AtpC2 from *Arabidopsis thaliana*, AtpC of *Chlamydomonas reinhardtii*, *Synechocystis*, *Escherichia coli* and mitochondrial AtpC subunit of *Arabidopsis thaliana*. The Cys residues, involved in the redox modulation of plant and algal plastid ATP synthase, and the highly conserved acidic residues, the object of the following study, are indicated with arrows.

Three conserved acidic residues in vicinity to the Cys residues forming the sulphhydryl bridge, namely D²¹¹, E²¹² and E²²⁶ (Fig. 4.10), were modified by oligonucleotide directed mutagenesis and the resulting modified *atpC1* gene was used to complement the *dpa1* mutation. From wild type genomic DNA the *atpC1* gene was amplified in a two step amplification with the primers atpC1-Sma-for, atpC1-mod-rev and atpC1-mod-for, atpC1-rev-xba (see scheme in Fig. 4.11A, B). The modified gene obtained was inserted in the cloning vector PCR-Script Amp SK(+) and the modification was confirmed by sequencing (Fig. 4.11C). The recombinant DNA was further isolated by restriction with the enzymes *SmaI*, *XbaI* and inserted in the binary vector pSeX001. Heterozygous plants for the *dpa1* mutation were transformed with *Agrobacterium* carrying the construct.

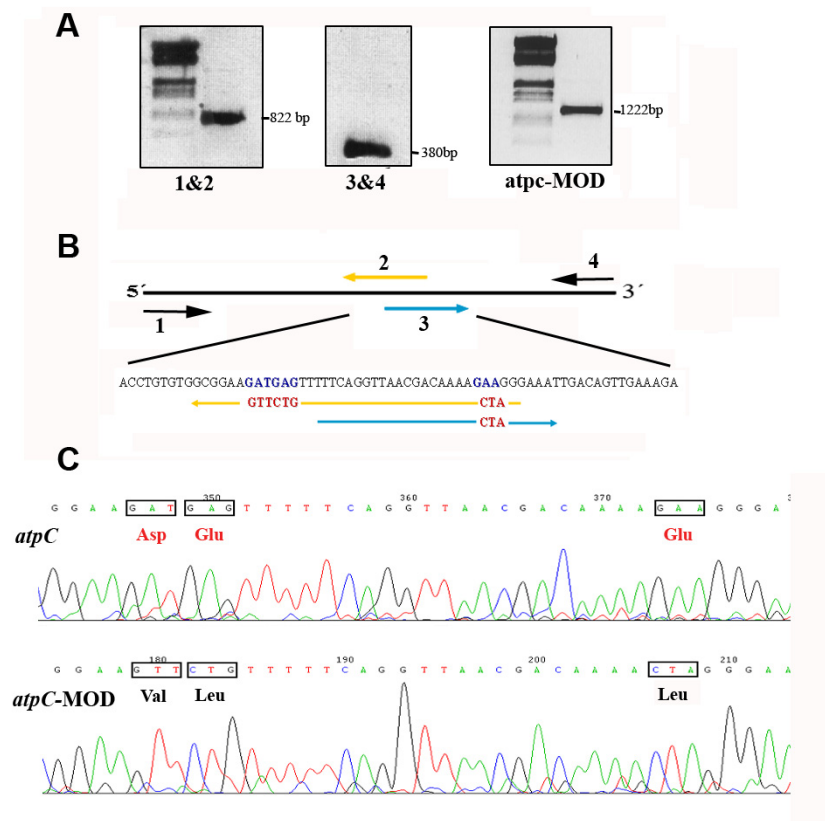


Figure 4.11. Oligonucleotide directed mutagenesis of the *atpC1* gene. **A.** Primers atpC1-Sma-for and atpC1-mod-rev (1&2) amplified a fragment of 822 bp; primers atpC1-mod-for and atpC1-rev-xba (3 & 4) a fragment of 380 bp, **B.**, details of the mutagenesis strategy, and **C.**, sequence analysis of wild type and mutant γ subunit.

4.2.1 ATP SYNTHASE ACCUMULATION IN ATPC-MOD TRANSFORMED LINES

Three independent *dpa1* mutant lines transformed with the modified *atpC1* gene (atpCMOD-c) were selected. The plants grew photoautotrophically and showed a phenotype comparable to wild type. Polypeptide analysis revealed that ATP synthase subunits accumulate in the transgenic lines in the same amount as in the wild type or *dpa1* mutant complemented with the wild type *atpC1* gene (atpC1-c). The charge modification of the γ subunit, due to the exchange of negatively charged amino acids with neutral ones of comparable size (D211V, E212L and E226L) caused a molecular weight shift in one-dimensional SDS PAGE (Fig. 4.12A). The change of the isoelectric point from 6.7 in AtpC1

to 8.6 in AtpCMOD was demonstrated by isoelectric focusing of membrane proteins, followed by Western analysis with γ subunit antibodies (Fig. 4.12B).

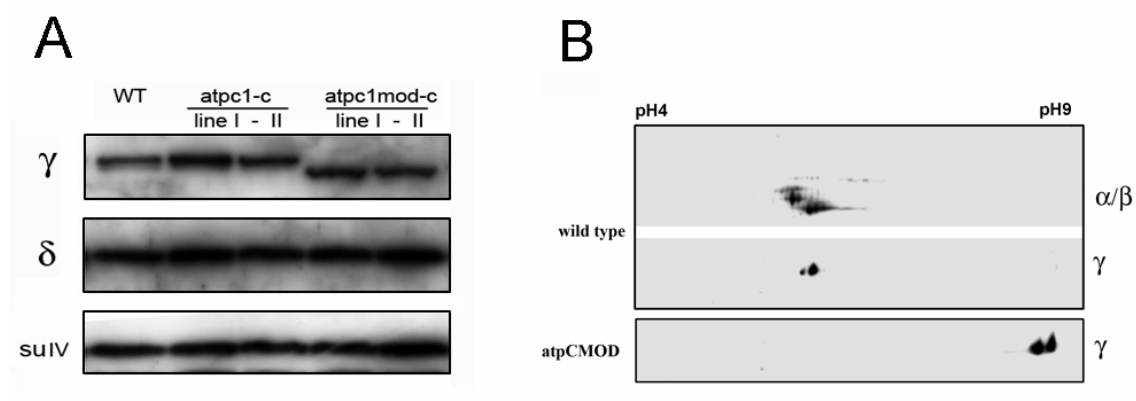


Figure 4.12. A. Western analysis of thylakoid membrane proteins from wild type (WT), two independent *dpa1* complemented plants (*atpc1-c*) and two independent *dpa1* mutant plants transformed with *Atpc1mod* (*atpc1mod-c*). The accumulation of ATP synthase subunits γ , δ , and of suIV of the cytochrome complex were analyzed. No difference in the levels of accumulation was observed. A shift in the apparent molecular weight of the γ -MOD compared to γ -wild type is visible in the one dimensional gel. **B.** 2D membrane protein separation (IEF-SDS gel) and γ subunit detection in wild type and *atpCMOD-c*. α and β subunits were localized at the same IEF point in the two preparations while the γ subunit focused at a more basic pH in *atpCMOD-c* in comparison to the wild type.

4.2.2 CHLOROPHYLL A FLUORESCENCE TRANSIENT AND THYLAKOID Δ pH IN ATPCMOD-C

Exposure of photosynthetically active thylakoid membranes to light results in the activation of the electron transport chain and consequent Δ pH across the membranes. Supply with ADP and Pi induces ATP synthesis which can be monitored as a decrease of the Δ pH due to ATP synthase mediated H^+ translocation. The ATP synthase activity as a function of the Δ pH was measured in thylakoid membranes from wild type or C1MOD-c plants (Fig. 4.13). The experiments were performed at three selected light intensities 12, 45 and 90 $\mu E m^{-2} sec^{-1}$). At 90 $\mu E m^{-2} sec^{-1}$ the Δ pH generated by photosynthetic electron transport was higher than at 12 or 45 $\mu E m^{-2} sec^{-1}$, indicating that the latter are sub-saturating conditions, optimal

to investigate the redox regulation of ATP synthase. DTT was employed to reduce the Cys residues and thus investigate the thiol regulation. No difference could be estimated in presence or absence of DTT in the wild type or C1MOD line (data not shown). This suggests that the thiol reduction is more difficult to induce in the native complex in comparison to the reconstituted $\alpha_3\beta_3\gamma$ subcomplex reported by other groups (Konno *et al.*, 2000; Nakanishi *et al.*, 2004). Moreover, the ATP synthase activity was comparable in the wild type and C1MOD-c plants excluding an inverse regulation of the ATP synthase under oxidizing conditions in the modified ATP synthase complex.

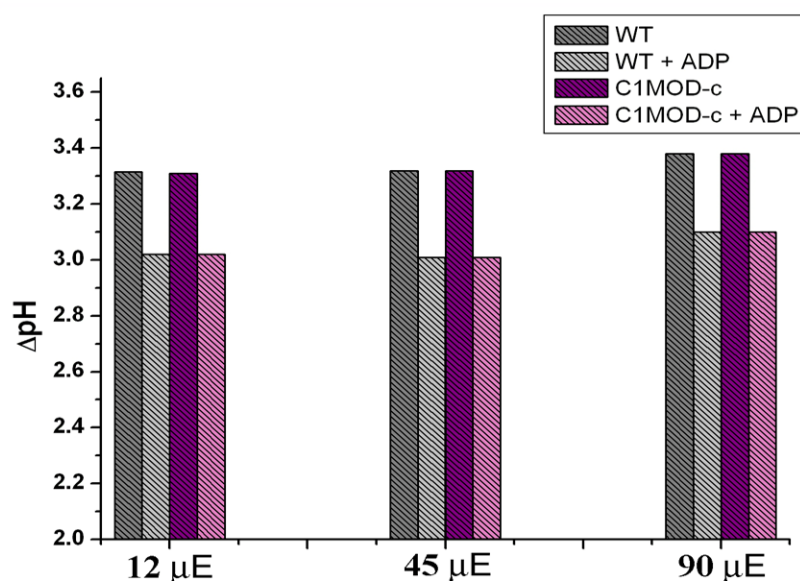


Figure 4.13. ATP synthesis measured as change in ΔpH calculated through aminoacridin fluorescence. The ΔpH was measured on intact thylakoid membranes isolated from wild type (grey) and AtpCMOD-c plants (lilac). The thylakoid were illuminated for 2 min at three different light intensities (12, 45, and 90 $\mu E m^{-2}sec^{-1}$) prior and after supply of ADP.

Another mutant of γ subunit was characterized in *Arabidopsis thaliana* (Govindjee and Spilotro, 2002). This mutant (*cfq*) was characterized for altered kinetics of the energy-dependent quenching during the dark-light transition. The mutant had a single amino acid exchange (E244K) localized 18 amino residues downstream the Asp (E226) substituted in the atpCMOD polypeptide. With a similar approach the non-photochemical quenching induction during fast dark-light transition was investigated in plants with modified γ subunit

Fig. 4.14). No difference to the wild type could be observed. The charged amino acid exchanges in AtpC1MOD have no significant influence on the non-photochemical quenching induction kinetics.

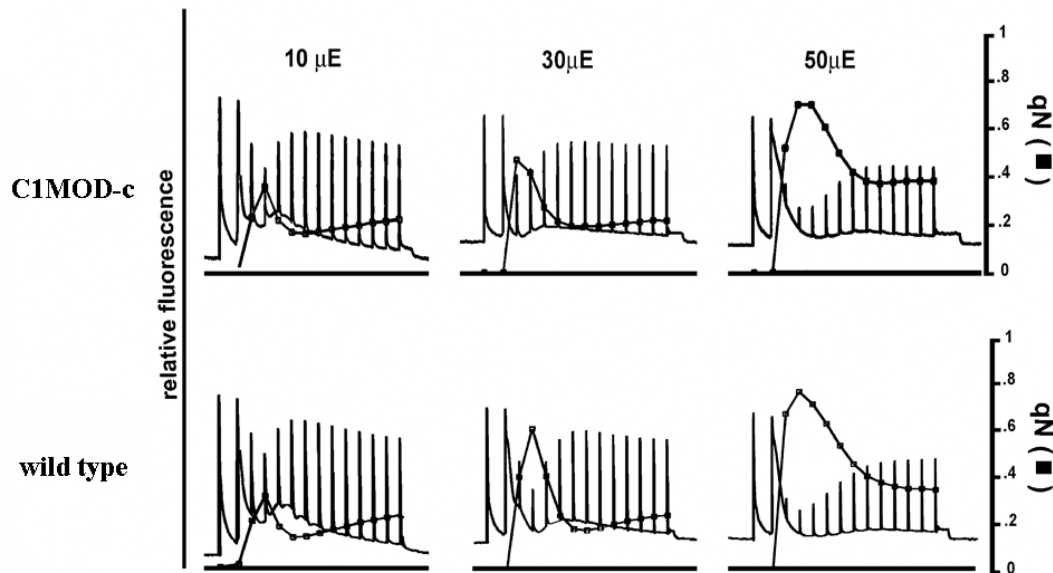


Figure 4.14. Chlorophyll *a* fluorescence pattern and non-photochemical quenching (qN) were investigated in wild type and AtpCMOD-*c* leaves. Plants grown at a light intensity of 100 $\mu\text{E}/\text{m}^2\text{s}$ were dark adapted for 10 min prior to recording the chlorophyll fluorescence at three selected light intensities (10, 30, and 50 $\mu\text{E}/\text{m}^2\text{s}$).

4.3 THE *ATPC2* GENE

Arabidopsis thaliana genome contains the *atpC1* gene encoding the plastid ATP synthase γ subunit, and an additional gene, *atpC2*, encoding a homologous protein of unknown function and localisation.

4.3.1 *ATPC2* IS LOCALIZED IN THE PLASTID

The reporter gene green fluorescent protein (GFP) was used to test if the putative transit peptide of AtpC2 protein is functional. The N-terminal sequence of the AtpC2 polypeptide

was cloned with a GFP expressing vector in order to localize the protein in the plant cell. 349 nucleotides were amplified from *atpC2* gene and cloned in the vector PCR-Script Amp SK(+) using the forward primer T7 and the reverse primer *atpC2*-kpn-rev. The amplicate was digested with *KpnI* and inserted in frame upstream into the *gfp* coding sequence of the pOL vector. Upon transient expression in *Nicotiana tabacum* protoplasts, the GFP localization was visualized (Fig. 4.15). Indeed, in accordance to the cellular localization prediction software for the AtpC2 protein, GFP was imported into the chloroplasts. This demonstrates that *atpC2* contains a functional targeting peptide suggesting that AtpC2, as AtpC1, is localized in the chloroplast.

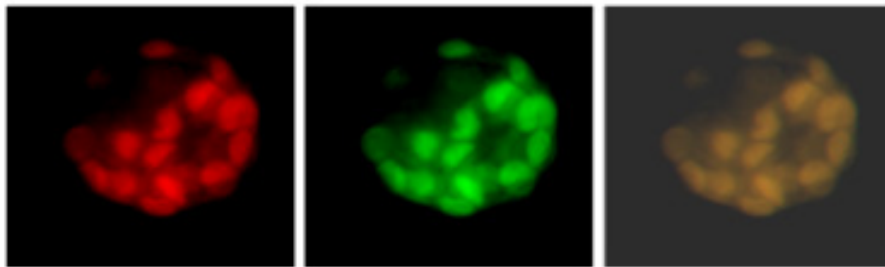


Figure 4.15. Visualization of GFP fluorescence in tobacco leaf protoplast cells. The GFP protein (green) fused to the AtpC2 transit peptide co-localized (merged picture on the right) with the autofluorescence of chloroplasts (red).

4.3.2 *ATPC2* IS EXPRESSED AT A VERY LOW LEVEL IN GREEN TISSUES

At the nucleic acid level the most diverged region between *atpC1* and *atpC2* is localized at the 5' end of the coding sequence. Primers were designed from this region to differentially quantify the mRNA populations of the two genes. By real time RT-PCR analyses the *atpC2* transcript was estimated to be, in leaf tissues, 100 - 150 times less abundant than that of *atpC1*. Moreover, *atpC2* transcript levels were found in comparable amounts in wild type and *dpa1* mutant plants.

4.3.3 OVEREXPRESSION OF *ATPC2* IN THE *DPA1* MUTANT

The very low expression of *atpC2* could be the reason why this gene was not able to compensate the loss of *atpC1* in *dpa1* or the function of the AtpC2 protein could be different from AtpC1. To discern these alternatives, plants heterozygous for the *dpa1* mutation were transformed with a suitable vector carrying the *atpC2* gene controlled by the constitutive strong promoter 35SRNACaMV. The full-length gene sequence was amplified from wild type genomic DNA with the primers *atpC2-sma-for* and *atpC2-xba-rev*. The product was cloned in the vector PCR-Script Amp SK(+) and after sequence analysis it was isolated by restriction with the enzymes *SmaI* and *XbaI*, and inserted into the binary vector pSeX001. Homozygous *dpa1* mutants expressing the transgene were selected on sulfonamide supplemented media and analyzed further.

4.3.3.1 Gene expression in the transformed lines

Real time RT-PCR analysis was used to quantify the levels of expression of the *atpC2* transgene in three selected independent transformed lines. For comparison the expression of *atpC1* in three *dpa1* complemented lines was also analyzed. The same amount of total RNA was employed for the cDNA synthesis with random primers. Specific primers for *atpC1* and *atpC2* were used for the quantification (see Materials). The *Actin2* gene was also quantified as an internal control and confirmed that equal amounts of transcripts were present in all the samples. *AtpC2* was indeed over-expressed in all the transformed lines (Fig. 4.16). With the exception of line II, in line I and III the level of the transgene was higher than *atpC1* RNA in wild type plants. In AtpC1-c plants *atpC1* transcripts were at least 10-fold overexpressed in comparison with wild type. In *dpa1* and *atpC2*-c plants a basic level of *atpC1* transcript was detected. This because the *atpC1* amplified region is at the 5' end of the gene, prior the T-DNA insertion. AtpC1-c lines overall showed a higher level of expression of the transgene (*atpC1*) in comparison to AtpC2-c (*atpC2*).

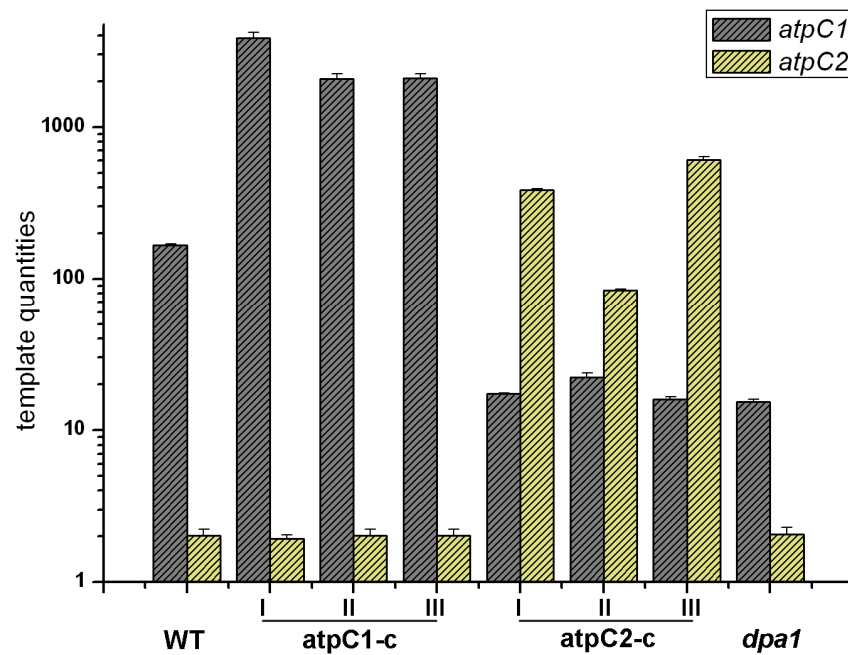


Figure 4.16. Quantities of *atpC1* (grey) and *atpC2* (yellow) transcript segments estimated by real time two-step RT-PCR. Wild type (WT), three independent lines (I-III) of *dpa1* complemented with *atpC1* (*atpC1-c*) or transformed with *atpC2* (*atpC2-c*) and the *dpa1* mutant were analyzed. 1 μ g of total RNA for each sample was used to produce the cDNA. The calibration curves for the quantification were obtained from the same genomic DNA for both genes so that the calculated values can be directly compared. The data, presented in a Log10 scale, are averages of three repetitions.

4.3.3.2 Protein accumulation in the transformed lines

An antigenic region of the predicted polypeptide encoded by the *atpC2* gene was chosen to obtain a specific antiserum for the γ_2 subunit (Fig. 4.17A). Western analysis on plants transformed with *atpC1* (*atpC1-c*) or *AtpC2* (*atpC2-c*) revealed that the antibody was indeed specific and did not recognize subunit γ_1 . γ_2 accumulated in *atpC2-c* lines to a different extent; other ATP synthase subunits α , β and δ followed the same pattern of accumulation. In all three lines the ATP synthase subunits never accumulated to the same amounts as in *AtpC1-c* complemented lines. The highest level of ATP synthase was reached in *AtpC2-c* line III, corresponding to 25% of the wild type level (Fig. 4.17B). Total proteins isolated from the same plants were analyzed for the accumulation of the protein encoded by the *sul* gene, the selectable marker of the pSeX001 vector used for transformation. The marker showed a homogeneous accumulation in the transformed lines.

A pulse labelling experiment with [³⁵S]-methionine (Fig. 4.17D) was performed to elucidate whether the low level of ATP synthase subunits accumulation in *atpC2-c* lines was due to an impaired translation of AtpC2. To reduce the complexity of labelling, synthesis of the plastid encoded proteins was blocked with chloramphenicol. In parallel, Western analysis with AtpC2 antibody was performed on two representative samples (*atpC1-c* and *atpC2-c*) in order to identify the band corresponding to AtpC2 (Fig. 4.17C). The filter was overexposed to reveal unspecific bands that were used as internal markers to facilitate the identification of the γ subunit in the *in vivo* labelling protein pattern (Fig. 4.17C, D). A band could be identified corresponding to the γ subunit clearly overexpressed in *atpC1-c* relative to the wild type (γ_1), (Fig. 4.17D). In *atpC2-c* the corresponding γ_2 band is less intensive than γ_1 in *atpC1* complemented lines but still revealed a higher accumulation level than in the wild type. This excluded that the translation of AtpC2 is limiting the ATP synthase accumulation in *AtpC2-c* plants. However, the pattern resulted in very dense protein bands thus precluding a precise quantification.

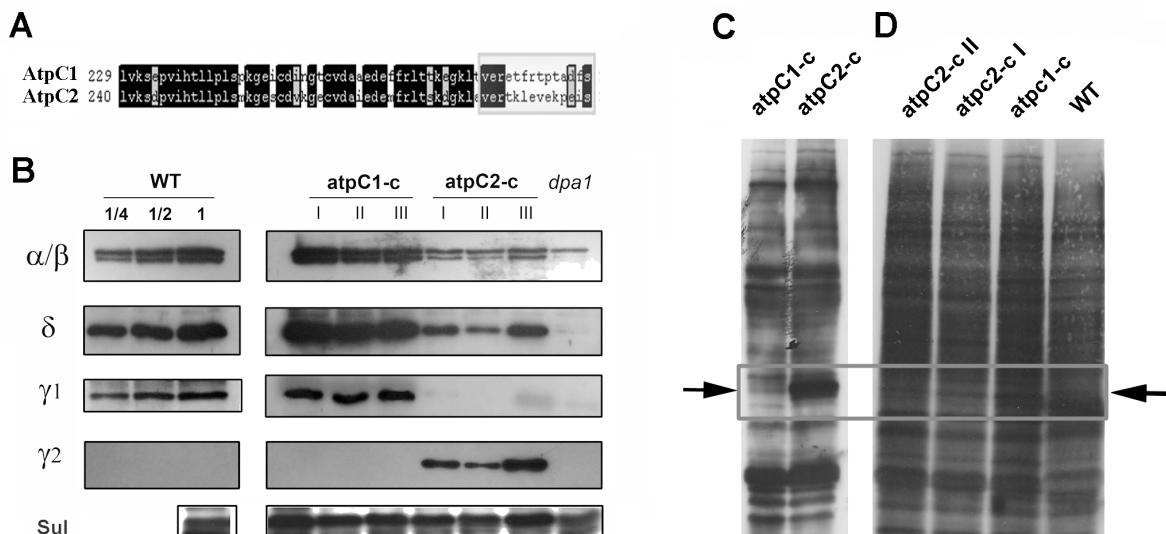


Figure 4.17. **A.** ApC2 peptide selected to generate an antiserum specific for the γ_2 subunit. **B.** Immunodetection of ATP synthase subunit (α , β , γ_1 , γ_2 and δ) on thylakoid membrane proteins isolated from three independent *dpa1* complemented line (*atpC1-c*), three *atpC2* transformed lines (*atpC2-c*), the *dpa1* mutant and wild type (WT) plants. Total protein extract from the same plants were analyzed for the expression of a protein (Sul) encoded by the binary vector used for nuclear transformation. **D.** *In vivo* labelling of nuclear encoded membrane proteins. **C.** Marked with an arrow the band corresponding to AtpC2 polypeptide, identified by Western analysis of *atpC2-c*.

4.3.3.3 *AtpC2* transformed lines are light sensitive

Chlorophyll fluorescence analysis (Fig. 4.18) confirmed the serological characterization of *AtpC2*-c lines (Fig. 4.17B). The mutants were partially complemented and revealed a light sensitivity that was intermediate between the wild type and *dpa1*. At very low light of $10 \mu\text{E m}^{-2}\text{s}^{-1}$ only *atpC2*-cII showed a sensitive development of non-photochemical quenching (qN). In the *atpC2*-cI line a higher light sensitivity than the wild type appeared at $30 \mu\text{E m}^{-2}\text{s}^{-1}$ while the light had to be increased to $50 \mu\text{E m}^{-2}\text{s}^{-1}$ to see an effect in *AtpC2*-cIII. In the three lines the levels of light sensitivity correspond to the abundance of ATP synthase complex accumulation estimated in each of them. In *AtpC2*-cIII, where the highest amount of enzyme was detected, less non-photochemical quenching was induced in comparison with other lines. Nevertheless, *AtpC2* expression is able to restore the photosynthetic efficiency (F_v/F_m) of 0.8 in the transformed lines, except in *AtpC2*-cII, where F_v/F_m is only ~ 0.65 .

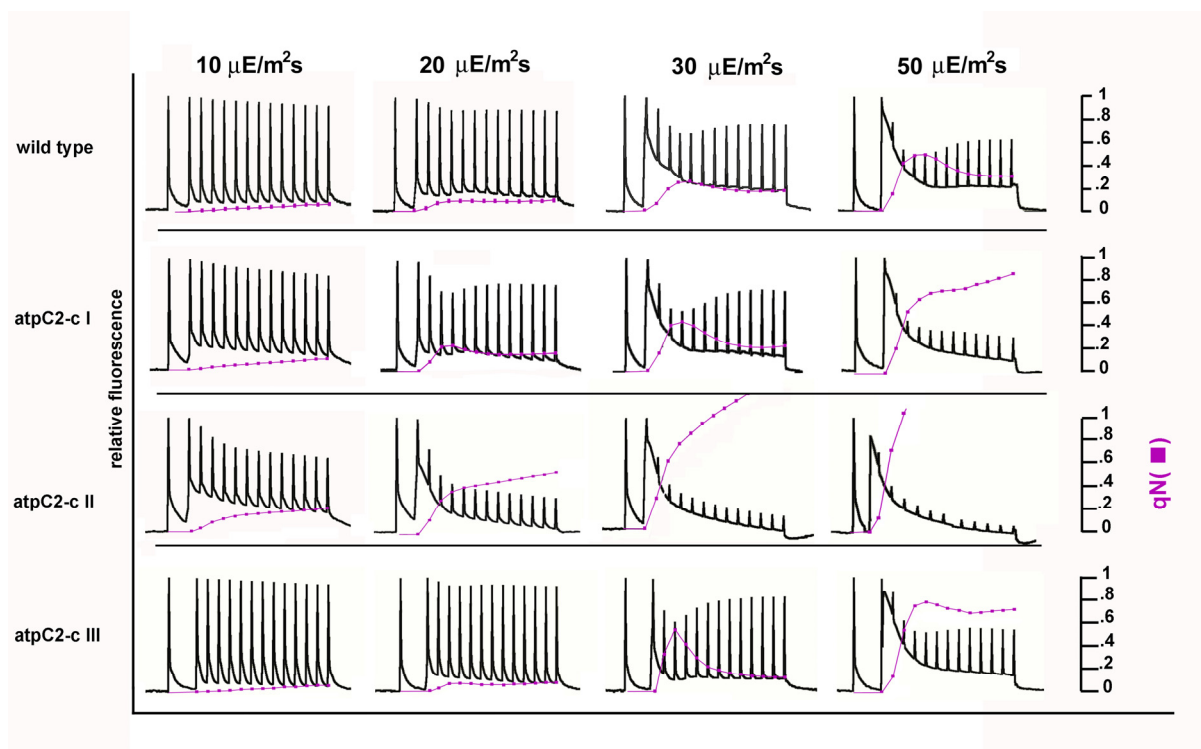


Figure 4.18. *In vivo* chlorophyll fluorescence induction and qN (■) analysis in wild type and three *dpa1* mutant lines transformed with 35SCaMV-*atpC2* (*atpC2*-c). A first saturating pulse was applied at time 0, after 1 minute actinic light was switched on and consecutive saturating pulses were applied at intervals of 20 seconds. The actinic light intensity was 10, 20, 30 and $50 \mu\text{mol of photons m}^{-2}\text{s}^{-1}$.

4.3.4 *ATPC2* KNOCK-OUT LINES

A BLAST search on Insertion Flank Sequences database using the *atpC2* gene sequence (<http://www.arabidopsis.org/Blast/>) allowed to identify the Salk insertion line N562789, which displayed 48 bp homology at position +794 bp relative to the start codon of the *atpC2* gene (Fig 4.19A). Seeds from this line were propagated and individual plants, homozygous for the T-DNA insertion, were identified by PCR. Combination of primers designed on the T-DNA and *atpC2* gene sequences (1&3, Fig. 4.19A) confirmed the presence of the T-DNA generating a 693 bp PCR product. Primers complementary to the region flanking the insertion (1&2, Fig. 4.19A) could not generate any amplificate confirming that the insertion lines were homozygous for the mutation. Due to the very low expression of the endogenic *atpC2* Western analysis would have been of no use to estimate the γ_2 accumulation, thus real time RT-PCR was performed to further characterize the knock-out lines (Fig. 4.19B). While *AtpC1* was expressed at the same level in wild type and *AtpC2* knock-out line, *AtpC2* was clearly reduced in the mutant line (0.46 +/- 0.15 vs 2.6 +/- 0.2). Although the mutation was confirmed, the plants were green, autotrophic and fertile. Immunological studies on selected ATP synthase subunits and chlorophyll *a* fluorescence analysis were comparable to data obtained from wild type.

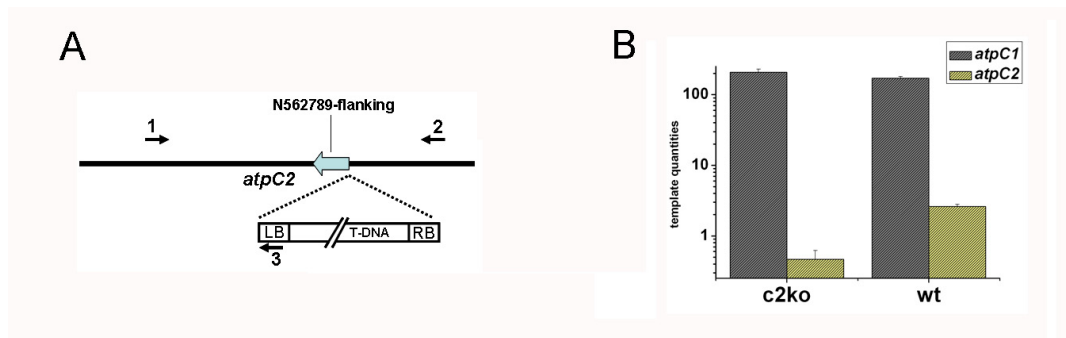
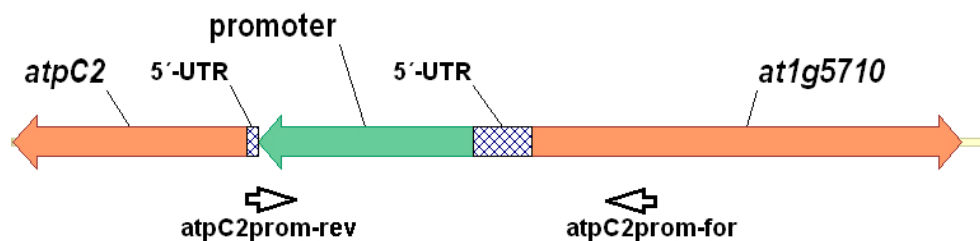


Figure 4.19. Characterization of *AtpC2* knock-out lines. **A.** Schematic presentation of T-DNA insertion and primers used to identify the homozygous lines. Primer 1 (*atpC2*-G16-for) and 2 (*atpC2*-rev-kpn) were chosen from the *atpC2* coding sequence before and after the predicted T-DNA insertion (blue arrow). Primer 3 (LBb1) was from the left border of the T-DNA. The PCR product using primers 1 and 3 demonstrated the insertion and the orientation of the T-DNA. **B.** Real time RT-PCR quantification of *atpC1* (grey) and *atpC2* (yellow) RNA segments in wild type (WT) and *atpC2* knock-out (c2ko) plants.

All together the experiments showed that the loss of function of the *atpC2* in plants grown under standard conditions did not reveal any visible phenotype. Therefore, a more comprehensive analysis was necessary to uncover the importance of this gene.

4.3.5 EXPRESSION ANALYSIS OF THE *ATPC2* PROMOTER

A GUS-GFP fusion protein was used as a marker gene to analyze and compare *atpC2* and *atpC1* promoter regions. 900 bp of 5' flanking region of the *atpC2* gene were cloned in a proper vector for promoter analysis in order to direct the expression of a chimeric GUS-GFP protein. The region comprised the presumable promoter starting at nucleotide -5 from the ATG start codon, until the 5' end of the At1g5710 gene (see Fig.4.20).



```

aaaccaaagacggcgattttgagagcagaggatttgcggtactcggatttgagttgggtttcgtaatcgaaga
tttgggocggcgtcgattgctcgaattcgaagagatcgcggcgggaaatgaggaatgtgggtgaattgcggcgg
agattgggtggagaaatgaggggtttcgccgagagaaatggagtagcattgtgagtagtgttgattgagtttt
agctccaaagtgggagcttagagaaatctgtgagaatagaagaggaagaagcgggttcgccaaggaggaaga
agatgcgagcgcgacctcaaaaaataaacggatcaattttatgtcgtggcctaaacgtgggtgatgctgattgacc
aagaaaaacaaaatgctaaatacacaacaacacaaggaccataatggaaataaaaaattgaggtcaaaattaaa
agtcggttccaaggaaatgttaggtactgttttgtattcatttgatatttagtaaccgcatttacaatatttct
ttttctgaaggactagagtttttatttgcataattttattttgattgttactttaagttcaatctcttcc
tatatatgaatctttaaagaaaatttcgtaattttcatatgctgactatagttgttgttttttggttttcta
ttaatttggtctattttagtaatttttattaggatttaggaggttattgatatttccctcgtttttctcatag
aaaaaaaaaaaaaactctaattttgactttttagtaatttttatatactgaccctaataaacatgataa
ttacagaaaaccctcaagttctctttctttgctcatttcttcacgagaagatgaaatcttaaacctctcaag
ttcagggtcttctttcccaaacgaaaatgacagg

```

Figure 4.20. Genomic 5'-*atpC2* flanking region. 900 bp were amplified with the primer atpC2prom-for and atpC2 prom-rev (boxed) and fused to a GUS-GFP chimeric protein. The amplified sequence is shadowed, and the ATG start codon of *atpC2* gene is in bold.

AtpC2prom-for and atpC2prom-rev primers were used to amplify the genomic region which was cloned using the Gateway cloning system first in pDONOR201 and afterwards in the binary vector. A similar approach was used to clone 900 bp of the *atpC1* promoter region with the primers atpC1prom-for and atpC1prom-rev (Table 2.1, Material).

The constructs were used to transform wild type *Arabidopsis* plants. Seedlings (T1 generation) were selected and analyzed for their GUS activity. 7 - 10 day-old seedlings showed a drastic difference in GUS expression driven either under *atpC1* or *atpC2* promoters. While transformants carrying *atpC1*::GUS-GFP exhibited high levels of GUS activity all over the seedlings (Fig. 4.21A), seedlings in which *atpC2* driven marker gene was incorporated in the genome had a very low GUS activity. Mainly, the signal was localized in the area of the root-hypocotyl junction (Fig. 4.21B). These interesting, but still preliminary, data require further analysis. A homogeneous population of transformants (T2 generation) will be analyzed to determine the potential role and importance of the *atpC2* gene in *Arabidopsis*.

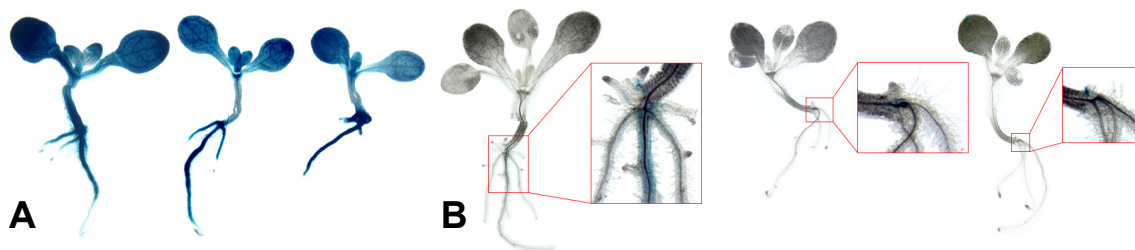


Figure 4.21. Analysis of the activity of the *atpC1* (A) and *atpC2* (B) promoters. Regions where *atpC2* promoter driven GUS expression was detected are magnified.

4.4 TOWARDS ORGANELLE TRANSFORMATION IN *ARABIDOPSIS*

For the development of plastid transformation in *Arabidopsis* the establishment of an efficient regeneration system and selection regime is essential.

4.4.1 EFFICIENT REGENERATION FROM COTYLEDON PROTOPLASTS

An efficient and reproducible regeneration protocol from protoplasts of *Arabidopsis thaliana* was established. Cotyledons from three different *Arabidopsis thaliana* accessions were chosen as sources for protoplast isolation. Several factors may contribute and be important to obtain high yields of uniform and healthy protoplasts which will be later able to regenerate. The best results were obtained with 8 day-old cotyledons grown under continuous light at 25°C and cold treated at +4°C for 24 h in the dark prior to isolation. After 1 h of incubation in MMC medium (preplasmolysis) the cell wall degrading enzymes were added to fresh MMC medium. Cotyledons were incubated in the dark at 25°C for 12 – 24 h and protoplasts were isolated following standard filtration, flotation, and sedimentation (Dovzhenko *et al.*, 1998) and finally immobilized in thin alginate layers (TAL) at the plating density of 1×10^5 ppl/ml.

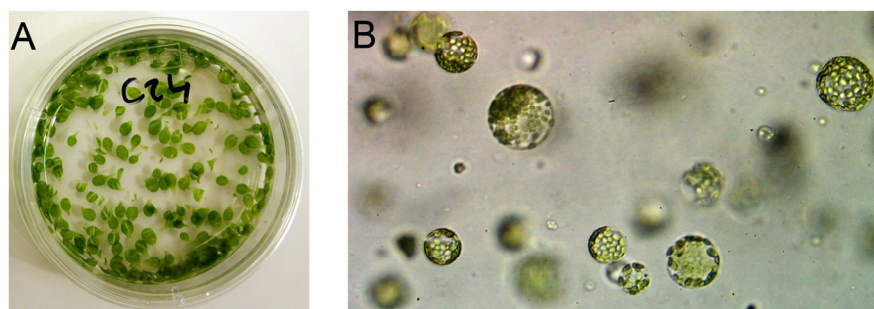


Figure 4.22. A. 8 day-old cotyledons prepared for digestion in a 3 cm diameter Petri dish. B. Freshly isolated protoplasts.

An important factor influencing the plating efficiency of embedded protoplasts and their regeneration capacity is cell density. Different combinations of volumes of culture medium were tested. Small volumes (1 - 2 ml) were detrimental resulting in low plating efficiencies 1 - 6% (Fig. 4.23A, B) versus 16% obtained in 4 ml culture medium in a 3 cm diameter Petri dish (Fig. 4.23C).

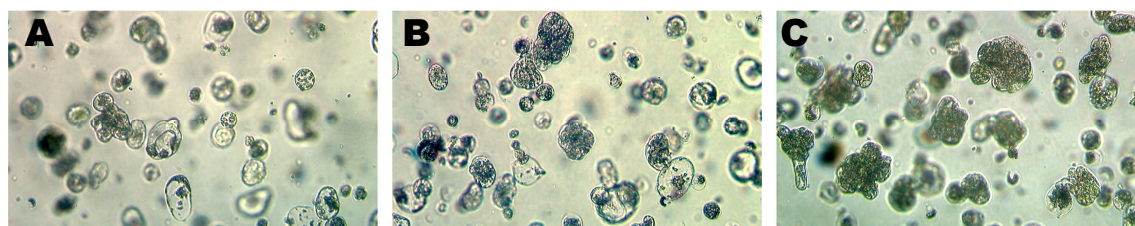


Figure 4.23. Colonies formation from protoplasts cultured in 1 ml (A), 2 ml (B) and 4 ml (C) of PCA medium.

Different phytohormone concentrations were tested. While the plating efficiencies were highest with 3 mg/l Dicamba and 0.5 mg/ml BAP (see Table 4.3), further replacement of the cytokinin BAP with auxin NAA (0.5 mg/l) resulted in fast divisions (first division 24 h after protoplasts isolation) at high efficiencies (20%). Protoplasts of the accession C24 exhibited the best results, reproduced in 4 independent isolations with plating efficiencies of 28%, 27%, 26%, and 30%, respectively.

Table 4.3 *Plating efficiency of cotyledon protoplasts in PCA medium with different hormone components (mg/l); accessions C24, Wassilewskija (Was) and Columbia (Col)*

Dicamba	BAP	C24	Was	Col
1	0.1	0.3%	2%	n/d
2	0.15	2.5%	1.3%	n/d
3	0.3	5.5%	2.7%	n/d
3	0.5	15.5%	5%	2.9%

The lowest plating density at which sustained cell divisions were observed and colonies formed was 5×10^3 to 1×10^4 ppl/ml. Typically, smaller cells (20 - 30 μm) divided first.

The majority of protoplasts (40 - 60 μm in diameter) divided after 2 - 3 days, forming microcolonies of 32 - 64 cells after additional 4 - 5 days of culture. After 12 - 14 days of culture in liquid medium, colonies became macroscopically visible (Fig. 4.24A) and the grids could be transferred to SRA medium for regeneration. First shoot formation was observed after 18 - 19 days of culture (Fig. 4.24B). For estimation of regeneration potential at least 30 protoplast derived calli were transferred to SRA medium (10 calli per 6 cm diameter Petri dish). For all three accessions the regeneration rate was 40 - 60% (Fig. 4.24C). Regenerates were transferred to Magenta vessels with RRA medium and successfully rooted (Fig. 4.24D). Regenerates were fertile and formed seeds under sterile conditions (Fig. 4.24E) (Dovzhenko *et al.*, 2003). Thus, the established protocol could be used either for PEG mediated transformation of *Arabidopsis* protoplasts or for biolistic delivery of the transgenes to protoplast-derived colonies.

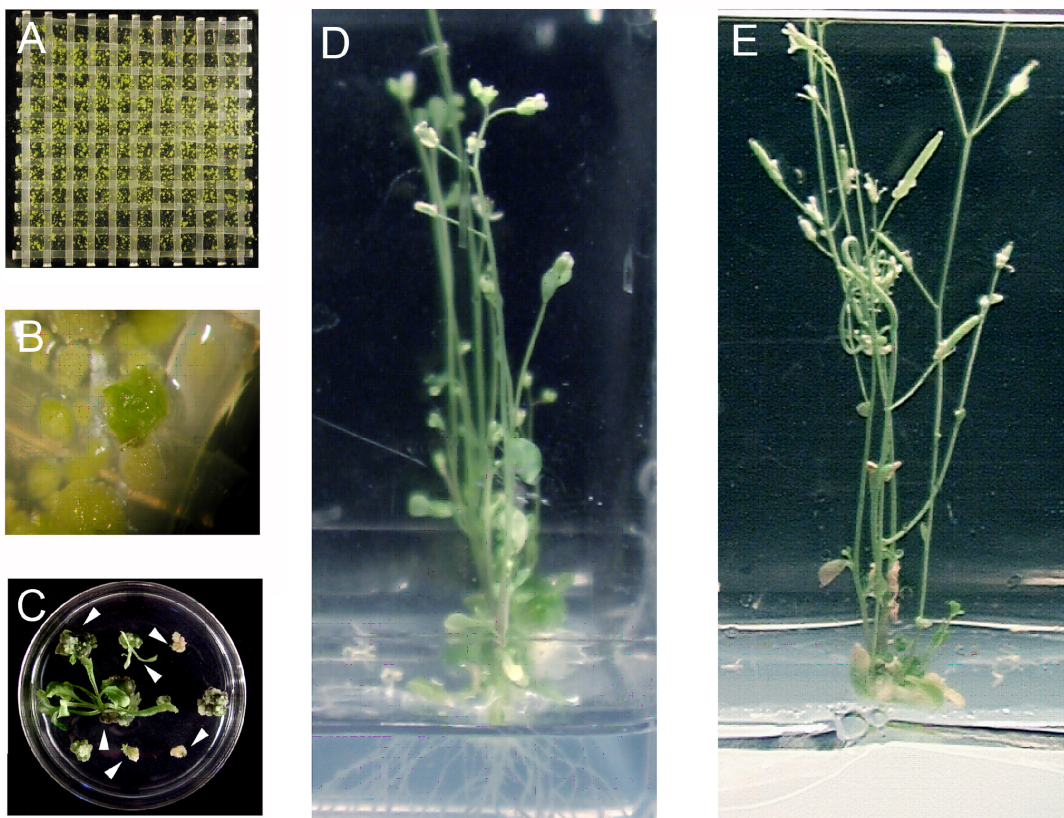


Figure 4.24. A. Protoplast derived colonies after two weeks of culture; B. Shoot initiation from a protoplast derived colony 19 days after protoplast isolation; C. Shoot regeneration after 5 weeks; D. Rooted regenerate after 7 weeks and E. Seeds formation after 9 weeks. (Experiment performed in cooperation with A. Dovzhenko in the laboratory of Prof. H.U. Koop, München, Germany)

4.4.2 DEVELOPMENT OF A SELECTABLE MARKER FOR *ARABIDOPSIS* PLASTID TRANSFORMATION

The marker gene, *aadA*, encodes an aminoglycoside 30-adenyltransferase, an enzyme that inactivates spectinomycin and streptomycin by adenylation. Although other marker genes have been proposed for plastid transformation of higher plants *aadA* remains the most widely used. In tobacco spectinomycin selection results in the recovery of a high frequency of plastid transformants (Svab & Maliga, 1993); in *Arabidopsis*, where plastid transformation is not as efficient, many spectinomycin resistance lines were either spontaneous mutants or the *aadA* gene was incorporated in the nucleus (Sikdar *et al.*, 1998).

The bacterial *sul* gene, fused to the Rubisco transit peptide, was proven to be a successful selectable marker for nuclear transformation in tobacco and *Arabidopsis thaliana*. The mechanism of resistance is basically different from *aadA*. While the latter one inactivates the antibiotic, *sul* encodes an enzyme insensitive to the drug. For a proper function the enzyme (DHPS) had to be imported into the chloroplast. The *sul* gene, cloned in a vector suitable for plastid transformation, could be employed as a potential selectable marker for plastid transformation in higher plants.

4.4.2.1 GFP mediated visualization of the SUL protein *in planta*

In order to optimize the selection conditions on sulfonamide, the green fluorescent protein (GFP) was chosen as additional visual marker to cope with the *sul* gene. A chimeric fusion protein comprising the DHPS resistance marker and the GFP was constructed. This chimeric protein had the double role to identify possible transformants at an early stage of selection and shoot regeneration, and to confirm the plastid transformation by localization. To test whether the fusion was not affecting the DHPS function a pilot experiment was performed. The chimeric protein fused to the Rubisco transit peptide (TP_{rbc}) was used for nuclear transformation of *Arabidopsis thaliana*. The *sul* gene fused to TP_{rbc} was amplified from the pSeX001 vector with the forward primer TP_{rbc}-sma-for and the reverse primer PhyBlink-rev. The *gfp* gene was amplified from the pGFP2 vector with the forward primer PhyBlink-for and the reverse primer GFP-bam-xba-rev. The two genes were fused in a second PCR

amplification step. For the fusion the *sul* stop codon was deleted during gene amplification and a 10-mer (GGGGIDKLDP) linker (Yamaguchi *et al.*, 1999) was introduced between the two proteins. The PCR product was cloned in the pPCR-Script Amp SK (+) cloning vector and sequenced. A fragment with the correct sequence was subsequently isolated by *Sma*I restriction and cloned in pPEX001 plasmid, a binary vector suitable for plant nuclear transformation, carrying the *pat* gene for Basta selection (Fig. 4.25).

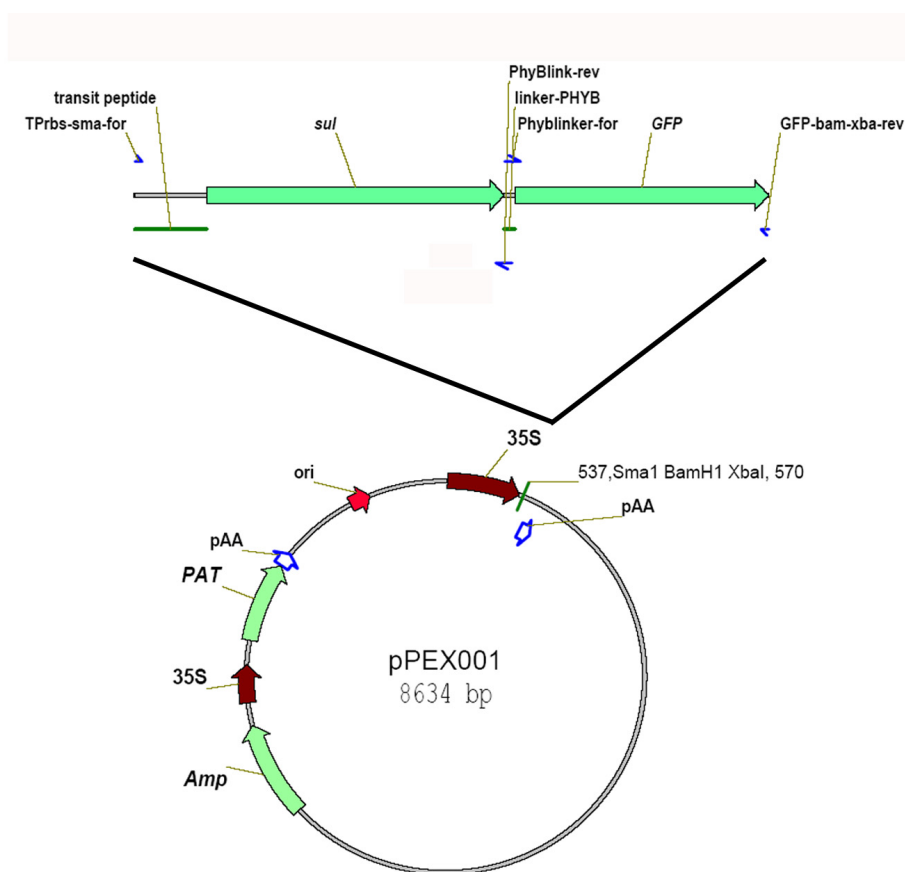


Figure 4.25. Construct used for tobacco transient expression and *Arabidopsis* stable transformation. The sequence interval of the Sul-GFP chimeric protein fused to TPrbc was cloned in the pPEX001 binary vector under constitutive 35S promoter from CaMV (35S). The primers used for the cloning are shown as blue arrows.

4.4.2.2 Sub-cellular localization of the Sul-GFP fusion protein

Transient expression of the SUL-GFP chimeric protein fused to the Rubisco transit peptide (rbcS) in tobacco protoplasts resulted in a green fluorescence that mostly colocalized with the red autofluorescence of chlorophyll (Fig. 4.26). These data confirmed that the TP-rbcS is able to direct the fusion protein into plastids. However, a punctate green fluorescence pattern not clearly localized was also visible in the cells.

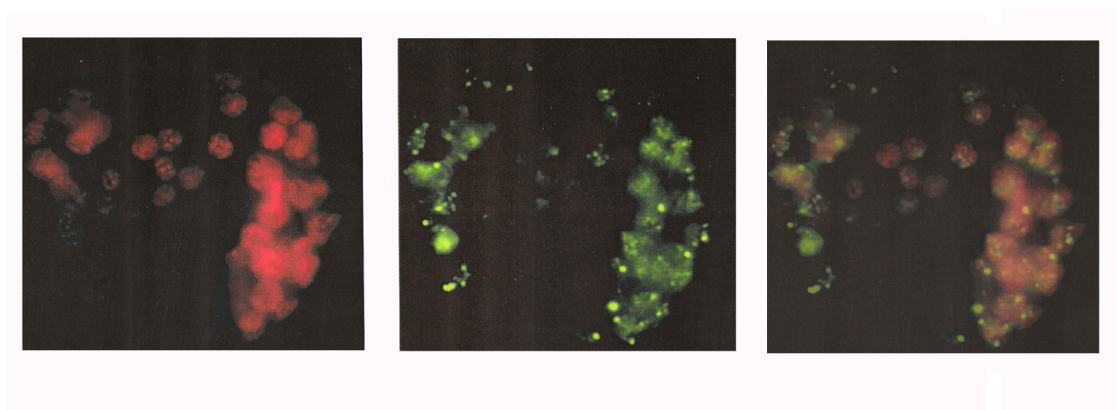


Figure 4.26. Visualization of GFP fluorescence in tobacco protoplast cells. The Sul-GFP fusion protein (green) mostly co-localized with the autofluorescence of chloroplast (red).

4.4.2.3 Sul-GFP efficiency as selectable marker

Arabidopsis plants were transformed using *Agrobacteria* carrying the pPEXOO1-*sul-gfp* vector. The seeds were successively plated on Basta supplemented media to identify the transformants. 15 independent lines, showing green fluorescence under microscope observation, were chosen among the Basta resistant plants. 100 seeds from each plant were plated in the presence either of Basta or sulfonamide. Plants transformed with the pSeX001 vector, i.e. expressing the Sul protein fused with the Rubisco TP, but no GFP, were also plated as a control. While all plants were able to grow under Basta selection, they showed no resistance to sulfonamide. However, the control plants suffered under Basta selection and proved resistance to sulfonamide. Most probably the GFP polypeptide, fused to the DHPS, affects the activity of the enzyme which fails to confer resistance to the antibiotic. Thus the Sul-GFP protein which potentially could be a valuable help, could not be used further for plastid transformation experiments.

4.4.2.4 Cloning of the *sul* gene in a vector for tobacco plastid transformation

Since the *Nicotiana tabacum in vitro* culture has been efficiently established and the plastome routinely transformed this species was chosen to optimize the conditions for the new selectable marker. The *EcoRV-aadA* vector (Regel *et al.*, 2001) was used for efficient transformation of tobacco chloroplasts, thus this vector was modified to test the *sul* gene as a marker. The *sul* coding sequence was amplified by PCR with Pfu polymerase using the pSeX001 binary vector as a template. The forward primer 5-*sul*-*NcoI* and the reverse primer 3-*sul*-*HindIII*, introducing the *NcoI* and *HindIII* restriction sites respectively, were used. The amplicate was cloned in the pPCR-Script Amp SK (+) cloning vector and sequenced. The *sul* gene was further isolated from the vector with the restriction enzymes *NcoI*, *HindIII* and introduced in the *puc18-aadA* cassette vector digested with the same enzymes.

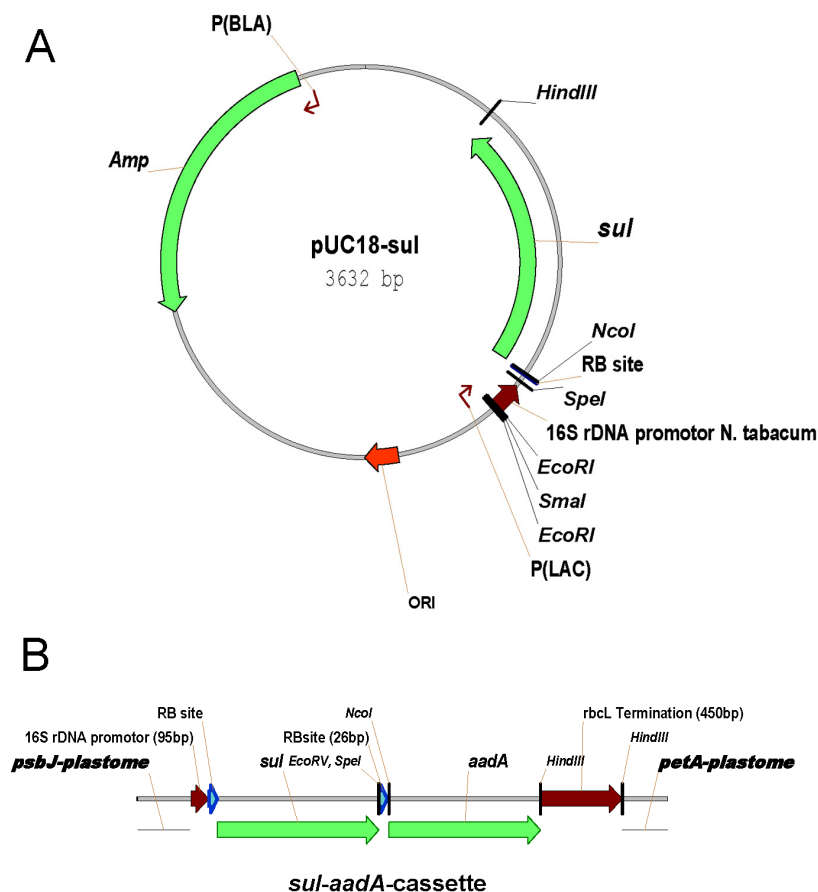


Figure 4.27. Recombinant *sul* gene constructs. **A.** *Sul* fused to the ribosome binding site and 16S promoter in the pUC18 cloning vector. **B.** Novel cassette used for tobacco plastid transformation.

The resulting construct (Fig. 4.27A) was digested with *SpeI* and *HindIII* and, upon Klenow polymerase treatment, the blunt ended fragment was inserted into the linearized and dephosphorilated *EcoRV-aadA* vector at the *EcoRV* site. The vector obtained contained both the *sul* and *aadA* genes each with a ribosome binding site but single promoter and terminator regulatory regions (Fig. 4.27B). The *aadA* gene encoding resistance to spectinomycin was cloned downstream the *sul* gene as additional control.

4.4.2.5 *Nicotiana tabacum* plastid transformation

Concentration series of sulfonamide drug were tested in order to find out the concentration that proved efficient and did not affect plant regeneration. The optimal selection concentration found was 20 mg/l of the drug. Twenty tobacco leaves were used for biolistic delivery of the recombinant plasmid *pEcoRV-sul-aadA*. The same protocol as for spectinomycin selection was adopted for sulfonamide selection. After three days of culture without selection pressure on RMOP medium leaves were cut into small pieces and transferred to RMOP medium containing either spectinomycin 500 mg/l or sulfonamide 20 mg/l. The experiment was repeated five times. While selection on spectinomycin yielded independent regenerates for each experiment, no sulfonamide resistance plantlets were obtained.

4.4.3 DHPS AND FOLATE BIOSYNTHESIS IN *ARABIDOPSIS*

In bacteria DHPS, the target of sulfonamide drugs, is part of a cluster of genes involved in folate biosynthesis. The resistance gene (*sul*) is present on various R plasmids. In higher plants DHPS is part of a bifunctional enzyme, which also exhibits HPPK activity, located in the matrix space of mitochondria (Mouillon *et al.*, 2002). In higher plants, the principal if not sole, site of folate biosynthesis is considered to be mitochondria (Sahr *et al.*, 2005). BLAST search analysis of the *A. thaliana* genome database was performed to isolate the *Arabidopsis* DHPS coding gene. Two cDNAs were identified corresponding to the genes At1g69190 and At4g30000. The two proteins encoded share a high level of homology except for 88 amino acids at the N-terminus of At4g30000 which encodes a putative mitochondrial signal peptide (Fig. 4.28).

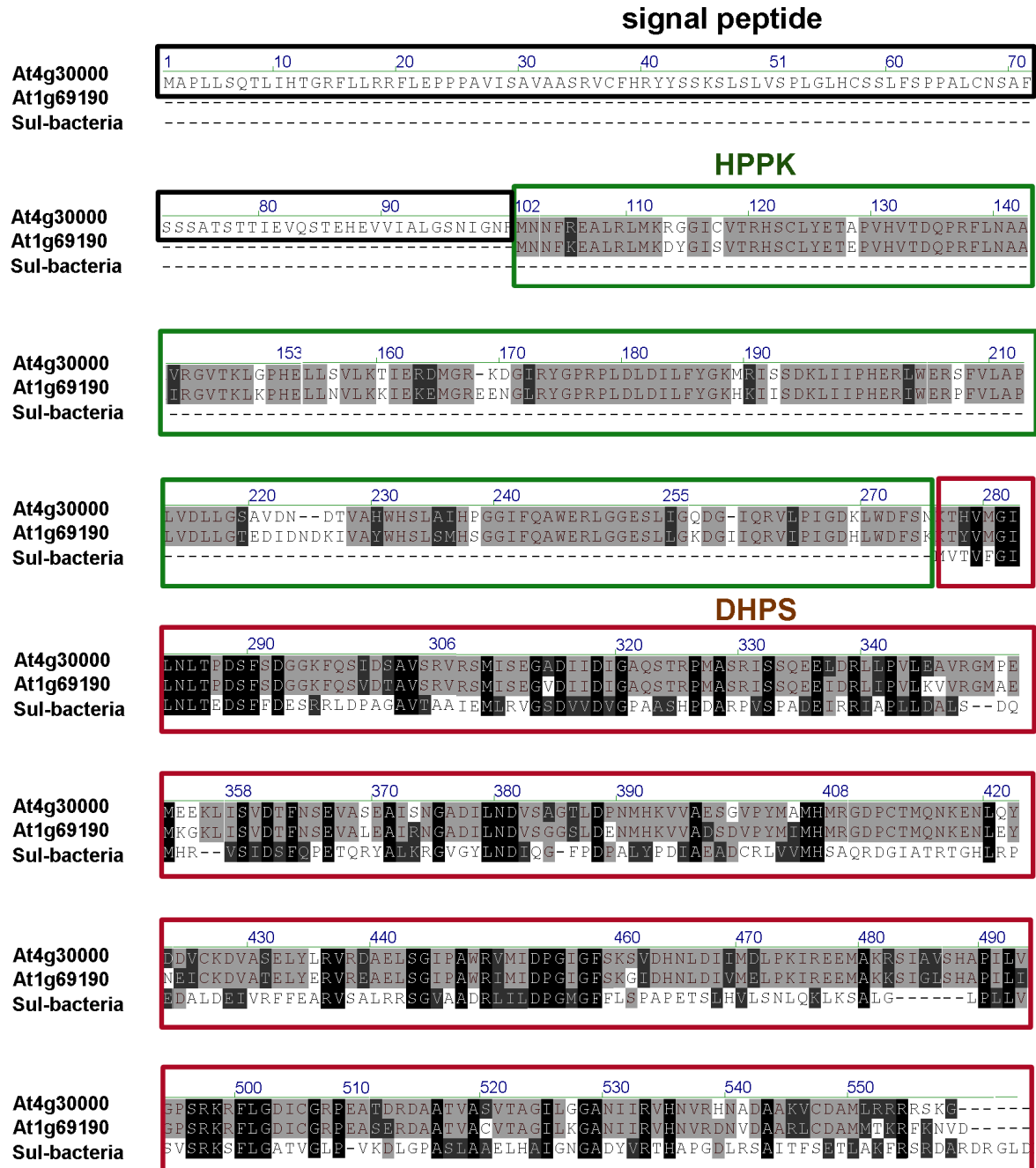


Figure 4.28. Comparison of DHPS predicted sequence encoded by *E. coli sul* gene and *Arabidopsis* At1g69190 and At4g30000 genes. The prokaryotic protein consists of 290 amino acids having DHPS activity. The *Arabidopsis* genes encodes a bifunctional enzyme with HPPK (green) and DHPS (red) activities. At4g30000 encodes a protein containing a hypothetical mitochondrial signal peptide at the N-terminus (black).

In a proteomics approach on *Arabidopsis* plants transformed with pSeX001 vector, *sul* encoded protein was identified in the mitochondrial cellular fraction (personal communication, Dr. H.P. Braun, Hannover). DHPS fused to transit peptide fragments of

different sizes were sequenced revealing that the enzyme was imported into the mitochondria and a misleading processing of the transit peptide was taking place. The mitochondrial translocation of the bacterial DHPS and the subsequent sulfonamide resistance was further investigated as this would imply the possibility to employ *sul* gene as a marker for mitochondrial transformation.

4.4.4 SULFONAMIDE RESISTANCE BY MITOCHONDRIAL TRANSLOCATION OF DHPS

The yeast CoxIV (cytochrome oxidase subunit IV) mitochondrial targeting signal was used to deliver the *sul* gene product to the mitochondria.

4.4.4.1 Localization of the CoxIV fusion protein

The CoxIV signal peptide was amplified from yeast DNA with the forward primer coxIV-for and the reverse primer coxIV-rev-Xho and cloned in frame with the GFP coding sequence at the *Xho*I restriction site of the pGFP2 plasmid. The amplificate consisted of 29 amino acids: 25 amino acid residues for the signal peptide and four belonging to the mature CoxIV protein (Köhler *et al.*, 1997). The vector was used for transient transformation of tobacco protoplasts. Microscopic observation (Fig. 4.29) confirmed the mitochondrial localization of GFP under the CoxIV signal peptide.

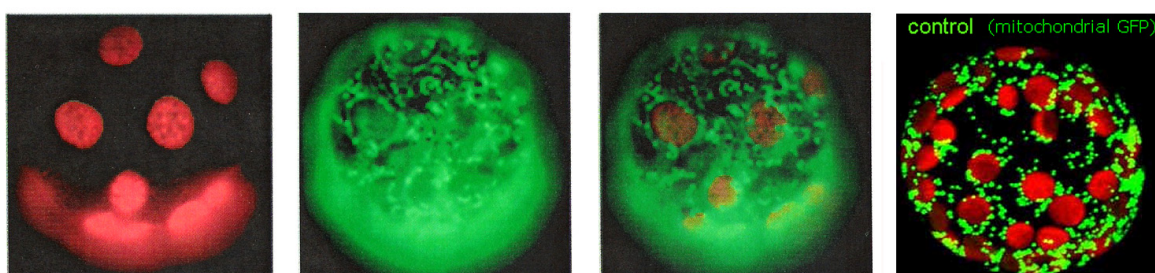


Figure 4.29. Visualization of GFP in tobacco protoplasts. The CoxIV-GFP fusion protein (green) localized in the typical pattern for mitochondria as shown in the control picture (Akashi *et al.*, 1998). There is no overlapping of the green fluorescence with the chlorophyll autofluorescence (red) in the merged picture.

4.4.4.2 Mitochondrial targeting of bacterial DHPS confers sulfonamide resistance to *Arabidopsis* plants

The CoxIV signal peptide was fused to the *sul* coding sequence and cloned into the pPEX001 vector. *Arabidopsis* plants were transformed with the construct obtained and the seeds were plated on Basta supplemented media to isolate the transformants. 15 independent lines were further propagated in order to produce the T2 generation. These seeds were analyzed for their resistance to sulfonamide. All selected lines demonstrated to be both, BASTA and sulfonamide resistant confirming that a mitochondrial translocation of *sul* encoded enzyme is able to confer resistance to sulfonamide.

4.4.5 BACTERIAL DHPS SPECIFIC ANTIBODY

An antigenic region of the predicted polypeptide encoded by the *sul* gene was chosen to obtain a specific antibody for the bacterial DHPS enzyme. A peptide of 15 amino acid residues, having low similarity with *Arabidopsis* encoded DHPS, was selected (Fig, 4.30). The specificity of the immunoserum obtained was tested on total protein isolated from wild type or plants transformed with the pSeX001 vector, thus expressing *sul* encoded enzyme. A specific signal of the expected size ~30 kDa was detected only in the transgenic line. The antibody was monospecific and did not recognize the plant HPPK-DHPS.

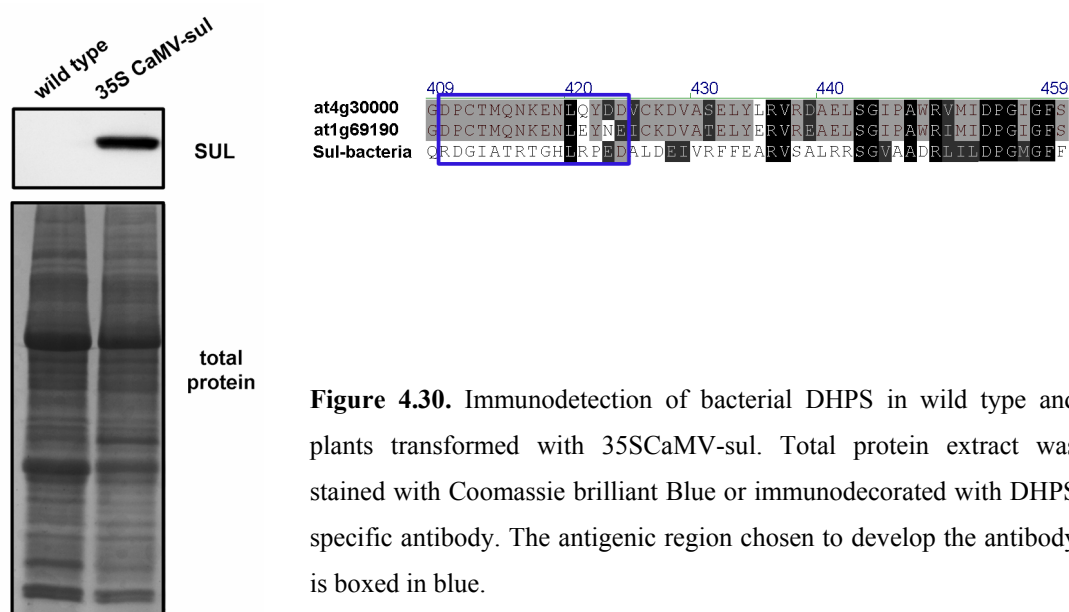


Figure 4.30. Immunodetection of bacterial DHPS in wild type and plants transformed with 35SCaMV-sul. Total protein extract was stained with Coomassie brilliant Blue or immunodecorated with DHPS specific antibody. The antigenic region chosen to develop the antibody is boxed in blue.

These antibodies are intended to be used in future analysis for immunolocalization. The localization of DHPS fused to rbcS or CoxIV transit peptide will be analyzed in plants growing with or without selection pressure.

5 DISCUSSION

5.1 THE γ SUBUNIT IS ESSENTIAL FOR ASSEMBLY OF THE PLASTID ATP SYNTHASE

The *dpa1* mutant which has been induced by a T-DNA insertion into the *atpC1* gene in *Arabidopsis thaliana* was investigated. *AtpC1* is one of the two genes encoding the γ subunit of the chloroplast ATP synthase in *Arabidopsis*. The lack of the γ subunit in *dpa1* affects the accumulation of all the other subunits in the photosynthetic complex (Fig. 4.3A). The second gene, *atpC2*, displays a very low endogenous expression and does not result in detectable amounts of the γ_2 subunit in the mutant (as well as in the wild type, Fig. 4.16B).

Biogenesis of ATP synthases in eubacteria and mitochondria proceeds through the assembly of the soluble F_1 followed by association to the transmembrane FO subcomplex (Klyonsky and Simoni, 1985; Hadikusumo *et al.*, 1988). The independence of assembly of the two subcomplexes is abolished in plastids of the green algae *Chlamydomonas* where a concerted assembly of CF_1 and CFO subunits has been reported for mutants affected in different subunits (Lemaire and Wollman, 1989; Robertson *et al.*, 1989; Smart *et al.*, 1991). The same holds true for *dpa1*, where lack of the nuclear encoded γ subunit affects the accumulation of all other nuclear- and plastid-encoded subunits that constitute the ATP synthase. A model for the assembly pathway that resulted from different mutant analyses and reconstitution experiments predicts an early stage formation of $\alpha\beta$ heterodimers followed by trimerization upon interaction with the γ subunit (Wollman *et al.*, 1999). *In vivo* labelling studies have shown that the plastid-encoded α and β proteins of the CF_1 subcomplex of 55.4 and 53.8 kDa, respectively, are translated at normal rates (Fig. 4.16D). Surprisingly, *de novo* synthesized α and β subunits are associated with the membrane even in the absence of the γ subunit in *dpa1*. This provides new insights into the assembly pathway of the plastid ATP synthase and may imply that either γ is not necessary for the formation of the $\alpha\beta$ hexamers prior to assembling into the membrane or that the $\alpha\beta$ dimer can already associate to the membrane mediated by yet unidentified chaperones in the chloroplast. In yeast mitochondria at least two chaperones play an important role in the assembly of the α and β subunits into the F_1 oligomer (Ackerman, S.H., 2002). The *atpC2* gene, when over-expressed, results in

an increased accumulation of ATP synthase in *dpa1* thylakoid membranes, albeit never at wild type levels (Fig. 4.16B). Thus a very low endogenous presence of γ_2 may be sufficient to contribute to the assembly of the $\alpha\beta$ subunits to the CFo in *dpa1*. On the other hand, binding of α and β to CFO mediated by δ and b' can not be excluded.

Overexpression of *atpCI* in complemented lines did not result in increased amounts of the ATP synthase complex, nor of the γ subunit, compared to the wild type (Fig. 4.16B). Thus, an increased expression of several or all genes of the ATP synthase might be necessary to regulate the abundance of the complex or, more likely, the regulation of complex abundance takes place at a translational or post-translational level.

5.2 LOSS OF THE CHLOROPLAST ATP SYNTHASE CAUSES HIGH NON-PHOTOCHEMICAL QUENCHING

Several ATP synthase mutants in *Chlamydomonas* have been shown to be light-sensitive (Majeran *et al.*, 2001) and the same is true for *dpa1*. As a consequence of the ATP synthase disruption, accumulation of a large electrochemical gradient through the thylakoid membrane that induces qE, the energetic component of NPQ, might be expected (Müller *et al.*, 2001). Therefore, quenching of the fluorescence was in fact also expected to occur in *Chlamydomonas* ATP synthase mutants. Surprisingly, the major effect in the *Chlamydomonas* mutants is a light intensity-dependent rise of the steady state fluorescence level (F_s) up to a level very close to F_m (Majeran *et al.*, 2001). It has been suggested that $\Delta \mu_{\text{H}^+}$ -dependent NPQ was not induced under the experimental conditions. In contrast to the alga, in *dpa1*, increasing light intensity results in an increased NPQ and a drop of F_s even below the initial dark F_o level (Fig. 4.4). This difference shows that fluorescence signals and quenching mechanisms differ significantly between green algae and higher plants. A different extent in the dissipation of excess absorbed light energy has been described in respect to the xanthophyll cycle for the *npq* mutants of *Chlamydomonas* and *Arabidopsis* (Niyogi *et al.*, 1997; Niyogi *et al.*, 1998). Inactivation of the violaxanthin de-epoxidase results in an impaired NPQ of 25% in *Chlamydomonas* and of 85% in *Arabidopsis*, suggesting a larger contribution of xanthophyll cycle-dependent NPQ in *Arabidopsis* compared with the green alga (Niyogi *et al.*, 1998).

5.3 POST-ILLUMINATION FLUORESCENCE INCREASE IS DUE TO RELAXATION OF THE THYLAKOID PROTON GRADIENT

The mechanism of fluorescence quenching and the unusual relaxation that occurs in darkness have been characterized. Analysis of the relaxation kinetics in the dark allowed to investigate different factors separately (Fig. 4.5). Far-red light did not influence the relaxation kinetics of the quenching in the dark. Therefore, the post-illumination fluorescence increase in the dark is not due to reduction of plastoquinone or Q_A (Fig. 4.5A). In the presence of the uncoupler nigericin strong quenching was abolished in *dpa1* and exciton quenching relaxed when nigericin was applied during fluorescence induction (Fig. 4.5C). These results demonstrate that a low luminal pH causes strong NPQ below the F_0 level in *dpa1*. This is in contrast to the *cfq* mutant that is affected by a decreased Δ pH across the thylakoid membrane due to a higher proton conductivity of the ATP synthase. Consequently, NPQ was decreased under moderate light intensities in *cfq* (Govindjee and Spilotro, 2002). High energy quenching, qE, as the main component of NPQ depends on low luminal pH, the activation of xanthophyll cycle and involves protonation of acidic amino acids on the LHCII polypeptides, in particular PsbS (Müller *et al.*, 2001). At lower temperatures, formation of zeaxanthin known to be involved in NPQ is slowed down (Niyogi *et al.*, 1998). The quenching kinetics and relaxation mechanisms in the dark are highly temperature-sensitive in *dpa1*. This suggests that NPQ in *dpa1* is due to the temperature-dependent activity of the violaxanthin de-epoxidase involved in the xanthophyll cycle. Application of the uncoupler nigericin clearly shows that relaxation of quenching in the darkness is due to dissipation of the pH gradient across the thylakoid membrane. Leakage of the membrane increases with increasing the temperature consistent with the temperature-dependent relaxation of quenching. However, it cannot be excluded an additional temperature effect on the quenching mechanism itself because the biophysical mechanism of chlorophyll de-excitation is still unknown (Horton *et al.*, 2005).

An increased F_0 in *dpa1* results in a reduced ratio F_v/F_m of 0.5 ± 0.1 as compared with 0.80 ± 0.02 in wild type. This is indicative of disturbances in PSII that may be related to a partial disconnection of the outer antenna or accumulation of reduced Q_A molecules. Because no ATP formation takes place, electron acceptors in the form of $NADP^+$ cannot be regenerated, and the photosystems suffer from photoreduction. However, far-red light which excites PSI

preferentially was unable even to partially reduce F_o of dark-adapted plants (data not shown) indicating that the increased F_o is independent of accumulation of reduced quinones. Moreover, under still moderate light intensities NPQ is able to quench up to 40% of F_o probably to protect PSII from photodestruction.

Substantial quenching below the initial F_o fluorescence level during illumination was also observed in several other *Arabidopsis* mutants such as *hcf109* (Meurer *et al.* 1996, 2002) and in a tobacco *psbF* point mutation (Bondarava *et al.*, 2003). This quenching also relaxes after switching off actinic light and reaches the F_o level with similar kinetics to those found in *dpa1*. Because investigation is missing whether far-red light or uncoupling had an effect on the quenching mechanism in these mutants, it remains to be shown whether the observed dark increase of fluorescence is due to reduction of quinones.

5.4 PHOTOPROTECTIVE ROLE OF qE

To identify proteins involved in qE, *Chlamydomonas* and *Arabidopsis* mutants with altered NPQ of chlorophyll fluorescence were isolated (Niyogi *et al.*, 1998; Li *et al.*, 2000). Two genes, *npq1* and *npq2*, are both involved in the xanthophyll cycle, whereas *npq4* encodes the PsbS protein. In *Chlamydomonas* a defect in the chloroplast ATP synthase did not allow a light-dependent increase in qE which leads to fast degradation of PSII (Majeran *et al.*, 2001). Even if PSII is affected in *dpa1* as evidenced by the lower value of F_v/F_m , no considerable effect on the accumulation of PSII proteins could be observed (Fig. 4.4B). Again, this suggests a protective role of qE on PSII. The *dpa1* mutant could develop a very high qE already under moderate light condition, but, if the PsbS protein was missing, the plant could no longer perform qE, consistent with an increased photoinhibition during a short-term high light stress (Fig. 4.8). Overexpression of PsbS increased the qE capacity in *Arabidopsis*. Furthermore, plants with higher qE capacity were more resistant to photoinhibition than the wild type (Li *et al.*, 2002). Increased qE was associated with decreased photosystem II excitation pressure and changes in the fractional areas distribution of the chlorophyll *a* fluorescence lifetime, except the chlorophyll centers, suggesting that qE protects from photoinhibition by preventing over-reduction of photosystem II electron acceptors. The important role of NPQ in photoprotection implies that NPQ itself has to be modulated in response to rapid changes of physiological conditions. Recently, it has been

shown that the chloroplast ATP synthase is involved in modulation of NPQ (Kanasava and Kramer, 2002). The proton conductivity of the enzyme, as estimated by measurement of the electrochromic shift at 520 nm, is altered at different CO₂ concentrations. This allows the modulation of the relationship between photosynthetic electron transport and NPQ. The *dpa1* mutant represents an extreme example with maximal proton accumulation which only relaxes through leakage of the membrane.

5.5 UP-REGULATION OF NUCLEAR PHOTOSYNTHETIC GENE EXPRESSION IN *DPA1*

In the *dpa1* mutant a preferential down-regulation of the differentially expressed genes is observed. A different, and more balanced, response of transcriptional regulation was observed for photosynthetic genes, for which about an equal number of genes were up- or down-regulated. The changes in the accumulation of transcripts for photosynthetic genes could be interpreted as a reaction of the plant to the altered physiological states of thylakoids due to the loss of ATP synthase function. It appears possible that under the conditions induced by the *dpa1* mutation particular components of the photosynthetic apparatus are more rapidly degraded and that corresponding nuclear genes are up-regulated as a compensatory response, e.g. genes of the ATP synthase. On the other hand, up-regulation of genes encoding the cytochrome *b₆/f* complex, e.g. *petM*, might result in higher levels of this complex (Fig. 4.3B and Table 4.2). Another possibility is that distinct subunits of the photosynthetic apparatus are down-regulated to decrease the photosynthetic activity of corresponding complexes that could be harmful in the absence of ATP synthase activity. However, a previous comparison of the differential expression of photosynthetic proteins and their transcripts in the *prp111-1* mutant (Kurth *et al.*, 2002) has shown that complex interdependencies of mRNA and protein levels can occur in photosynthetic mutants. This includes situations where nuclear genes are up-regulated but the levels of corresponding proteins are decreased, due to the interaction of plastome- and nuclear-encoded proteins in photosynthetic multiprotein complexes (Kurth *et al.*, 2002). However, taken together, the transcriptional regulation of photosynthetic genes differs from the general trend (Fig. 4.9), clearly indicating that the plant might be able to monitor the altered photosynthetic state due to loss of ATP synthase activity and to respond by regulating the expression of appropriate photosynthetic genes.

5.6 *ATPC2* IN *ARABIDOPSIS* AND HIGHER PLANTS

Arabidopsis contains two genes encoding for the chloroplast gamma subunit, *atpC1* and *atpC2* (Inohara *et al.*, 1991). By comparison of the primary sequence of AtpC1 and AtpC2 it was suggested that both proteins contain an N terminal transit peptide of 50 and 60 amino acids respectively and GFP visualization proved that AtpC2 transit peptide is able of chloroplast localization. Nevertheless AtpC1 was found to be the predominant species in illuminated plants and *atpC1* knock out mutation revealed that the second gene cannot compensate for the gene loss.

Pairwise comparison between the γ subunit mature forms from different plants revealed a higher homology between AtpC1 and γ subunit of other sources rather than AtpC1 and AtpC2 of *Arabidopsis* (Fig. 5.1). This suggests that the γ subunits of higher plants, so far isolated, are encoded by *atpC1* gene orthologs. Possibly the *atpC2*, due to its very low expression, could not be isolated in higher plants other than *Arabidopsis*.

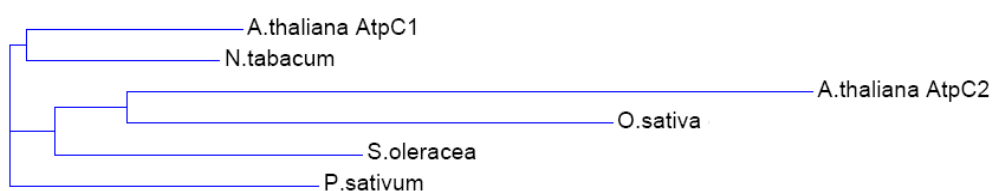


Figure 5.1 Phylogenetic analysis of the chloroplast ATP synthase gamma subunit proteins. The phenogram was produced with VectorNTI software using AlignX application , matrix BLOSUM62mt2.

5.7 IS *ATPC2* A FUNCTIONAL γ SUBUNIT?

Under normal growth conditions *atpC2* is expressed more than 100 times less than *atpC1*. This low abundance could be the reason why *atpC2* cannot complement the *atpC1* loss of function. Over-expression of *atpC2* in *dpa1* was performed in order to investigate this hypothesis. The gene was successfully transcribed and at least in two lines a higher level of

expression than of *atpC1* in wild type plants was confirmed. However, the ATP synthase as a complex s never accumulated in the transformed lines at the same level as in the wild type (Fig. 4.17B) and chlorophyll fluorescence measurements (Fig. 4.18) revealed a general higher development of qE in the transformed lines. At a first view it appeared that AtpC1 and AtpC2 are not fully interchangeable; AtpC2 is unable to completely complement the *dpa1* mutant.

On the other hand, all three lines are viable and can be propagated on soil in the homozygous state. AtpC2 is actually able to accumulate a functional ATP synthase complex and partially rescues the mutant. Therefore, it has been shown that the low expression of *atpC2* is the limiting factor to functionally complement *dpa*. The fact that the amount of the γ_2 subunit correlates with the different capacity to perform qE in the different lines,, i.e. the higher the protein accumulation the lower qE confirms that AtpC2, *per se*, is a functional γ subunit. The limiting step seems to be the ability to accumulate the enzyme as in the wild type. With *in vivo* labeling experiments (Fig. 4.17D) it was intended to investigate whether loss of complete complementation by AtpC2 was due to impaired translation efficiency or complex stability. A band could be identified that accumulated at higher level in *atpC1* and *atpC2* complemented lines in comparison to the wild type although, due to the very dense protein pattern, it was difficult to estimate the AtpC2 efficiency of translation *versus* AtpC1. Even if it remains to be understood whether AtpC2 is translationally or post-translationally regulated, it is questionable whether the low accumulation is related to a possible function of AtpC2.

The subcomplex formed by $\alpha_3\beta_3\gamma$ is a functional ATPase with ATP hydrolysis activity; it is conceivable that AtpC2 could assemble an active ATP hydrolysis complex. Moreover, if γ_2 cannot form a stable attachment to CFo, its expression could balance the relative proportion of the two activities under changing environmental or tissue-specific conditions. Mature AtpC1 and AtpC2 γ subunits share 72% homology while the similarity between AtpC1 and other γ subunits is higher. From a closer observation of the polypeptide sequences (Fig. 5.2) it emerges that the lower similarity is due also due to amino acids which are otherwise highly conserved in the other species. Specific features that have been demonstrated to play a critical role for the γ function, like the Cys involved in thiol modulation, the Glutammic acid causing the *cfq* phenotype (Govindjee and Spilotro, 2002), the C-terminal α -helix,

important for the γ - β interaction (Boltz and Frasch, 2005). They are conserved in subunit γ_2 . The γ subunit has a central position in the ATP synthase complex, it is surrounded by the $(\alpha\beta)_3$ ring with which it interacts during the catalysis. Other important interactions are with CF_o ring which drives the γ rotation and with ϵ subunit. The structure is a coiled coil from the N- and C-terminal α helices. The differences with other γ subunits that have been pointed out by the alignment in AtpC2 might influence the structure of the γ and/or the interaction with other subunits.

5.8 REGULATION OF *ATPC1* AND *ATPC2* EXPRESSION

To disclose the function of *atpC2* a classic forward genetic approach was applied. The loss of function of *atpC2* in T-DNA insertion knock-out plants did not cause any strong visible phenotype, as *dpa1* for example. Additional information about the endogenous expression of *atpC2* could help in hypothesizing its function. The expression profiles of *atpC1* and *atpC2* in different tissues were investigated using the publicly available software Genevestigator[®] (Zimmermann *et al.*, 2004) (<https://www.genevestigator.ethz.ch/at/>) (Fig. 5.3). The low endogenous expression of *atpC2* was confirmed this way. In leaf tissue *atpC2* is ~100 times less abundant than *atpC1*. A higher amount of *atpC2* transcript is found in seed, shoot apex and rosette. Only in radicles from seedlings the two genes are expressed in comparable amounts. Interestingly the relatively higher level of *atpC2* expression is found in those tissues where *atpC1* is expressed at a relatively lower level. The comparison of the regulatory region of the two genes proposed by Inhoara *et al.* (1991) did not reveal similar motives between the two genes. A GT-1 binding site typical of light responsive genes like Rubisco (Green *et al.*, 1987) and phytochrome (Kay *et al.*, 1989) are found in the control region of *atpC1*, but not of *atpC2*.

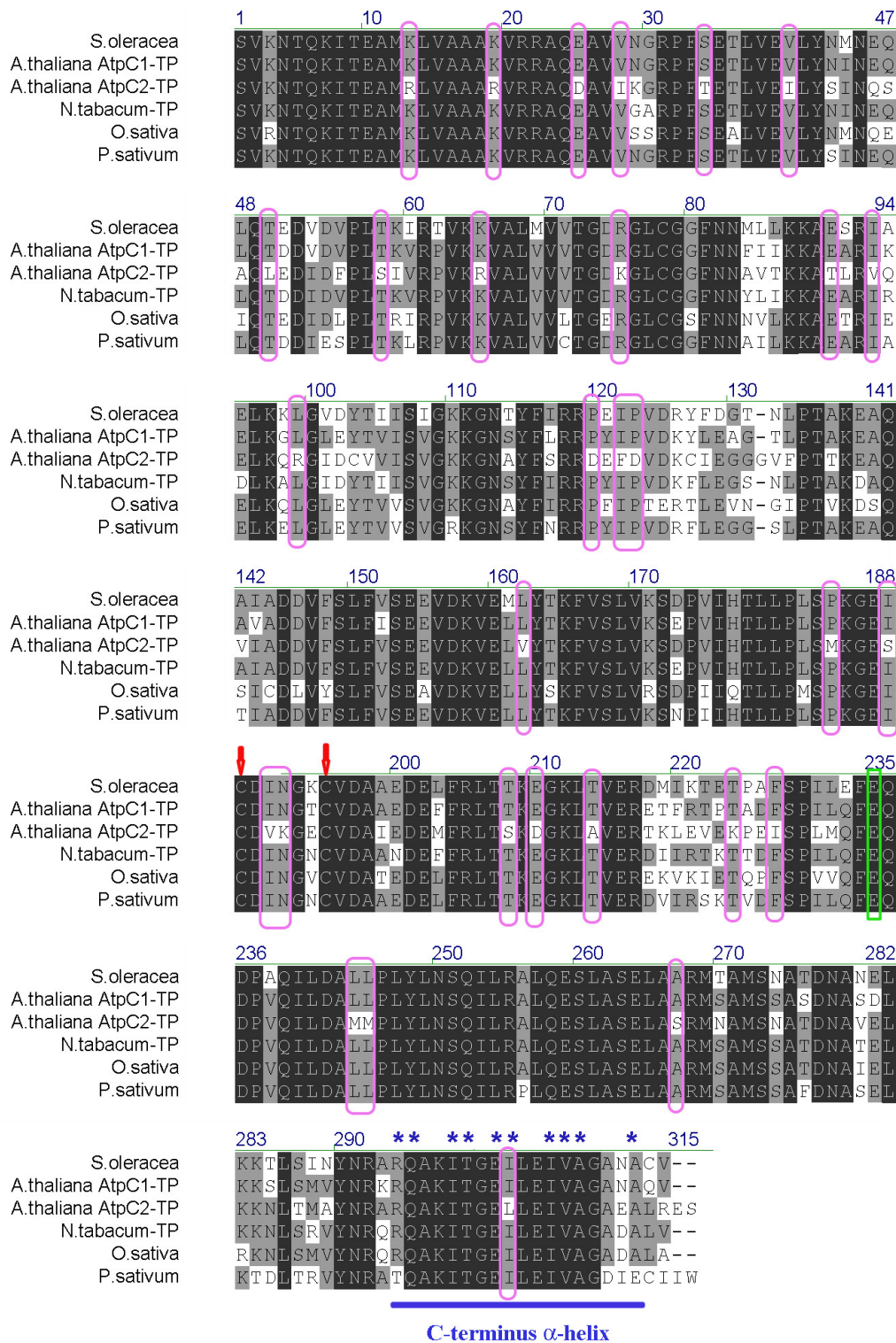


Figure 5.2 Protein alignment of mature γ subunits from different sources. The amino acids residues conserved in all the subunits are shaded in black. Boxed in pink amino acids conserved in all γ_1 subunits but in γ_2 . The Cys involved in thiol modulation are indicated with red arrows. The amino acid causing the *cfq* phenotype are boxed in green. The C-terminal α helix is important for interaction with β subunits. In detail, the amino acids marked with asterisks have been demonstrated to play a direct role for the γ - β interaction (Boltz and Frasch, 2005).

Only a unique sequence was found in both promoters AA(T or A)₂ ACTCTAATT(C or T)₂(T or G)ATC(C or T)TTTGT which could be important for transcriptional regulation (Inhoara *et al.*, 1991).

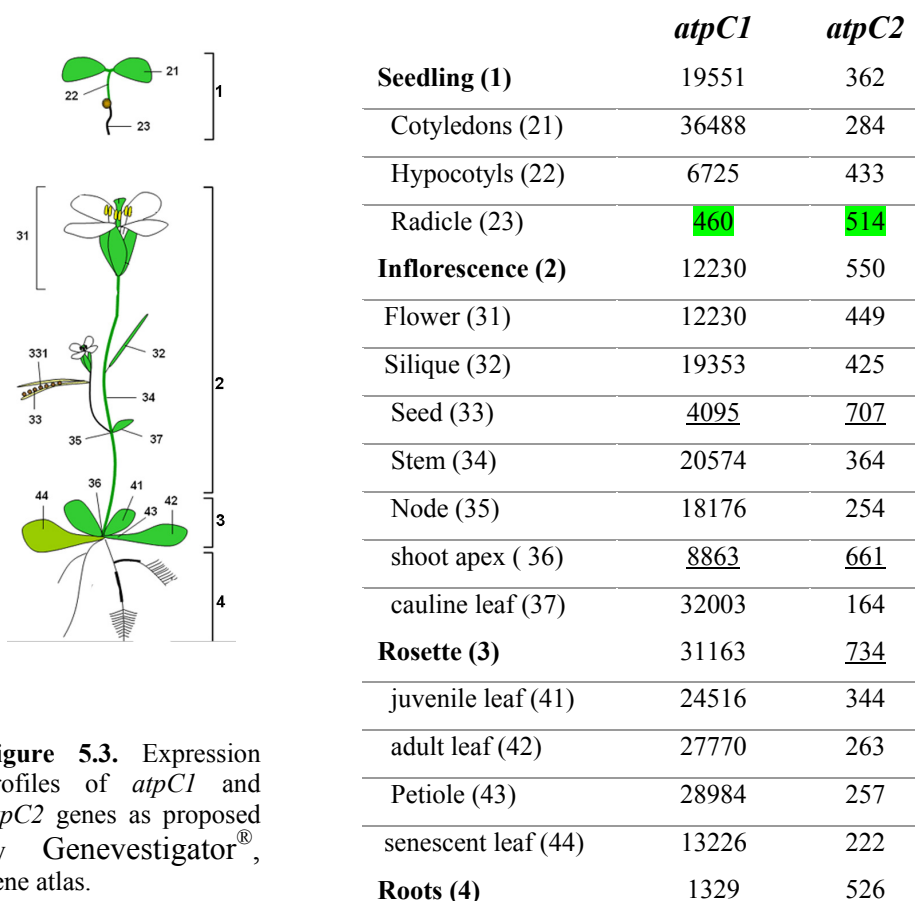


Figure 5.3. Expression profiles of *atpC1* and *atpC2* genes as proposed by Genevestigator[®], gene atlas.

We performed a promoter analysis cloning 900 bp of the 5' flanking region of both genes. Preliminary observations could be made on T1 transformants (Fig. 4.20). The GUS staining confirmed the gene expression data according to which *atpC2* is expressed at a low level in green tissues. The *atpC1* promoter regulated GUS accumulation revealed an overall high level of expression in almost all tissues. The *atpC2* promoter induced a GUS staining accumulation localized at the root-hypocotyl junction. These data are in agreement with the expression profile on seedlings where a higher level of *atpC2* transcripts is seen in the radicles. Although this is valuable information, the *atpC2* function remains elusive. Once the uniform T2 seeds will be available the promoter analysis will be performed testing different developmental stages and growth conditions.

5.9 IN VIVO ANALYSIS OF ATP SYNTHASE THIOL MODULATION

The two Cys residues are responsible for thiol modulation of chloroplast γ subunit as has been demonstrated introducing the missing nine-residue sequence into *Synechocystis* (Fig. 1.3) and restoring the γ thiol modulation in this organism (Werner-Grüne *et al.*, 1994). Since then, several reconstitution experiments with chimeric $\alpha_3\beta_3\gamma$ complex, where α and β were from F1 prokaryotic origin and recombinant γ from spinach CF1, were performed in order to characterize the mechanism of thiol modulation (Hisabori *et al.*, 1997, Hisabori *et al.* 1998, Konno *et al.*, 2000, Bald *et al.*, 2001, Nakanishi *et al.*, 2004). In Konno *et al.* (2000) it was shown that the substitution of three negatively charged amino acid residues of the regulatory region of the γ subunit with neutral ones (E210A–D211A–E212A in Fig. 4.10) made the complex activity insensitive to DTT. On the other hand, the deletion of the same residues had the effect to inverse the redox regulatory function, i.e., reduction caused a decrease of the ATP hydrolysis activity. Furthermore, with the same chimeric complex an inverse redox regulation of the γ rotation was observed (Nakanishi *et al.*, 2004). Two of the charged amino acids modified in AtpC1MOD corresponded to two that were investigated by Konno and coworkers (2000). In an ATP synthesis assay no difference could be found in comparison to the wild type complex, under oxidizing conditions (Fig. 4.13). On the other hand we could not induce DTT reduction and observe thiol modulation in our system. It is conceivable that a DTT interaction with a native complex may be more problematic than working with an isolated CF1 subcomplex. Thus further improvements for the analysis of thiol modulation on a native complex are needed.

The third charged amino acid which was modified in AtpC1MOD (E226) was more distant from the two Cys residues forming the sulphhydryl bridge (Fig. 4.10). In the *Arabidopsis thaliana cfq* mutant (Govindjee and Spilotro, 2002), a single modification of another highly conserved glutamic acid group (E244K) in the γ subunit influenced the non-photochemical induction kinetics. Moreover, the *cfq* mutant grown in a 16 h photoperiod exhibited a slightly stunted growth. Although the authors do not explain why this amino acid causes such a phenotype we expected that the mutation of a close, also highly conserved negatively charged amino acid residue could have a similar effect. The non-photochemical quenching induction during dark-light transition at the conditions adopted in our chlorophyll fluorescence analysis is not altered in the mutant plants. The plants also did not exhibit an

altered growth phenotype when grown on soil under standard green house condition. Evidently, the two glutamic acid residues, although highly conserved among plant γ subunits and not far localized between each other, do not share functional features.

5.10 EFFICIENT *IN VITRO* REGENERATION FROM COTYLEDON PROTOPLASTS OF *ARABIDOPSIS THALIANA*

The sole report on meaningful *Arabidopsis* plastid transformation (Sikdar *et al.*, 1998) suffered from the ability to obtain fertile plants after *in vitro* regeneration from plant leaves. The authors suggested that the lack of fertility could be due to extensive polyploidy of leaf tissue. We have chosen young cotyledons as starting material and, as a first step, developed an efficient regeneration system from cotyledons derived protoplast.

Different factors were essential for rapid division of cotyledon protoplasts. The TAL technique (Luo and Koop, 1997) was one of the key steps for fast and successful shoot regeneration from leaf protoplasts of *A. thaliana* (Luo and Koop, 1997), *Oenothera hookeri* (Kuchuk *et al.*, 1998), *Nicotiana tabacum* (Dovzhenko *et al.*, 1998), the closely related species *Brassica napus* and from callus protoplasts of *Beta vulgaris* (Dovzhenko and Koop, 2003). This technique proved to be essential for fast development of *Arabidopsis* cotyledon protoplasts as well.

Protoplast embedding using filter-sterilised alginic acid solution and the addition of ammonium succinate, 20 mM for tobacco (Dovzhenko *et al.*, 1998), and 2.5 mM for *Arabidopsis* (Masson and Paszkowski, 1992) leaf protoplasts were beneficial. However, both had a detrimental effect on cotyledon protoplast development. In contrast to sugarbeet protoplasts (Hall *et al.*, 1997), the antioxidant *n*-propylgallate inhibited cell divisions even at low concentrations (0.05 mM). Modifications in mineral and organic composition of PCA culture medium (Luo and Koop, 1997) resulted in fast cell divisions and high plating efficiencies up to 30%. Protoplasts of accession C24 exhibited the highest plating efficiency. Optimal concentrations of casein hydrolysate, L-glutamine, coconut water (Sigma, St. Louis, Mo., U.S.A.), Mg^{2+} , and Ca^{2+} were determined (see Methods).

Further improvement of the phytohormone composition (Table 4.2) allowed to obtain first cell divisions within only 24 h after protoplast isolation. Replacement of the cytokinin 6-benzylaminopurine (0.15 mg/l) with the artificial auxin α -naphthylacetic acid (0.5 mg/l) resulted in fast divisions at high frequencies. Thus, cotyledon protoplasts do not require cytokinins for divisions and colony formation. Higher volumes of protoplast culture medium (4 ml) were advantageous, resulting in higher plating efficiencies in comparison to 1 or 2 ml (Fig. 4.23).

The established regeneration system is efficient and protoplast growth with subsequent regeneration is very fast; rooted regenerates were obtained after 7 weeks (Fig. 4.24D). The method described could be useful for somatic hybridisation experiments. It may also be useful for the generation of nuclear transformants via direct gene transfer. However, our main interest lies in the ability to perform plastid transformation in *A. thaliana*. Polyethylene glycol treatment of protoplasts is a means to introduce foreign DNA into chloroplasts of higher plants (Golds *et al.*, 1993). Bombardment of *Arabidopsis* leaves resulted in only a few transformants that were sterile (Sikdar *et al.*, 1998), and a protoplast-based system could be an efficient alternative. Freshly isolated protoplasts or protoplast-derived microcolonies could be useful for either the polyethylene glycol method or the biolistic method (Huang *et al.*, 2002).

5.11 DEVELOPMENT OF *SUL* AS A SELECTABLE MARKER

A breakthrough in chloroplast transformation technologies was the development of the first chloroplast specific resistance marker, a bacterial aminoglycoside 3'-adenylyltransferase gene (*aadA*) conferring resistance to a number of antibiotics of the aminoglycoside type, including spectinomycin and streptomycin. The AAD protein catalyzes the divalent transfer of an AMP residue from ATP to spectinomycin, thereby converting the antibiotic into an inactive form that no longer inhibits protein biosynthesis on prokaryotic 70 S ribosomes as present in the chloroplast. For many years *aadA* has been the most effective selection system for chloroplast transformants. Alternative selectable markers for tobacco chloroplast were more recently described: betaine aldehyde dehydrogenase (Daniell *et al.*, 2001) and *aphA-6* (Huang *et al.*, 2002).

Arabidopsis, as other Brassicaceae, demonstrates a higher level of resistance to spectinomycin; seedlings bleach but the growth is not arrested (Zubko and Day, 1998). This makes *aadA* an unfavourable selectable marker for *Arabidopsis*. The importance of an efficient selectable marker was proven with the introduction of the *aadA* itself. Earlier a chloroplast 16 S ribosomal RNA gene engineered to be resistant to spectinomycin and streptomycin was utilized for chloroplast transformation, but with efficiencies 100 times lower than *aadA* (Svab and Maliga, 1993).

As the *sul* gene fused to the Rubisco small subunit transit peptide seemed to be an efficient marker in nuclear transgenic *Arabidopsis* it was decided to engineer the gene for chloroplast transformation. In preliminary experiments using tobacco for plastid transformation we could not obtain sulfonamide resistant plastid transformants. The utilization of a visual marker, as GFP, could provide a useful tool to optimize the selection condition, allowing the visual identification and isolation of possible transformants (Siderov *et al.*, 1999). Unfortunately, the fusion seemed to interfere with the catalytic function of the DHPS enzyme.

As already explained, the idea to use *sul* as a chloroplast marker was based on the evidence that the fusion with a chloroplast transit peptide was able to confer resistance to the sulfonamide drug. However, the tetrahydrofolate biosynthetic pathways in higher plants has a unique and complex subcellular compartmentation split between three compartments (see Introduction, Fig. 1.5). In this model the HPPK-DHPS enzyme, target of sulfonamids is located in the mitochondria. In pea leaves the protein is synthesized with a mitochondrial signal peptide, its activity is detected only in mitochondria and Southern analyses suggested a single copy of the gene in the genome (Rebeille' *et al.*, 1997). Nevertheless subcellular compartmentation of DHPS-HPPK was not investigated.

The sulfonamide resistance that was observed in *Arabidopsis* nuclear transformants carrying the Rubisco small subunit transit peptide-*sul* fusion could arise from a dual targeting of the protein to chloroplast and mitochondria. Indeed a proteomics analysis carried out on *Arabidopsis* plants transformed with pSeX001 vector revealed the presence of the DHPS polypeptide in the mitochondria. The sequences showed different truncations of the transit peptide indicating that import and processing of the peptide were impaired. A standard *in*

in vitro assays for import into isolated pea chloroplasts and mitochondria demonstrated that, while chloroplast protein import is highly specific because mitochondrial proteins were not imported to any detectable levels into the organelle, pea mitochondria imported a range of chloroplast protein precursors with the same efficiency as chloroplasts (Cleary *et al.*, 2002). The import capability of mitochondria, combined with the selective pressure of the sulfonamide drug, could indeed drive the DHPS to the organelle so that the observed resistance of the transformed plants would arise from the mitochondrial targeting of the protein marker, rather than from plastid targeting.

When *sul* was fused to the CoxIV signal peptide, specific for mitochondria localization (Köhler *et al.*, 1997), the transformants were resistant to sulfonamide. This confirms that the site for *de novo* folate biosynthesis is the mitochondrion and the localization of HPPK-DHPS is also in this organelle. However, in *Arabidopsis* two genes encode a HPPK-DHPS protein (Fig. 4.28). Comparison of the predicted polypeptide revealed a high level of homology for the two functional domains (HPPK and DHPS) and an N-terminal extension, presumably the mitochondrial signal peptide, for one of them. The second gene, lacking any signal peptide, codes a putative cytosolic HPPK-DHPS. An alternative cytosolic biosynthetic pathway can not be excluded at this stage. Moreover, it is interesting to note that in other eukaryotes like *P. falciparum* (Triglia and Cowan, 1994) or *P. carinii* (Volpe *et al.*, 1992) the reported ORF sequences coding for HPPK/DHPS do not indicate the presence of a signal peptide. Moreover the cytoplasmatic HPPK-DHPS would also have a preferential access to the substrates, since H₂Pterin is believed to be synthesized in the cytosol and *pABA* has also to cross the cytosol to reach the mitochondria.

In any case, whether a cytosolic pathway takes place or only a mitochondrial one, there is no evidence for a chloroplast DHPS activity. This definitely excludes a use of *sul* as a marker for plastid transformation. Interestingly, this opens the possibility to use *sul* as a marker for mitochondrial transformation.

Mitochondrial transformation has been achieved to date only in *Saccharomyces cerevisiae* (Johnston *et al.*, 1988; Fox *et al.*, 1988) and *Chlamydomonas reinhardtii* (Randolph-Anderson *et al.*, 1993). The transformation in yeast and in the alga is dependent on the ability to grow non-lethal mitochondrial mutants and to genetically manipulate restoring the

mutated function. This approach can bypass the lack of an antibiotic, specifically affecting the mitochondria, for which a suitable resistance gene could be used as selectable marker. However, this strategy cannot be applied to multicellular eukaryotes such as higher plants. A more general selection system was proposed (Mireau *et al.*, 2003) based on the RNase Barnase and Barstar, a specific Barnase inhibitor. The RNase was cytoplasmically synthesized and targeted to the mitochondria, and the inhibitor encoding gene, Barnase, was integrated to the mitochondrial genome and represented the gene marker. This was the first report of gene insertion in a wild type mitochondrial chromosome. The system is elegant although elaborate. A general antibiotic-based selection system would certainly be preferable. Moreover, no further reports on mitochondrial transformation using this system have followed. Targeting of the DHPS to mitochondria has been demonstrated to confer resistance to sulfonamide in higher plants. Thus, *sul* could be an obvious solution to construct marker that will finally open the way to mitochondrial transformation in higher plants.

6 SUMMARY

ATP synthase is one of the major photosynthetic complexes that represents one of the smallest molecular motors known in nature. The rotating γ subunit is a key feature of this enzyme. It contains features specific for the chloroplast ATP synthase. In this work the γ subunit has been functionally analyzed in *Arabidopsis thaliana*.

- The nuclear gene *atpC1* encoding the γ subunit of the plastid ATP synthase has been inactivated by T-DNA insertion mutagenesis. In the seedling-lethal *dpa1* mutant the absence of detectable amounts of the γ subunit destabilizes the entire ATP synthase complex and consequently photophosphorylation is abolished. However, *in vivo* protein labelling analysis suggests that assembly of the ATP synthase α and β subunits into the thylakoid membrane still occurs in *dpa1*. Further effects of the mutation include an increased light sensitivity of the plants and an altered photosystem II activity. A high non-photochemical quenching develops with increasing actinic light intensity. It has been shown that a high proton gradient is responsible for most quenching (qE). The photoprotective role of qE was further demonstrated in the double mutant *dpa1* x *psbS* in which PsbS, essential factor for qE, is missing. Expression profiling of 3292 nuclear genes encoding mainly chloroplast proteins demonstrates that most organelle functions are down-regulated while the mRNA expression of some photosynthesis genes is significantly up-regulated, probably to compensate for the defect in *dpa1*.

- The expression of a second gene copy, *atpC2*, is unaltered in *dpa1* and is not sufficient to compensate for the lack of *atpC1* expression. The two proteins, AtpC1 and AtpC2, share less similarity than AtpC1 of *Arabidopsis* with γ subunits of other plant species suggesting that the γ subunits so far isolated in other plant species are AtpC1 orthologs. It has been established that AtpC2 is also imported into the chloroplast. Therefore, it is likely that the chloroplast ATP synthase complexes contain both *atpC1* and *atpC2* encoded γ subunits. However, the *atpC2* gene is expressed more than hundred times at a lower level than *atpC1* and array data show the differential and tissue specific expression of the two genes. The function of AtpC2 could not be revealed by inactivating the gene. Overexpression of *atpC2*

in *dpa1* generated viable lines with an ATP synthase complex containing only γ_2 , although the wild type phenotype is not completely restored.

The second part of this work regarded the optimization of conditions for plastid transformation in *Arabidopsis thaliana*.

- An efficient and fast regeneration system from cotyledon protoplasts was established for *Arabidopsis thaliana* accessions C24, Columbia, and Wassilewskija. Culture conditions and media compositions were optimized for the development of protoplasts embedded in thin alginate layers. Unexpectedly, the absence of cytokinins had a positive effect on cell development. Moreover, combined adjustment of NAA and Dicamba concentrations resulted in high plating efficiencies of up to 30%, followed by shoot regeneration within only 19 days after protoplast isolation. The protocol is reproducible, efficient, extremely fast, and regenerated plants are fertile. Thus, this cotyledon-based system could prove useful for studying plant cell and molecular biology in *A. thaliana*.

- The *sul* gene appeared to be a potential novel candidate as selectable marker for plastid transformation. However, genetic and molecular studies demonstrated that *sul* can not be used for this purpose. On the other hand a new function of *sul* appeared. The gene could be the missing marker for mitochondria transformation in higher plants.

LITERATURE

Abrahams, J.P., Leslie, A.G, Lutter, R., and Walker, J.E. (1994) Structure at 2.8 °A resolution of F1-ATPase from bovine heart mitochondria. *Nature* 370, 621–628.

Ackerman, S.H. (2002) Atp11p and Atp12p are chaperones for F(1)-ATPase biogenesis in mitochondria. *Biochim Biophys Acta* 1555, 101-105.

Alonso, J.M., Stepanova, A.N., Leisse, T.J., Kim, C.J., Chen, H., Shinn, P., Stevenson, D.K., Zimmerman, J., Barajas, P., Cheuk, R., Gadrinab, C., Heller, C., Jeske, A., Koesema, E., Meyers, C.C., Parker, H., Prednis, L., Ansari, Y., Choy, N., Deen, H., Geralt, M., Hazari, N., Hom, E., Karnes, M., Mulholland, C., Ndubaku, R., Schmidt, I., Guzman, P., Aguilar-Henonin, L., Schmid, M., Weigel, D., Carter, D.E., Marchand, T., Risseuw, E., Brogden, D., Zeko, A., Crosby, W.L., Berry, C.C. and Ecker, J.R. (2003) Genome-wide insertional mutagenesis of *Arabidopsis thaliana*. *Science* 301, 653-657.

Akashi, K., Grandjean, O., and Small, I. (1998) Potential dual targeting of an *Arabidopsis* archaeobacterial-like histidyl-tRNA synthetase to mitochondria and chloroplasts . *FEBS Lett.* 431, 39-44.

Amann, K., Lezhneva, L., Wanner, G., Herrmann, R.G. and Meurer J. (2004) Accumulation of phosysten one1, a member of a novel gene family, is required for accumulation of [4Fe-4S] cluster-containing chloroplast complexes and antenna proteins. *Plant Cel.* 16, 3084-3097.

Arabidopsis Genome Initiative (2000) Analysis of the genome sequence of the flowering plant *Arabidopsis thaliana*. *Nature* 408, 796–815.

Arechaga, I., and Jones, P.C. (2001) The rotor in the membrane of the ATP synthase and relatives. *FEBS Lett.* 494, 1-5.

Arnon, D.I. (1949) Copper enzymes in isolated chloroplasts. Polyphenoloxidase in *Beta vulgaris*. *Plant Physiol.* 24, 1-13.

Bald, D., Noji, H., Yoshida, M., Hirono-Hara, Y., and Hisabori, T. (2001) ATPase activity of a highly stable a3b3c subcomplex of thermophilic F1 can be regulated by the introduced regulatory region of γ subunit of chloroplast F1. *J. Biol. Chem.* 276, 39505–39507.

Basset, G.J., Quinlivan, E.P., Ravanel, S., Rebeille', F., Nichols, B.P., Shinozaki, K., Seki, M., Adams-Phillips, L.C., Giovannoni, J.J., Gregory, III, J.F. et al. (2004) Folate synthesis in plants: the p-aminobenzoate branch is initiated by a bifunctional PabA-PabB protein that is targeted to plastids. *Proc. Natl. Acad. Sci. U.S.A.* 101, 1496–1501.

Bechtold, N., and Pelletier, G. (1998) In planta *Agrobacterium*-mediated transformation of adult *Arabidopsis thaliana* plants by vacuum infiltration. *Methods Mol. Biol.*, 82, 259-266.

Blum, H., Beier, H. and Gross, H.J. (1987) Improved silver staining of plant proteins, RNA and DNA in polyacrylamide gels. *Electrophoresis* 8, 93-99.

Bolle, C., Kusnetsov, V.V., Herrmann, R.G., and Oelmuller, R. (1996) The spinach *AtpC* and *AtpD* genes contain elements for light-regulated, plastid-dependent organ-specific expression in the vicinity of the transcription start sites. *Plant J.* 9, 21-30.

Boltz, K.W. and Frasch, K.D. (2005) Interactions of γ T273 and γ E275 with the β Subunit PSAV segment that kinks the γ subunit to the catalytic site Walker homology B Aspartate are important to the function of *Escherichia coli* F1Fo ATP synthase. *Biochemistry* 44, 9497-9506.

Bondarava, N., De Pascalis, L., Al-Babili, S., Goussias, C., Golockj, J. R., Beyer, P., Bock, R., and Krieger-Liszay, A. (2003) Evidence that cytochrome *b₅₅₉* mediates the oxidation of reduced plastoquinone in the dark. *J. Biol. Chem.* 278, 13554–13560.

Boydton, J.E., Gillham, N.W., Harris, E.H., Hosler, J.P., Johnson, A.M., Jones, A.R., Randolph-Anderson, B.L., Robertson, D., Klein, T.M., Shark, K.B., and Sanford, J.C. (1988) Chloroplast transformation in *Chlamydomonas* with high velocity microprojectiles. *Science* 240, 1534–1538.

Bradford, M.M. (1976) A rapid and sensitive method for the quantification of microgram quantities of protein utilizing the principle of protein-dye binding. *Anal. Biochem.* 72, 248-254.

Cleary, S.P., Tan, F.C., Nakrieko, K.A., Thompson, S.J., Mullineaux, P.M., Creissen, G.P., von Stedingk, E, Glaser, E, Smith, AG, Robinson, C. (2002) Isolated plant mitochondria import chloroplast precursor proteins *in vitro* with the same efficiency as chloroplasts. *J. Biol. Chem.* 277, 5562-5566.

Clough, S.J., and Bent, A.F. (1998) Floral dip: a simplified method for *Agrobacterium*-mediated transformation of *Arabidopsis thaliana*. *Plant J.* 16, 735-743.

Dal Bosco, C., Lezhneva, L., Biehl, A., Leister, D., Strotmann, H., Wanner, G. and Meurer, J. (2004) Inactivation of the chloroplast ATP synthase gamma subunit results in high non-photochemical fluorescence quenching and altered nuclear gene expression in *Arabidopsis thaliana*. *J. Biol. Chem.* 279, 1060-1069.

Daniell, H., Muthukumar, B. and Lee, S.B. (2001) Marker free transgenic plants: engineering the chloroplast genome without the use of antibiotic selection. *Curr. Genet.* 39, 109-116.

- Demming-Adams, B.** (1990) Carotenoids and photoprotection in plants: a role for the xanthophyll zeaxanthin. *Biochim. Biophys. Acta* 1020, 1–24.
- Dovzhenko, A.,** Bergen, U. and Koop, H.U. (1998) Thin-alginate-layer technique for protoplast culture of tobacco leaf protoplasts: shoot formation in less than two weeks. *Protoplasma* 204, 114-118.
- Dovzhenko, A.,** Dal Bosco, C., Meurer, J. and Koop, H.U. (2003) Efficient regeneration from cotyledon protoplasts in *Arabidopsis thaliana*. *Protoplasma* 222, 107-111.
- Dovzhenko, A.,** and Koop, H.U. (2003) Sugarbeet (*Beta vulgaris* L.): shoot regeneration from callus and callus protoplasts. *Planta* 217, 374-381.
- Engelbrecht, S., and Junge, W.** (1997) ATP synthase: a tentative structural model. *FEBS Lett.* 414, 485-491.
- Falk, G., and Walker, J. E.** (1988) DNA sequence of a gene cluster coding for subunits of the FO membrane sector of ATP synthase in *Rhodospirillum rubrum*. Support for modular evolution of the F1 and FO sectors. *Biochem. J.* 254, 109–122.
- Feldmann, K.A.** (1991) T-DNA insertion mutagenesis in *Arabidopsis*: mutational spectrum. *Plant J.* 1, 71-82.
- Fox, T.D.,** Sanford, J.C., and McMullin, T.W. (1988) Plasmids can stably transform yeast mitochondria lacking endogenous mtDNA. *Proc Natl Acad Sci US A.* 85, 7288-7292.
- Gold, T.,** Koop, H.U., and Maliga, P. (1993) Stable plastid transformation in PEG-treated protoplasts in *Nicotiana tabacum*. *Biotechnology* 11, 95–97.
- Govindjee and Spilotro** (2002) An *Arabidopsis thaliana* mutant, altered in the γ subunit of the ATP synthase, has a different pattern of intensity dependent changes in non-photochemical quenching and kinetics of the P-to-S fluorescence decay. *Funct. Plant Biol.* 29, 425–434.
- Green, P.J.,** Kay S.A., and Chua N.H. (1987) Sequence-specific interactions of a pea nuclear factor with light-responsive elements upstream of the *rbcS-3A* gene. *The EMBO Journal* 6, 2543-2549.
- Groth, G.,** and Pohl, E. (2001) The structure of the chloroplast F1-ATPase at 3.2 Å resolution. *J. Biol. Chem.* 276, 1345–1352.
- Groth, G.,** and Strotmann, H. (1999) New results about structure, function and regulation of the chloroplast ATP synthase (CF₀CF₁). *Physiol. Plant.* 106, 142–148.

Guerineau, F., Brooks, L., Meadows, J., Lucy, A., Robinson, C., and Mullineaux, P. (1990) Sulfonamide resistance gene for plant transformation. *Plant Mol. Biol.* 15, 127-136.

Hadi, M.Z., Kemper, E., Wendeler, E. and Reiss, B. (2002) Simple and versatile selection of *Arabidopsis* transformants. *Plant Cell Rep.* 21, 130–135.

Hadikusumo, R. G., Meltzer, S., Choo, W. M., Jean-Francois, M. J. B., Linnane, A. W., and Marzuki, S. (1988) The definition of mitochondrial H⁺ ATPase assembly defects in mit- mutants of *Saccharomyces cerevisiae* with a monoclonal antibody to the enzyme complex as an assembly probe. *Biochim. Biophys. Acta* 933, 212–222.

Hall, R.D., Riksen-Bruinsma, T., Weyens, G., Lefebvre, M., Dunwell, J.M., Van Tunen, A., Krens, F.A. (1997) Sugar beet guard protoplasts demonstrate a remarkable capacity for cell division enabling applications in stomatal physiology and molecular breeding. *J Exp Bot* 48, 255–263.

Hanson and Roje (2001) One-carbon metabolism in higher plants. *Annu. Rev. Plant Physiol. Plant Mol. Biol.* 52, 119-137.

Herrmann, R.G. and Westhoff, P. (2001) Thylakoid biogenesis and dynamics: The result of a complex phylogenetic puzzle. In: Regulation of photosynthesis (Aro, E.-M. and Andersson, B., eds). Dordrecht: Kluwer Academic Publishers, pp. 1-28.

Hisabori, T., Kato, Y., Motohashi, K., Kroth-Pancic, P., Strotmann, H., Amano, T. (1997) The regulatory functions of the gamma and epsilon subunits from chloroplast CF1 are transferred to the core complex, alpha3beta3, from thermophilic bacterial F1. *Eur. J. Biochem.* 247, 1158-1165

Hisabori T, Motohashi K, Kroth P, Strotmann H & Amano T (1998) The formation or the reduction of a disulfide bridge on the c subunit of chloroplast ATP synthase affects the inhibitory effect of the e subunit. *J. Biol. Chem.* 273, 15901–15905.

Holt, N.E., Fleming, G.R., and Niyogi, K.K. (1984) Toward an understanding of the mechanism of non-photochemical quenching in green plants. *Biochemistry* 43, 8281-8289.

Hou, B.K., Zhou, Y.H., Wan, L.H., Zhang, Z.L., Shen, G.F., Chen, Z.H., and Hu ZM. (2003) Chloroplast transformation in oilseed rape. *Transgenic Res.* 12, 111-114.

Huang, F.C., Klaus, S.M.J., Herz, S., Zou, Z., Koop, H.U. and Golds, T.J. (2002) Efficient plastid transformation in tobacco using the *aphA-6* gene and kanamycin selection. *Mol Gen Genomics* 268, 19–27.

- Inohara, N.**, Iwamoto, A., Moriyama, Y., Shimomura, S., Maeda, M., and Futai, M. (1991) Two genes, *atpC1* and *atpC2*, for the gamma subunit of *Arabidopsis thaliana* chloroplast ATP synthase. *J. Biol. Chem.* 266, 7333–7338.
- Johnston, S.A.**, P.Q. Anziano, K. Shark, J.C. Sanford, and R.A. Butow. (1988) Mitochondrial transformation in yeast by bombardment with microprojectiles. *Science* 240, 1538-1541.
- Junesch, U.**, Gräber, P. (1991) The rate of ATP-synthesis as a function of ΔpH and $\Delta\phi$ catalyzed by the active, reduced H^+ -ATPase from chloroplasts. *FEBS Lett.* 294, 275–278.
- Junge, W.** (2004) Protons, proteins and ATP. *Photosynth. Res.* 80, 197-221.
- Khan, M.S., and Maliga, P.** (1985) Fluorescent antibiotic resistance marker for tracking plastid transformation in higher plants. *Nat. Biotechnol.* 17, 910-915.
- Kay, A.S.**, Nagatani, A. Keith, B., Deak, M., Furuya, M. and Chua, N.-H. (1989) Rice phytochrome is biologically active in transgenic tobacco. *Plant Cell* 1, 775-782.
- Kanazawa, A.**, and Kramer, D. M. (2002) *In vivo* modulation of non-photochemical exciton quenching (NPQ) by regulation of the chloroplast ATP synthase. *Proc. Natl. Acad. Sci. U. S. A.* 99, 12789–12794.
- Ketcham, S.R.**, Davenport, J.W., Warncke, K., McCarty, R.E. (1984) Role of the γ subunit of chloroplast coupling factor 1 in the light dependent activation of photophosphorylation and ATPase activity by dithiothreitol, *J. Biol. Chem.* 259, 7286–7293.
- Klionsky, D.J.**, and Simoni, R.D. (1985) Assembly of a functional F1 of the proton-translocating ATPase of *Escherichia coli*. *J. Biol. Chem.* 260, 11207–11215.
- Köhler, R.H.**, Zipfel, W.R., Webb, W.W., Hanson, M.R. (1997) The green fluorescent protein as a marker to visualize plant mitochondria *in vivo*. *Plant J.* 11, 613-621.
- Konec, C.**, Martini, N., Szabados, L., Hroudá, M., Bachmair, A. and Schell, J. (1994) Specialized vectors for gene tagging and expression studies. In: *Plant Molecular Biology Manual*. Vol. B2 (Gelvin, S.B. and Schilperoort, R.A., eds). Dordrecht: Kluwer Academic Publishers, pp. 1-22.
- Konno, H.**, Yodogawa, M., Stumpp, M. T., Kroth, P., Strotmann, H., Motohashi, K., Amano, T., and Hisabori, T. (2000) Inverse regulation of F1-ATPase activity by a mutation at the regulatory region on the γ subunit of chloroplast ATP synthase. *Biochem. J.* 352, 783–788.

Koop, H.U., Steinmüller, K., Wagner, H., Rößler, C., Eibl, C. and Sacher, L. (1996) Integration of foreign sequences into the tobacco plastome via polyethylene glycol-mediated protoplast transformation. *Planta* 199, 193-201.

Krysan, P.J., Young, J.C. and Sussman, M.R. (1999) T-DNA as an insertional mutagen in *Arabidopsis*. *Plant Cell* 11, 2283-2290.

Kuchuk, N., Herrmann, R.G., Koop, H.U. (1998) Plant regeneration from leaf protoplasts of evening primrose (*Oenothera hookeri*). *Plant Cell Rep* 17, 601–604.

Kuromori, T., Hirayama, T., Kiyosue, Y., Takabe, H., Mizukado, S., Sakurai, T., Akiyama, K., Kamiya, A., Ito, T. and Shinozaki, K. (2004) A collection of 11800 single-copy Ds transposon insertion lines in *Arabidopsis*. *Plant J.* 37, 897-905.

Kurth, J., Varotto, C., Pesaresi, P., Biehl, A., Richly, E., Salamini, F., and Leister, D. (2002) Gene-sequence-tag expression analyses of 1,800 genes related to chloroplast functions. *Planta* 215, 101–109.

Legen, J., Misera, S., Herrmann, R. G., and Meurer, J. (2001) Map positions of 69 *Arabidopsis thaliana* genes of all known nuclear encoded constituent polypeptides and various regulatory factors of the photosynthetic membrane: a case study. *DNA Res.* 8, 53–60.

Lemaire, C. and Wollman, F.A. (1989) The chloroplast ATP synthase in *Chlamydomonas reinhardtii*. II. Biochemical studies on its biogenesis using mutants defective in photophosphorylation. *J. Biol. Chem.* 264, 10235–10242.

Lezhneva, L., Amann, K. and Meurer, J. (2004) The universally conserved HCF101 protein is involved in assembly of [4Fe-4S]-cluster-containing complexes in *Arabidopsis thaliana* chloroplasts. *Plant J.* 37, 174-185.

Li, X.-P., Bjorkman, O., Shih, C., Grossman, A. R., Rosenquist, M., Jansson, S., and Niyogi, K. K. (2000) A pigment-binding protein essential for regulation of photosynthetic light harvesting. *Nature* 403, 391–395.

Li, X. P., Muller-Moule P., Gilmore, A. M., and Niyogi, K. K. (2002) PsbS-dependent enhancement of feedback de-excitation protects photosystem II from photoinhibition. *Proc. Natl. Acad. Sci. U. S. A.* 99, 15222–15227.

Luo, Y. and Koop, H.U. (1997) Somatic embryogenesis in cultured immature zygotic embryos and leaf protoplasts of *Arabidopsis thaliana* ecotypes. *Planta* 202, 387–396.

Majeran, W., Olive, J., Drapier, D., Vallon, O., and Wollman, F. A. (2001) The light sensitivity of ATP synthase mutants of *Chlamydomonas reinhardtii*. *Plant Physiol.* 126, 421–433.

- Maliga, P.** (2003) Progress towards commercialization of plastid transformation technology. *Trends Biotechnol.* 1, 20-8. Review.
- Martienssen, R.A.** (1998) Functional genomics: probing plant gene function and expression with transposons *Proc. Natl. Acad. Sci. USA* 95, 2021-2026.
- Masson, J., and Paszkowski, J.** (1992) The culture response of *Arabidopsis thaliana* protoplasts is determined by the growth conditions of donor plants. *Plant J.* 2, 829–833.
- Menz, R.I.,** Walker, J.E., and Leslie, A.G. (2001) Structure of bovine mitochondrial F(1)-ATPase with nucleotide bound to all three catalytic sites: implications for the mechanism of rotary catalysis. *Cell* 106, 331-341.
- McMaster, G.K.** and Carmichael, G.G. (1977) Analysis of single and double-stranded nucleic acids on polyacrilamid and agarose gels by using glyoxal and acridine orange. *Proc. Natl Acad. Sci. USA* 74, 4835-4838.
- Meurer, J.,** Meierhoff, K. and Westhoff, P. (1996) Isolation of high-chlorophyll-fluorescence mutants of *Arabidopsis thaliana* and their characterization by spectroscopy, immunoblotting and RNA gel hybridization. *Planta* 198, 385–396.
- Meurer, J.,** Plücker, H., Kowallik, K.V. and Westhoff, P. (1998) A nuclear-encoded protein of prokaryotic origin is essential for the stability of photosystem II in *Arabidopsis thaliana*. *EMBO J.* 17, 5286–5297.
- Meurer, J.,** Lezhneva, L., Amann, K., Gödel, M., Bezhani, S., Sherameti, I., and Oelmüller, R. (2002) A peptide chain release factor 2 affects the stability of UGA-containing transcripts in *Arabidopsis* chloroplasts. *Plant Cell* 12, 3255–3269.
- Mireau, H.,** Arnal, N., and Fox T. D. (2003) Expression of Barstar as a selectable marker in yeast mitochondria. *Mol Gen Genetics* 270, 1-8.
- Mouillon, J.M.,** Ravel, S., Douce, R., and Rebeille, F. (2002) Folate synthesis in higher-plant mitochondria: coupling between the dihydropterin pyrophosphokinase and the dihydropteroate synthase activities. *Biochem J.* 363, 313-9.
- Müller, P.,** Li, X.-P., Li, X-P., and Niyogi, K. K. (2001) Non-Photochemical Quenching. A response to excess light energy. *Plant Physiol.* 125, 1558–1566.
- Murashige, T.** and Skoog, F. (1962) A revised medium for rapid growth and bioassays with tobacco tissue cultures. *Physiol Plant.* 15, 473-497.

Nakanishi, H-U., Nakanishi, Y. Konno H., Motohashi, K., Bald D., and Hisabori, T. (2004) Inverse Regulation of Rotation of F1-ATPase by the Mutation at the Regulatory Region on the γ Subunit of Chloroplast ATP Synthase. *J. Biol. Chem.* 279, 16272–16277.

Nalin, C.M and McCarty, R.E. (1984) Role of a disulfide bond in the γ subunit in activation of the ATPase of chloroplast coupling factor1. *J. Biol. Chem.* 259, 7275–7280.

Nelson, N. (1992) Organellar proton-ATPases. (1992) *Curr Opin Cell Biol.* 4, 654-60. Review.

Niyogi, K. K., Björkman, O., and Grossman, A. R. (1997) Chlamydomonas Xanthophyll Cycle Mutants Identified by Video Imaging of Chlorophyll Fluorescence Quenching. *Plant Cell* 9, 1369–1380.

Niyogi, K.K., Grossman, A.R., and Bjorkman, O. (1998) Arabidopsis mutants define a central role for the xanthophyll cycle in the regulation of photosynthetic energy conversion. *Plant Cell* 10, 1121–1134.

Niyogi, K.K., Li, X.P., Rosenberg, V., Jung, H.S. (2005) Is PsbS the site of non-photochemical quenching in photosynthesis? *J Exp Bot.* 375-82. Epub 2004 Dec 20. Review.

O'Neill, C., Horvath, G.V., Horvath, E., Dix, P.J. and Medgyesy, P. (1993) Chloroplast transformation in plants: polyethylene glycol (PEG) treatment of protoplasts is an alternative to biolistic delivery systems. *Plant J.* 3, 729–738.

Oster, G., and Wang, H. (1999). ATP Synthase: Two rotary molecular motors working together. In: *Encyclopedia of Molecular Biology*, (ed. T. Creighton) New York:Wiley. pp. 211-215.

Race, H. L., Herrmann, R. G., Martin, W. (1999). Why have organelles retained genomes? *Trend Genet.* 15, 364-370.

Rebeille, F., Macherel, D., Mouillon, J.M., Garin, J. and Douce, R. (1997) Folate biosynthesis in higher plants: purification and molecular cloning of a bifunctional 6-hydroxymethyl-7,8-dihydropterin pyrophosphokinase/7,8-dihydropteroate synthase localized in mitochondria. *EMBO J.* 16, 947–957.

Regel, R., Ivleva, N. B., Zer, H., Meurer, J., Shestakov, S. V., Herrmann R. G., Pakarasi H. B., Ohad I. (2001) Deregulation of electron flow within photosystem II in the absence of the PsbJ protein. *The Journal of Biological Chemistry*, 276 41473-41478.

Richly, E., Dietzmann, A., Biehl, A., Kurth, J., Laloi, C., Apel, K., Salamini, F., and Leister, D. (2003) Covariations in the nuclear chloroplast transcriptome reveal a regulatory master-switch *EMBO Rep.* 4, 491-498.

- Robertson, D.**, Woessner, J.P., Gillham, N.W., and Boynton, J.E. (1989) Molecular characterization of two point mutants in the chloroplast *atpB* gene of the green alga *Chlamydomonas reinhardtii* defective in assembly of the ATP synthase complex. *J Biol Chem.* 264, 2331-2337.
- Ross, S.A.**, Zhang, M.X., and Selman, B.R. (1995) Role of the *Chlamydomonas reinhardtii* coupling factor 1 gamma-subunit cysteine bridge in the regulation of ATP synthase. *J Biol Chem.* 270, 9813-9818.
- Ruf, S.**, Hermann, M., Berger, I.J., Carrer, H., and Bock, R. (2001) Stable genetic transformation of tomato plastids and expression of a foreign protein in fruit. *Nat Biotechnol.* 19, 870-5.
- Sahr, T.**, Ravanel, S. and Rebeille, F. (2005) Tetrahydrofolate biosynthesis and distribution in higher plants. *Biochemical Society Transactions* 33, 758-762.
- Sambrook, J.**, Fritsch, E.F. and Maniatis, T. (1989) Molecular cloning – a laboratory manual. 2 ed. Cold Spring Harbor, New York, USA: Cold Spring Harbor Laboratory Press.
- Schwarz, O.**, Schurmann, P., and Strotmann, H. (1997) Kinetics and thioredoxin specificity of thiol modulation of the chloroplast H⁺-ATPase. *J Biol Chem.* 272, 16924-7.
- Seelert, H.**, Poetsch, A., Dencher, N.A., Engel, A., Stahlberg, H., Müller, D.J. (2000) Proton –powered turbine of a plant motor. *Nature* 405, 418-419.
- Sidorov, V.A.**, Karsten, D., Pang, S.Z., Hajdukiewicz, P.T.J., Staub, J.M., and Nehra, N.S. (1999) Stable chloroplast transformation in potato: use of green fluorescent protein as a plastid marker. *Plant J.* 19, 209–216.
- Sikdar, S.R.**, Serino, G., Chaudhuri, S. and Maliga, P. (1998) Plastid transformation of *Arabidopsis thaliana*. *Plant Cell Rep.* 18, 20–24.
- Smart, E. J.**, and Selman, B. R. (1991) Isolation and characterization of a *Chlamydomonas reinhardtii* mutant lacking the g-subunit of chloroplast coupling factor 1 *Mol. Cell. Biol.* 11, 5053–5058.
- Stock, D.**, Leslie, A.G., Walker, J.E. (1999) Molecular architecture of the rotary motor in ATP synthase. *Science* 286, 1700-1705.
- Strotmann, H.**, and Bickel-Sandkötter, S., (1977) Energy-dependent exchange of adenine nucleotides on chloroplast coupling factor (CF1). *Biochim. Biophys. Acta* 460, 126-135.
- Strotmann, H.**, Thelen, R., Müller, W., and Baum, W. (1990) A delta pH clamp method for analysis of steady-state kinetics of photophosphorylation. *Eur. J. Biochem.* 193, 879–886.

Strotmann, H., Shavit, N. and Leu, S. (1998) Assembly and function of the chloroplast ATP synthase. In: The molecular biology of chloroplast and mitochondria in *Chlamydomonas* (Rochaix, J.D., Goldschmidt-Clermont, M. and Merchant, S., eds. Norwell, MA: Kluwer Academic Publishers, 477–500.

Svab, Z., Hajdukiewicz, P.T.J. and Maliga, P. (1990) Stable transformation of plastids in higher plants. *Proc. Natl. Acad. Sci. U. S. A.* 87, 8526–8530.

Svab, Z. and Maliga, P. (1993) High-frequency plastid transformation in tobacco by selection for a chimeric *aadA* gene. *Proc. Natl. Acad. Sci. U.S.A.* 90, 913-917

Szabados, L., Kovacs, I., Oberschall, A., Abraham, E., Kerekes, I., Zsigmond, L., Nagy, R., Alvarado, M., Krasovskaja, I., Gal, M., Berente, A., Redei, G.P., Haim, A.B. and Koncz, C. (2002) Distribution of 1000 sequenced T-DNA tags in the *Arabidopsis* genome. *Plant J.* 32, 233-242.

Till, B.J., Reynolds, S.H, Greene, E.A., Codomo, C.A., Enns, L.C., Johnson, J.E., Burtner, C., Odden, A.R., Young, K., Taylor, N.E., Henikoff, J.G., Comai, L., and Henikoff, S. (2003) Large-Scale Discovery of Induced Point Mutations With High-Throughput TILLING. *Genome Res.*, 13, 524-530.

Triglia, T. and Cowman, A.F. (1994) Primary structure and expression of the dihydropteroate synthase gene of *Plasmodium falciparum*. *Proc. Natl Acad. Sci. USA*, 91, 7149-7153.

Vision, T. J., Brown, D. G., and Tanksley, S. D. (2002) The origins of genomic duplications in *Arabidopsis*. *Science* 290, 2114–2117.

Volpe, F., Dyer, M. , Scaife, J.G. , Darby, G. , Stammers, D.K. and Delves, C.J. (1992) The multifunctional folic acid synthesis *fas* gene of *Pneumocystis carinii* appears to encode dihydropteroate synthase and hydroxymethyldihydropterin pyrophosphokinase. *Gene*, 112, 213-218.

Wedel, N., Klein, R., Ljungberg, U., Andersson, B., and Herrmann, R.G. (1992) The single-copy gene *psbS* codes for a phylogenetically intriguing 22 kDa polypeptide of photosystem II. *FEBS Letters* 314, 61–66.

Werner-Grüne, S., Gunkel, D., Schumann, J, and Strotmann, H. (1994) Insertion of a "chloroplast-like" regulatory segment responsible for thiol modulation into gamma-subunit of FOF1-ATPase of the cyanobacterium *Synechocystis* 6803 by mutagenesis of *atpC*. *Mol Gen Genet.* 244, 144-150.

Wise, E.M. and Abou-Donia, M.M. (1975) Sulfonamide resistance mechanism in *Escherichia coli*: R plasmids can determine sulfonamide-resistant dihydropteroate synthases. *Proc Natl Acad Sci U S A.*, 72, 2621-2625.

Wittwer, C.T., Ririe, K.M., Andrew, R.V., David, D.A., Gundry, R.A. and Balis, U.J. (1997a) The LightCycler: a microvolume multisample fluorimeter with rapid temperature control. *Biotechniques* 22, 176-181.

Wittwer, C.T., Herrmann, M.G., Moss, A.A. and Rasmussen, R.P. (1997b) Continuous fluorescence monitoring of rapid cycle DNA amplification. *Biotechniques* 22, 130-131, 134-138.

Wollman, F.A., Minai, L. and Nechushtai, R. (1999) The biogenesis and assembly of photosynthetic proteins in thylakoid membranes. *Biochim. Biophys. Acta* 1411, 21-85.

Yamaguchi, R., Nakamura, M., Mochizuki, N., Kay, S.A., and Nagatani, A. (1999) Light-dependent translocation of a phytochrome B-GFP fusion protein to the nucleus in transgenic *Arabidopsis*. *Journal of Cell Biology* 145: 437-445.

Zimmermann, P., Hirsch-Hoffmann, M., Hennig, L., Gruissem, W. (2004). GENEVESTIGATOR. Arabidopsis Microarray Database and Analysis Toolbox. *Plant Physiol.* 136, 2621-2632.

Zubko, M.K. and Day, A. (1998) Stable albinism induced without mutagenesis: a model for ribosome-free plastid inheritance. *The Plant Journal* 15, 265-271.

ACKNOWLEDGEMENTS

This work was performed at the Department I of the Botanical Institute of the Ludwig-Maximilians-Universität in Munich in the laboratory of Prof. Dr. R.G Herrmann.

Vielen Dank Prof. Herrmann for the possibility to perform my PhD in a laboratory with excellent working features and characterized by an international breath, for the possibility to attend conferences and meetings where I could personally meet remarkable scientists, and for reviewing this work.

Vielen Dank to Dr. Jörg Meurer for supervising this work, for assigning to me interesting projects, for giving me the freedom to develop my own ideas and trusting in my capabilities. Thank you for the readiness to help in everyday situations especially when my basic knowledge of German could be an handicap for me.

Vielen Dank to the collaborators who enriched this work:

Prof. Dr. H.U. Koop who welcomed me in his laboratory where I learned everything I know about the “microscopic” world of protoplasts. Dr. Alexander Dovzhenko for awaking my interest and introducing me to “Mr. and Mrs.” Protoplasts.

Prof. Dr. H. Strotmann for the photophosphorylation data and for his helpfulness during my stay in his laboratory in Düsseldorf.

Prof. Dr. Wanner for the electron micrograph.

Prof. Dr. D. Leister for the array data.

Vielen Dank to Prof. Dr. H. Scheer for reviewing this work.

Thanks to Prof. I. Ohad for his kindness and educative suggestions.

Thank you to all people and colleagues that I have encountered during these five years. I remember with affection the first very pleasant visit to Munich thanks to Anna, Irina, and Lena. I’m grateful to Rainer Maier’s group, especially Julia, Anja, Michi and Christian that

helped me to get integrated at the beginning, to Jarda with his interesting stories and always ready to help with any computer problems. Thanks to Lada for pushing me to persevere in learning German and the nice time spent together. Thanks to Won, Serena, Reha, Peter, Lina, Elli, Jefferson, Cordelia, Patricia, Petra, Uwe, Martha, Stephan, Pavan, Sabine, Martina, and Holger that contributed to the friendly atmosphere in the laboratory.

Grazie a Giusy with whom I started this experience. Thanks for sharing a flat for three years in friendship, for many moments together and her merry character that helped me to take easier difficult moments.

Thanks to Sasha for his lovely taking care of me.

Thanks to my friends whose feelings were stronger than the distance. Thanks to Luca. Thanks to Roby and Teo. Thanks to my movies provider Davide.

Grazie alla mia famiglia che non conosce confini. Grazie per l'indefessa fiducia nelle mie capacita' e il continuo incoraggiamento.

CURRICULUM VITAE

Personal data

Family name: Dal Bosco
First name: Cristina
Date of Birth: 08th May 1974
Place of Birth: Tregnago (VR), Italy
Nationality: Italian
Marital status: Single



Academic education

10.1994 - 07.2000 Study at the Faculty of Sciences, University of Verona., Italy.
Degree in Plant Biotechnology with 107/110.

03.1999 - 07.2000 working on the degree thesis: „Analysis of the expression of a cold induced gene in barley: effect of plastid development and plastoquinone redox state”. In the molecular biology laboratory of the Experimental Institute for Cereal Research, Section of Fiorenzuola d’Arda (PC), Italy.

Head of the Department:

Dr. A.M. Stanca

Supervisor:

Prof. Dr. R. Bassi

Dr. L. Cattivelli

11.2000 - 12.2006 working on PhD thesis at the Botanisches Institute of the Ludwig Maximilians-Universität, Munich, Germany

Head of the Department:

Prof. Dr. R. G. Herrmann

Supervisor:

Dr. Jörg Meurer

Publications:

Proceedings after Congress participation:

Dal Bosco C, Lezhneva L, Leister D, Strotmann H, Wanner G, Meurer J. Inactivation of the ATPase gamma subunit in *Arabidopsis thaliana*.* Proceeding of “FEBS Advanced Course: Origin and Evolution of Mitochondria and Chloroplasts” April 2001 Hvar, Kroatien.

* Award for the third best poster

Dal Bosco C., Dovzhenko A., Meurer J., Koop HU. Efficient protoplast isolation, culture and regeneration from leaves and cotyledon of *Arabidopsis thaliana*. Proceeding of "Biotechnology Approaches for Exploitation and Preservation of Plant Resources" 23-31 May 2002 Yalta, Ukraine.

Dal Bosco C., Strotmann H., and Meurer J. ATP synthase gamma subunit AtpC2 in *Arabidopsis thaliana* Proceeding of International FEBS Advanced Lecture on the "Origin and Evolution of Mitochondria and Chloroplasts," 12 - 17 March 2005 in Wildbad Kreuth, Germany,

Dal Bosco C., Herrmann R.G. and Meurer J. Biogenesis and function of the thylakoid membrane system in higher plants. Proceeding of 2nd Summer School in Proteomic Basics "From Samples to Sequence" 31.07. - 06.08.2005 Kloster Neustift, Bozen, Italy

Journal:

Dal Bosco C., Busconi M., Govoni C., Baldi P., Stanca A.M., Crosatti C., Bassi R., Cattivelli L. (2003) Cor Gene expression in barley mutants affected in chloroplast development and photosynthetic electron transport. *Plant Physiol.* 131, 793-802.

Dovzhenko A., Dal Bosco C., Meurer J., Koop H.U. (2003) Efficient regeneration from cotyledon protoplasts in *Arabidopsis thaliana*. *Protoplasma.* 222, 107-111.

Dal Bosco C., Lezhneva L., Biehl A., Leister D., Strotmann H., Wanner G., Meurer J. (2004) Inactivation of the chloroplast ATP synthase gamma subunit results in high non-photochemical fluorescence quenching and altered nuclear gene expression in *Arabidopsis thaliana*. *J Biol Chem.* 279, 1060-1069. Epub 2003 Oct 23.

Ohad I., Dal Bosco C., Herrmann R.G., Meurer J. (2004) Photosystem II proteins PsbL and PsbJ regulate electron flow to the plastoquinone pool. *Biochemistry* 43, 2297-2308.

Courses Participations

FEBS Advanced Course: Origin and Evolution of Mitochondria and Chloroplasts"
April 2001 Hvar, Kroatien.

2nd Summer School in Proteomic Basics "From Samples to Sequence".
31.07. - 06.08.2005 Kloster Neustift, Bozen, Italy.

EHRENWÖRTLICHE VERSICHERUNG

Hiermit versichere ich, daß ich die vorliegende Arbeit selbständig und nur unter Verwendung der angegebenen Hilfsmittel und Quellen angefertigt habe.

Zudem erkläre ich, dass ich keine früheren Promotionsversuche unternommen habe.

München, 21.01.2006

Cristina Dal Bosco